Detecting and Understanding Nitric Oxide Formation during Nitrogen Cycling in Microbial Biofilms

Dissertation
zur Erlangung des Grades eines
Doktors der Naturwissenschaften
-Dr. rer. nat.-

Fachbereich Biologie/Chemie der
Universität Bremen

vorgelegt von

Frank Schreiber

Bremen
Mai 2009

Diese Arbeit wurde in der Zeit vom Mai 2006 bis Mai 2009 am Max-Planck-Institut für marine Mikrobiologie im Rahmen der International Max-Planck Research School for Marine Microbiology (IMPRS MarMic) angefertigt.

1. Gutachter: Prof. Dr. Bo Barker Jørgensen
2. Gutacherin: Prof. Dr. Barbara Reinhold

Überzeugt von dem rein menschlichen Ursprung alles Menschlichen, ist er also immer unterwegs – ein Blinder, der sehen möchte und weiß, dass die Nacht kein Ende hat. Der Stein rollt wieder. …. Der Kampf gegen Gipfel vermag ein Menschenherz auszufüllen. Wir müssen uns Sisyphos als einen glücklichen Menschen vorstellen.

aus „Der Mythos von Sisyphos"
von Albert Camus

Preface

Nitric Oxide (NO) is a remarkable molecule and, even though not obvious for us, it is ubiquitously present in low concentrations. It is essential for biogeochemical nitrogen cycling in sediments and waters, an important component of the atmospheric chemistry, and it regulates many functions in microorganisms and in multicellular organisms including humans. The discovery that NO is a central signaling molecule for the regulation of blood pressure sparked its fame, despite of being a simple gaseous molecule, resulting in its selection as the molecule of the year in 1992, followed by the award of the Nobel Prize in Physiology and Medicine in 1998 for the main investigators involved (R.F. Furchgott; F. Murad, and L.J. Ignarro). However, it was already recognized by T. Yamanaka in 1956 that NO was an active biomolecule. He showed NO formation by cell-free extracts that contained bacterial cytochromes and hypothesized that it is an intermediate in denitrification. This hypothesis was given wide acceptance when bacterial NO reductase of denitrifiers was isolated at the end of 1980ies. Somewhat later (1993) the signaling role of NO in bacteria was established by showing its involvement in regulating the oxidative stress response mediated by the SoxRS system, which was followed by many other examples.

This thesis started with the ambitious goal of establishing a signaling role for NO in complex microbial communities organized in biofilms. Before assessing the signaling role of NO, however, I had to realize that even reliable detection of NO in these environments at the relevant scale was not possible. Moreover, the manifold reactions of the nitrogen cycle that can possibly produce NO cause a considerable uncertainty about the processes that are responsible for NO formation. Thus, I learned a lesson every researcher receives: "Go to the lab and eat humble pie, but keep your big ideas in mind." Literally, this meant the development of an NO microsensor that is suitable for measurements in biofilms and sediments, and its application to complex microbial communities in dental and nitrifying/denitrifying biofilms. Application of the NO

microsensor, together with other microsensors, resulted in knowledge of the micro-environment and the activity of nitrogen cycling pathways, and allowed the rather firm assignment of accompanied NO formation to specific pathways.

But what about the 'big ideas'? Following the transient formation of NO in the nitrifying/denitrifying biofilm suggested that NO formation overshoots during perturbation of an active nitrogen cycling pathway. This overshoot is counteracted immediately, possibly on the enzyme level within this complex community. This is far from proving a signaling function but it shows a high degree of regulation of free NO concentrations and highlights the importance of NO for the functioning of the whole community. NO formation by the dental microbial community led us to the exciting hypothesis that a human-associated biofilm community may interact with the host *via* NO, because NO is known to be involved in shaping the immune response in the gum. The definitive establishment of NO signaling within and out of complex microbial communities organized in biofilms clearly awaits a concerted effort of microbial ecologists and molecular biologists in the future. This is certainly a task which could fill a researcher's life.

Acknowledgements

Contents

Chapter 1

Introduction

Chemistry and biology of nitric oxide

Chemical reactions of NO

Nitric Oxide (NO) is a gaseous, hydrophobic radical that plays various roles in biological systems due to its remarkable chemical properties. NO reacts with O_2 to form different oxidation products depending on whether the reaction takes place in the gas or aqueous phase (78). In the gas phase, NO and O_2 react to nitrogen dioxide (NO_2), a brown gas, which is in dynamic balance with its dimeric form, dinitrogen tetroxide (N_2O_4).

$$2\,NO + O_2 \rightarrow 2\,NO_2 \leftrightarrow N_2O_4 \tag{1}$$

The maximal solubility of NO is ~2 mM and it diffuses with ~ $2.21 \times 10^{-5}\,cm^2\,s^{-1}$ (4, 138) in water at 25°C. In the aqueous phase at neutral pH, NO reacts with O_2 to form nitrite (NO_2^-) and protons (54).

$$2\,NO + O_2 \rightarrow 2\,NO_2 \tag{2}$$

$$2\,NO_2 + 2\,NO \leftrightarrow 2\,N_2O_3$$
$$2\,N_2O_3 + 2H_2O \rightarrow 4\,NO_2^- + 4H^+ \tag{3}$$

The kinetics of the reaction is of second order dependence on NO concentrations and of first order dependence on O_2 concentrations with a rate constant of ~ $6 \times 10^6\,M^{-2}s^{-1}$. This results in a half-life of NO in the range of minutes to hours in oxygenated aqueous solutions if present in nanomolar concentrations (10, 61).

Nitric oxide forms chemically if NO_2^- is exposed to low pH levels. Nitrite and protons form an equilibrium with nitrous acid (HNO_2) with a pK_a of 3.2. Nitrous acid decomposes *via* dinitrogen trioxide (N_2O_3) to NO and NO_2 (93) by reactions that are essentially reverse to those shown in equation 3.

$2 \, NO_2^- + 2 \, H^+ \leftrightarrow 2 \, HNO_2$

$2 \, HNO_2 \rightarrow N_2O_3 + H_2O$

$N_2O_3 \rightarrow NO + NO_2$ (4)

The acidic decomposition of NO_2^- to NO is used to prepare NO standard solutions in the laboratory. Here, $NaNO_2$ is acidified under anoxic conditions with sulfuric acid (H_2SO_4) in the presence of sodium iodide (NaI). In this reaction NO, iodine (I_2) and sodium hydrogen sulfate ($NaHSO_4$) are formed (equation 5). Traces of NO_2 that may arise due to O_2 contamination can be removed by directing the gas stream through concentrated sodium hydroxide (NaOH).

$2 NaNO_2 + 2 NaI + 4 H_2SO_4 \rightarrow 2 NO + I_2 + 2 H_2O + 4 NaHSO_4$ (5)

NO in Eukaryotes

In eukaryotic organisms, NO is synthesized from arginine, O_2 and NADPH by NO synthase (NOS) in a tightly controlled enzymatic reaction (Figure 1) (14). The fast diffusion of NO, its hydrophobicity and its reactive nature make NO an ideal messenger molecule that can easily cross cell boundaries and quickly disappear again.
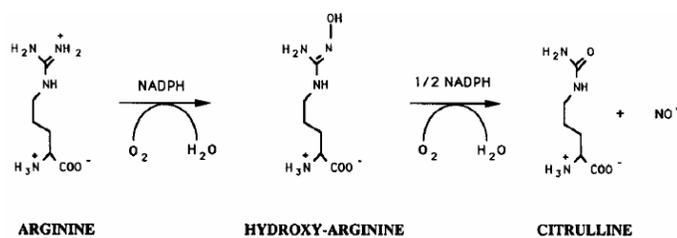
Figure 1. Biosynthesis of NO from aginine by NO synthase. Taken from Bredt & Snyder (14).

Nitric oxide-mediated signaling contributes to blood pressure regulation in vertebrates. Here, NO is formed in endothelial cells and diffuses to the adjacent smooth muscle to

initiate signaling events that cause its relaxation, resulting in vasodilatation. Furthermore, NO regulates platelet aggregation in the vascular system and acts as a neurotransmitter in the brain and the peripheral autonomic nervous system. Moreover, NO is produced by various cell types of the immune system (13). Here, NO is involved in the regulation of the inflammatory response and can serve directly as an antibacterial molecule. Interestingly, pathways that employ NO as messenger molecule or antibacterial agent are well conserved throughout the evolution of eukaryotic multicellular organisms (92).

In recent years a novel, NOS-independent pathway for NO formation in the human body has been described (73, 74). This pathway is based on the reduction of NO_2^- to NO, which is chemically mediated under acidic conditions or by enzymes that exhibit NO_2^- reductase activity (e.g. deoxyhemoglobin). Physiological evidence suggests that the NO_2^--dependent pathway is an alternative route for NO formation under hypoxic and acidic conditions, because NOS-dependent NO formation is impossible in the absence of O_2. Accordingly, NO formation from NO_2^- occurs in situations of decreased O_2 concentrations for hypoxic blood pressure regulation or in the acidic gut upon swallowing NO_2^--rich saliva. Nitrite in humans is formed by oxidation of NOS-derived NO or, more importantly, from ingested, dietary nitrate (NO_3^-), which is reduced by bacteria in the mouth. The latter pathway is termed the entero-salivary circulation of NO_3^- (Figure 2). Here, NO_3^- is taken up from food sources and is absorbed into blood in the intestine. Blood NO_3^- is concentrated by salivary glands leading to concentrations in the micromolar to millimolar range in saliva. Subsequently, NO_3^- is converted to NO_2^- by NO_3^--reducing bacteria in the oral cavity. Swallowed NO_2^- is absorbed into blood and enters the vascular system. Finally, NO_3^- and NO_2^- are excreted through urine and saliva. Bacterial reduction of NO_3^- to NO_2^- in the oral cavity actively regulates blood NO_2^- concentrations and thus affects the NO_2^--dependent pathway of NO formation (45, 134). Currently, it is assumed that bacteria that perform this reaction are located exclusively on the tongue. However, in chapter 4 it is shown that bacteria in dental plaque are an important component of N-cycling in the human mouth and are thus important for NO_2^--dependent NO formation in humans.
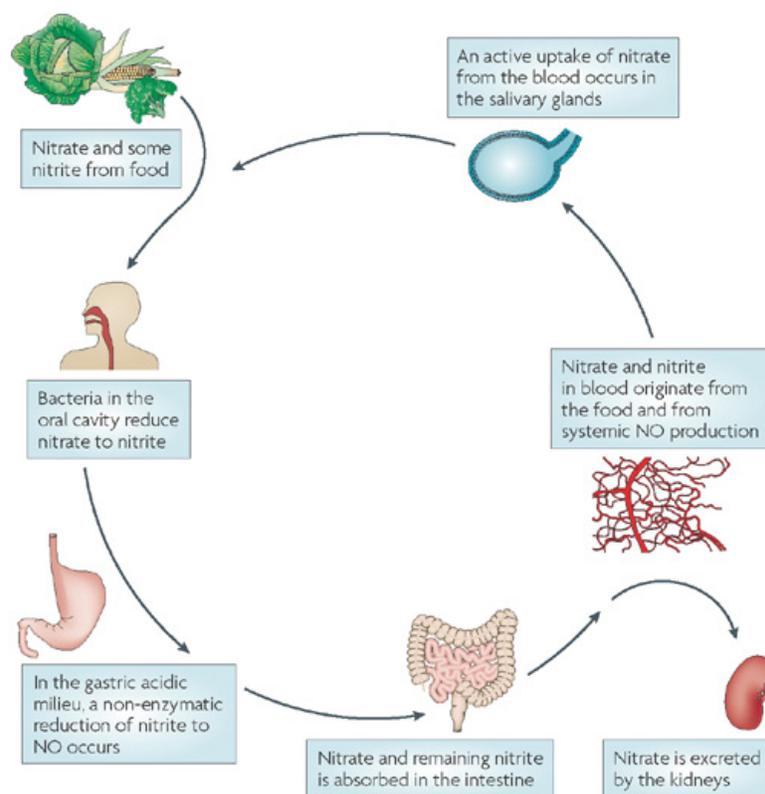
Figure 2. The entero-salivary circulation of nitrate in humans. Taken from Lundberg et al. (74).

Biochemistry of NO related functions in eukaryotes and bacteria

The biochemical basis for the signaling function of NO is the reaction with proteins *via* different, complex pathways involving its redox-related species (NO^+-nitrosonium and NO^--nitroxyl) and other reactive nitrogen species. These reactions result in specific posttranslational modifications of proteins in the target cells including the formation of metal-nitrosyl complexes (MeNO) by reaction with transition metal centers, S-nitrosothiols by S-nitrosylation of regulatory and/or active site cysteine thiols, and nitrotyrosines by nitration of tyrosine moieties (46, 51, 114). These NO-induced modifications cause conformational changes that lead to activation or inhibition of enzymes, which subsequently affect downstream signaling events (Figure 3). Specificity of NO to a certain protein is conveyed by the NO concentrations and the ambient redox

conditions. In addition, the reaction of NO with heme iron of hemoglobin, cysteine thiols of albumin and peptides such as glutathione forms NO adducts with longer lifetimes. These adducts preserve NO bioactivity in a transportable pool. Controlled release of NO is affected by allosteric and redox-based mechanisms that alter FeNO and S-nitrosothiol reactivity (48, 111). The best studied example is the conformational change of soluble guanylate cyclase (sGC) that mediates vasorelaxation upon NO signaling. Nitric oxide is produced by NOS in endothelial cells that diffuses to the adjacent smooth muscle cells. Here, NO binds to a heme group of sGC that has to be in the ferrous sate. This binding severs the bond between the heme group and a bound histidine residue, resulting in a conformational change that prompts the enzyme to produce cyclic GMP (cGMP). cGMP causes further downstream signaling processes that lead to relaxation of the smooth muscle around a blood vessel (46).
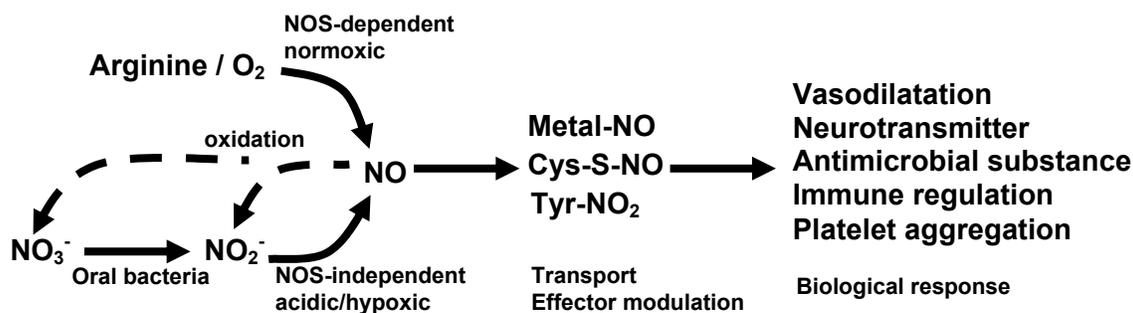
Figure 3. Paradigm of NO Biochemistry. NO synthase (NOS) converts L-arginine in the presence of O_2 to NO. Alternatively, NO may be formed from NO_2^- if ingested NO_3^- is reduced by oral bacteria. The reaction of NO with metal centers of proteins, cysteine-thiols or tyrosine moieties provides a means to tailor its lifetime and transport properties, and to elicit its specific biological responses. Dashed lines represent the back-oxidation of NOS-derived NO to NO_2^- or NO_3^- by reaction with O_2.

In biological systems, NO has a lifetime of a few seconds, thus its decay is much faster than its slow reaction in oxic, aqueous solutions. Controlled formation of O_2 radicals or certain Fe- and thiol-containing proteins that are reactive towards NO represent specific pathways to terminate NO mediated signaling events. The fast reaction of NO with superoxide (O_2^-) to form peroxynitrite ($ONNO^-$) has a second order rate constant of $\sim$10 ×

10^9 M^{-1}s^{-1} and, thus, even outcompetes the reaction of superoxide dismutase with O_2^-. Massive formation of ONNO$^-$ additionally accounts for several toxic effects, because it is very reactive towards biological molecules (125). A comparable toxic effect arises from the fast reaction of NO with oxyhemoglobin to NO_3^- and methemoglobin (54). Methemoglobin has an oxidized ferric iron instead of ferrous iron and is, thus, unable to carry O_2.

In addition to its signaling function, NO plays an important role in host defense against microbial pathogens. Nitric oxide-related toxicity for bacteria is exerted by its reaction with metal centers and thiols in bacterial proteins. Thus, similar biochemical mechanisms underlie NO-dependent physiological signaling and antimicrobial action (114). Nitric oxide-related antimicrobial actions are mainly exerted on bacteria within phagocytes, which are immune system cells that ingest bacteria and produce NO by NOS activity. In contrast, NO in infected tissue may rather be produced as a signal to modulate the immune response. Molecular consequences of NO toxicity involve the inhibition of bacterial respiration, DNA replication and DNA repair. Interaction of NO with reactive O_2 species, produced by phagocytes, results in synergistic cytotoxic effects due to the formation of ONNO$^-$ (31, 95, 114).

Bacteria have evolved sophisticated regulatory mechanisms to counteract cytotoxic effects of NO. As in eukaryotes, NO reacts with NO-responsive transcriptional regulators, which are modified by NO at cysteine thiols and transition metal cofactors, such as heme, non-heme Fe, Fe-S and zinc. These regulators commonly affect regulons, which are involved in responses to oxidative stress, NO detoxification or respiratory NO metabolism (88, 112, 113). Two widespread enzymatic functions are known to support the detoxification of NO in addition to respiratory NO reductases of denitrifying bacteria (denitrification will be dealt with in the following sections). Flavodiiron NO reductase (flavorubredoxin, NorVW) mediates the anaerobic detoxification of NO to N_2O (37, 43). In contrast, NO dioxygenase (flavohemoglobins, Hmp) mediates the O_2-dependent detoxification of NO to NO_3^- (38). In *Pseudomonas aeruginosa* NO, produced by NO_2^-

reduction, is involved in biofilm dispersal at sublethal concentrations (6), indicating that this event was mediated by a signaling function of NO, which was, however, not proven in this work. Taken together, NO is viewed as a signaling molecule not only in eukaryotes, but also in bacteria. However, solid signaling functions between bacteria in single-species and multi-species communities are not established.

The microbial nitrogen cycle

The element nitrogen is an essential nutrient for all living organisms, because it is a critical component of proteins and DNA (33). In turn, microorganisms have evolved a wide array of anabolic and catabolic reactions that make nitrogen bioavailable and that use oxidized and reduced nitrogen compounds for energy metabolism (Figure 4). The central anabolic process in the nitrogen cycle (N-cycle) is the fixation of atmospheric dinitrogen (N_2) to ammonium (NH_4^+). Nitrogen fixation is widely distributed among bacteria and archaea with a wide range of different physiologies. The central enzyme in N_2-fixation is O_2-senitive nitrogenase. However, N_2-fixation also occurs in oxic environments (28).

Nitrogen exists mainly in a reduced state within cells, where it is bound in proteins and other organic molecules. Free NH_4^+ is formed following cell death, lysis and organic matter degradation. Ammonium is oxidized to NO_3^- by nitrification; an aerobic, two-step process that involves NH_4^+-oxidation to NO_2^- and NO_2^--oxidation to NO_3^-. Denitrification and dissimilatory nitrate reduction to ammonium (DNRA) use NO_3^- and NO_2^- as electron acceptors for oxidation of reduced organic carbon or reduced sulphur compounds. Denitrification is the respiratory reduction of NO_3^- and NO_2^- *via* the intermediates NO and N_2O to the final product N_2 (142). In contrast, organisms that perform DNRA reduce NO_3^- and NO_2^- to the final product NH_4^+ (81). In addition, NO_2^- can be reduced by anaerobic ammonium oxidation (anammox) with N_2 as final product (121). More recently, it has been shown that methane (CH_4) can be oxidized anaerobically with NO_3^- as electron acceptor (DAMO) (97). In a contributed work in chapter 5 it is shown that this

process does not follow the 'conventional' denitrification sequence. Rather, the process involves the formation of intermediary O_2 -instead of N_2O- from NO. Oxygen is used as substrate for methane monooxygenase to activate CH_4 to methanol. In contrast to dissimilatory uses of NO_3^- reduction, assimilatory NO_3^- reduction leads to NH_4^+ formation with energy expenditure in environments were NH_4^+ is scarce.

Figure 4. The microbial N-cycle with special emphasis on catabolic reactions that lead to NO formation as intermediate or by-product. Processes depicted with dashed lines require O_2, whereas processes depicted with straight lines require the absence of O_2. Denitrification may also occur under oxic conditions depending on the habitat. Anabolic N_2 fixation is O_2-sensitive, but also occurs in oxic environments. DNRA is dissimilatory nitrate reduction to ammonium, Anammox is anaerobic oxidation of NH_4^+ and DAMO is denitrification coupled to anaerobic methane oxidation, bypassing N_2O as an intermediate. Nitric oxide as intermediate of anammox is postulated by genomic analysis.

Phylogeny, biochemistry and NO formation of N-cycle pathways

Denitrification

Denitrification is performed by facultative anaerobic microorganisms, which are phylogenetically found in all kingdoms of life (*Bacteria*, *Archaea* and *Eukarya*) (33). Denitrification coupled to organic carbon oxidation is referred as to heterotrophic denitrification. However, oxidation of ferrous iron, reduced sulphur compounds and hydrogen can be coupled to denitrification by autotrophic microorganisms (118, 142). Denitrification is commonly assumed to occur exclusively under anoxic conditions. However, it has been shown that certain pure cultures and microbial communities in certain habitats perform denitrification under oxic conditions (72). In a contributed work in chapter 5 it is shown that aerobic denitrification occurs in sediments of an intertidal sandflat (Janssand, North Sea), which are exposed to fluctuating O_2 concentrations.

The reductive sequence ($NO_3^- \rightarrow NO_2^- \rightarrow NO \rightarrow N_2O \rightarrow N_2$) of denitrification is mediated by periplasmic and membrane-bound enzymes (Figure 5). Periplasmic (Nap) or membrane-bound (Nar) NO_3^- reductases mediate the reduction of NO_3^- to NO_2^-. The key enzyme for NO formation during denitrification is NO_2^- reductase (Nir). Purification and characterization of Nir from several bacteria revealed two entirely different periplasmic enzymes; a heme-containing cytochrome cd_1 Nir (NirS) and a copper-containing Nir (NirK) (24). Reduction of NO to N_2O is mediated by respiratory NO reductases (Nor). Catalytic subunits of Nor are homologous to catalytic subunits of enzymes of the heme-copper oxidase superfamily, which are mainly comprised of respiratory, terminal O_2 reductases (143). Respiratory Nor proteins are integral membrane proteins that fall into two groups: one is a cytochrome *bc* complex that can use c-type cytochromes as electron donors (cNor), whereas the other one lacks a cytochrome *c* component and accepts electrons from quinols (qNor). All bacteria that contain cNor are capable of denitrification. In contrast, bacteria that contain qNor are mainly classified as non-denitrifying, pathogenic bacteria and denitrification is a less conspicuous trait (49, 143).

In pathogenic bacteria, qNor might mainly function in NO detoxification and additionally aid to survive anoxia when expressed in concert with Nir as shown for *Neisseria spp.* (3, 98). Notably, cNor is not a proton-pump and takes up electrons and protons from the periplasm. Rather, proton extrusion during electron flow to NO is due to the activity of upstream coupling sites (143). The final step in denitrification is mediated by N_2O reductase (Nos), a multi-copper enzyme that reduces N_2O to N_2. Similar to NO_3^- reduction, N_2O reduction can proceed as an autonomous respiratory process (142).
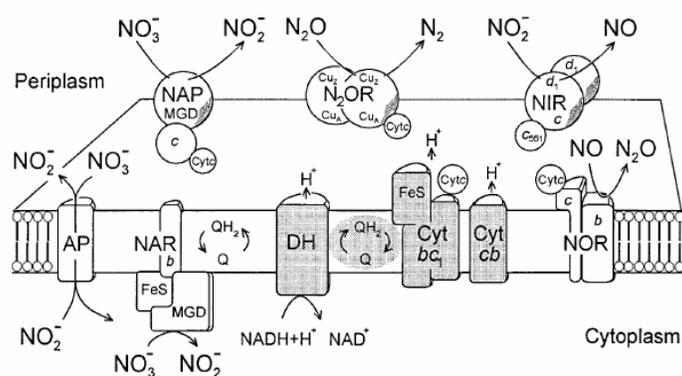
Figure 5. Organization and sidedness of the anaerobic electron transfer chain of the denitrifier *Pseudomonas stutzeri*. The shaded areas represent the components of the constitutive aerobic respiratory chain consisting of an NADH dehydrogenase complex (DH), quinone cycle (Q, QH_2), cytochrome bc_1 complex (Cyt bc_1), and the cytochrome cb terminal oxidase complex (Cyt cb). The respiratory denitrification system comprises membrane-bound (NAR) and periplasmic (NAP) NO_3^- reductases, NO_2^- reductase (NIR), NO reductase (NOR), and N_2O reductase (N2OR). Abbreviations: FeS, iron-sulfur centers; b, c, and d_1, heme B, heme C, and heme D_1, respectively; cyt c, unspecified c-type cytochromes accepting electrons from the bc_1 complex and acting on N2OR and NOR; cyt c_{551}, cytochrome c_{551}; AP, postulated NO_3^-/NO_2^- antiporter. Taken from Zumft (142).

Steady-state concentrations of NO during denitrification are strongly dependent on the affinity of Nor to NO. The K_m-value of Nor is very low (0.25 and 0.4 µM) resulting in low nanomolar NO steady state concentrations during denitrification, which are independent of NO_3^-, NO_2^- and cell concentrations (44, 139). The dominant exogenous signals that induce synthesis of denitrification systems are low O_2 tensions and the presence of a respirable NO_x (142). Nitrate induces the expression of NO_3^- reduction systems, while NO is the central signal for the induction of Nir and Nor, which are

controlled interdependently at both the transcriptional and the enzymatic levels to prevent accumulation of toxic NO (143). In contrast, concentrations of non-toxic N_2O do not affect N_2O reduction. Accumulation of N_2O is often observed during transitions from anoxic to oxic conditions or vice versa, because, as compared to Nir and Nor, inhibition of Nos by O_2 is more pronounced and expression of Nos is slower (7, 83, 89, 117).

DNRA

DNRA is a strictly anaerobic process that has been documented in various facultative, and obligate, anaerobic bacteria. DNRA proceeds in two steps, involving reduction of NO_3^- to NO_2^- and a six-electron reduction from NO_2^- to NH_4^+. Filamentous sulphur bacteria of the genus Thioploca have been shown to couple hydrogen sulphide oxidation with DNRA (90). Moreover, DNRA can be coupled to oxidation of reduced organic carbon compounds. DNRA can proceed *via* a cytoplasmic and a periplasmic pathway, both of which are performed by characteristic enzyme systems (81). The cytoplasmic pathway is mediated by a membrane-bound NO_3^- reductase (Nar) and a cytoplasmic NO_2^- reductase (NirB or NirB-NirD). In contrast, the periplasmic pathway is mediated by periplasmic NO_3^- and cytochrome *c* NO_2^- reductases, Nap and Nrf (Figure 6). During the cytoplasmic pathway energy is conserved by ATP generation *via* substrate-level phosphorylation using NO_2^- as an electron sink for the oxidation of fermentable substrates. In contrast, in the course of the periplasmic pathway electrons are transferred from primary substrates (e.g. formate, NADH and H_2) *via* a quinone-pool to Nrf. Thus, the pathways are sometimes distinguished as the respiratory reduction of NO_3^- to NH_4^+ (periplasmic pathway) and the ('true') dissimilatory or fermentative NO_3^- reduction to NH_4^+ (cytoplasmic pathway) (110). The cytoplasmic pathway is almost exclusively restricted to a few groups of facultative, anaerobic bacteria that thrive in NO_3^--rich habitats. Conversely, many pathogenic and enteric bacteria that survive anoxic, NO_3^--limited environments possess the periplasmic pathway.
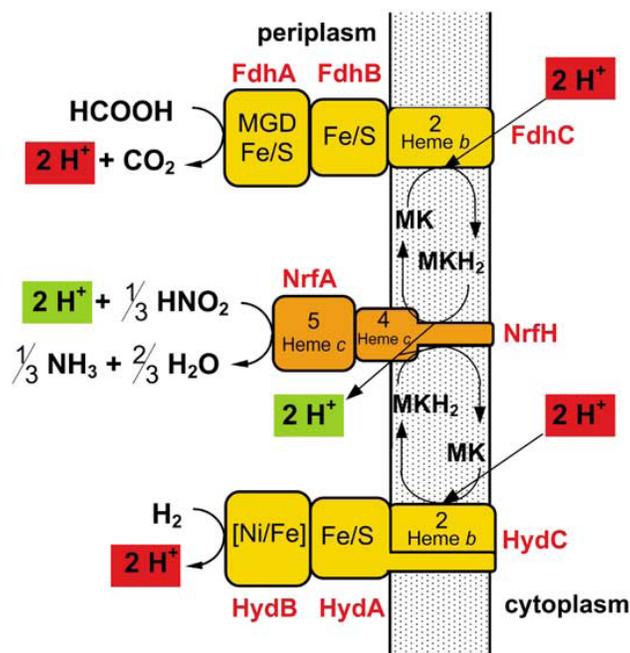
Figure 6. Enzyme complexes involved in electron transport from formate or H_2 to NO_2^- in the periplasmic DNRA pathway of in *Wolinella succinogenes*. The names of the protein subunits making up formate dehydrogenase (Fdh), hydrogenase (Hyd) or cytochrome *c* nitrite reductase (Nrf) are shown in red. Nitrite is supplied by reduction of NO_3^- by periplasmic NO_3^- reductase (Nap), which is not depicted. The hypothetical mechanism of Δp generation is depicted by protons drawn with different color backgrounds. A red background denotes protons that are involved in the electrogenic oxidation of formate or H_2 by MK thus generating Δp by a redox loop mechanism. Protons with a green background are involved in the electro-neutral reduction of NO_2^- by MKH_2, and do not contribute to Δp generation. Substrates and products of the redox reactions are drawn in their neutral forms for simplicity. MK, menaquinone, MGD, molybdenum linked to molybdopterin guanine dinucleotide; Fe/S, iron-sulfur centers. Taken from Simon (110).

Nitric oxide and N_2O turnover by bacteria that perform DNRA has been investigated in *Escherichia coli* and *Salmonella typhimurium*. In *E. coli*, NO formation is mediated by Nrf under anoxic conditions in the presence of NO_3^- and NO_2^- (20). Nitric oxide detoxifying enzymes, such as flavorubredoxin, may further reduce NO to N_2O (Figure 4). On the other hand, *E. coli* Nrf possesses NO reductase activity contributing to detoxification of exogenously generated NO (127). Aerobic and anaerobic NO formation in *S. typhimurium* is mediated by membrane-bound NO_3^- reductase Nar. Under aerobic conditions, however, activity of NO detoxifying Hmp oxidizes NO resulting in non-detectable concentrations (41). In a contribute work in chapter 5 it is shown that an

attenuated strain of *S. typhimurium*, which only infects cancerous tissues, can lead to high amounts of NO in the micro-environment of infected tumors, providing a promising approach for anti-cancer therapy.

Anammox

The anaerobic oxidation of NH_4^+ to N_2 with NO_2^- as electron acceptor is carried out by autotrophic bacteria that are distinct members of the phylum Planctomycetes (119). Anammox involves hydrazine (N_2H_4) as an intermediate, which is oxidized to N_2 by an hydroxylamine oxidoreductase-like protein located inside a unique membrane-bound organelle (anammoxosome) (121). Based on thermodynamic calculations and genomic evidence it was postulated that N_2H_4 formation is mediated by hydrazine hydrolase combining NH_4^+ and NO (Figure 7). Necessary NO might be formed by reduction of NO_2^- by NirS, which is present in the anammox genome (122). Fixation of CO_2 occurs at the expense of electrons that are generated by oxidation of NO_2^- to NO_3^- and by involving reverse electron flow.
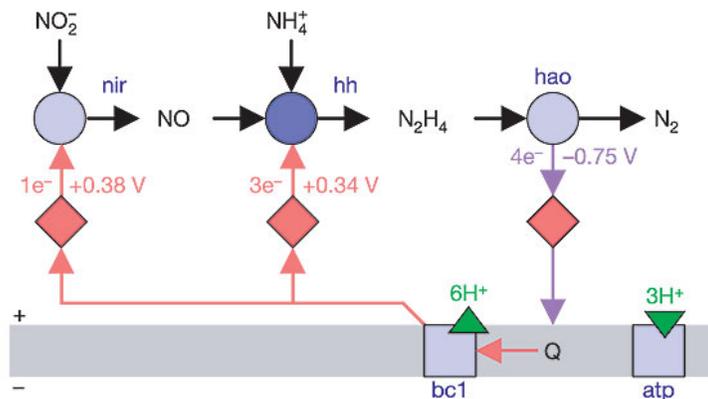
Figure 7. Postulated central anammox catabolism with NO as intermediate, electron transport and energy conservation. Nir, nitrite reductase; hh, hydrazine hydrolase; hao, hydroxylamine oxidoreductase-like protein; red diamonds, cytochromes; red arrows, reductions; purple arrows, oxidations. Taken from Strous et al. (122).

Currently, formation of NO and N_2O by anammox bacteria is not well understood. Accumulation of low NO (7 nM) and high N_2O concentrations (60 µM) by anammox has been demonstrated in an anaerobic enrichment culture consisting of 74% anammox bacteria (120). Despite the potential relevance of NO as a catabolic intermediate, anammox bacteria are able to reduce NO to N_2O, possibly with the genome encoded NO detoxifying enzymes flavorubredoxin and bacterial hemoglobin (58, 100).

Aerobic ammonium oxidation

Aerobic NH_4^+-oxidation to NO_2^- is performed by chemoautotrophic ammonia-oxidizing bacteria (AOB). AOB form a monophyletic cluster within the beta-subclass of Proteobacteria, except *Nitrosococcus*, which forms a separate branch within the gamma-subclass of Proteobacteria. In addition to AOB, NH_4^+-oxidation can be performed by mesophilic Crenarchaeota (65).
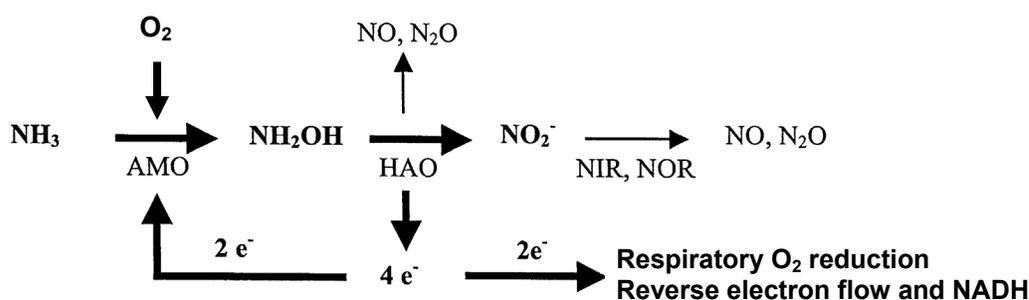
Figure 8. Pathways of NH_3 oxidation and NO and N_2O formation in AOB. Bold arrows and nitrogen compounds indicate major fluxes. AMO, ammonia monooxygenase; HAO, hydroxylamine oxidoreductase; NIR, nitrite reductase; NOR, nitric oxide reductase. Modified from Arp & Stein (5).

In AOB, NH_4^+ is first oxidized to hydroxylamine (NH_2OH) by ammonia monooxygenase (Amo) (Figure 8). The formation of NH_2OH results from the reduction of one O atom of O_2 with two electrons from NH_3 and the insertion of O into NH_3. The second O atom is reduced to H_2O with two electrons that are generated during further oxidation of NH_2OH.

Hydroxylamine oxidoreductase (Hao) mediates the oxidation of NH_2OH to NO_2^- resulting in the formation of four electrons. Two electrons are returned to Amo. The remaining two electrons are available for O_2-respiration to generate a proton gradient for ATP-synthesis and for the formation of NADH by reverse electron flow used as reducing equivalents for CO_2-fixation (5).

Several studies have demonstrated the production of NO and N_2O by pure cultures of AOB (60, 71, 107), but the mechanism is not completely understood. Generally, two different pathways are inferred (Figure 8). First, the catalytic cycle of Hao involves NO as an intermediate, which may lead to NO and N_2O release under certain physiological conditions (52). Second, the activity of nitrifier-encoded Nir and Nor reduces NO_2^- to NO and N_2O, termed nitrifier denitrification (12, 96, 102). In both pathways, O_2 and NH_4^+ are required to form NH_2OH as a substrate for Hao and as the electron donor for NO_2^- reduction. The activity of Nir and Nor is thought to confer tolerance to NO_2^- and NO that are produced during NH_4^+-metabolism. This is supported by genetic experiments showing that Nir expression in the AOB model organisms *Nitrosomonas europaea* was less repressed by the NO_2^- responsive regulator (NsrR) at increasing levels of NO_2^- (8).

Aerobic nitrite oxidation

The second step of nitrification is performed by chemolithoautotrophic nitrite-oxidizing bacteria (NOB), which are phylogenetically unrelated to AOB. NOB cluster mainly within the alpha-, gamma and delta-subclass of Proteobacteria, except for *Nitrospira*, which represents its own phylum (124). The key-step in NO_2^--oxidation is mediated by nitrite oxidoreductase (Nxr), which oxidizes NO_2^- to NO_3^- (Figure 9). The resulting electrons are used for O_2-respiration to generate a proton gradient for ATP-synthesis and for the synthesis of NADH by reverse electron flow used as reducing equivalents for CO_2-fixation (34).
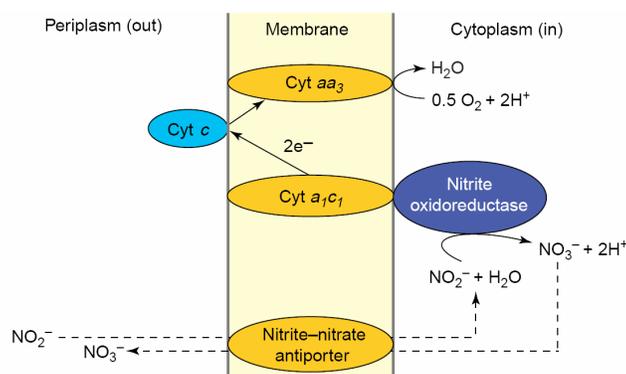
Figure 9. Simplified scheme of the aerobic energy metabolism of nitrite-oxidizing bacteria of the genus Nitrobacter. Energy is conserved by proton translocation by Cyt *aa3* creating a proton motive force. Abbreviations: Cyt, cytochrome. Taken from Costa et al. (21).

NOB form NO and N_2O under anaerobic conditions in the presence of NO_3^- and pyruvate. Here, Nxr functions in reverse direction mediating NO_3^- reduction to NO_2^- (35). NOB actively express NirK, which co-purifies with Nxr, in the presence of NO_2^- and if O_2 concentrations are low (1, 115). Nitric oxide generated by NOB-NirK is thought to direct cellular electron flux either toward O_2 respiration at high O_2 concentrations or toward NADH synthesis by reversibly inhibiting cytochrome oxidase at low O_2 concentrations (115).

NO and N_2O formation in mixed microbial communities

Environmental significance

Nitric oxide and N_2O are atmospheric trace gases that influence atmospheric chemistry and the greenhouse effect, which fostered investigations of NO and N_2O emissions from various environments. Large amounts of NO are formed in the stratosphere by photo-oxidation of biologically produced N_2O, which is mainly emitted from the ocean and soils (23, 116). In the stratosphere, NO and NO_2 determine the earth ozone (O_3) distribution by participating in a set of reactions that transfer O_3 to O_2. Conversely, high NO concentrations in the troposphere mainly result from combustion of fossil fuels and

lead to production of O_3 *via* photochemical smog reactions (23). Substantial amounts of atmospheric NO are formed from N_2 and O_2 by lightning discharge (137).

Besides being a stratospheric source for NO, N_2O is a potent greenhouse gas displaying a steadily increasing atmospheric concentration (Figure 10) (116). The infrared radiative forcing of one N_2O molecule is 206 times that of one CO_2 molecule resulting overall in a 6% contribution of N_2O to the anthropogenic greenhouse effect, despite its low atmospheric concentration (~310 ppbv) (116). Current estimates of the N_2O budget contain large uncertainties with respect to the sources, impairing effective strategies to mitigate its further increase in atmospheric concentrations.
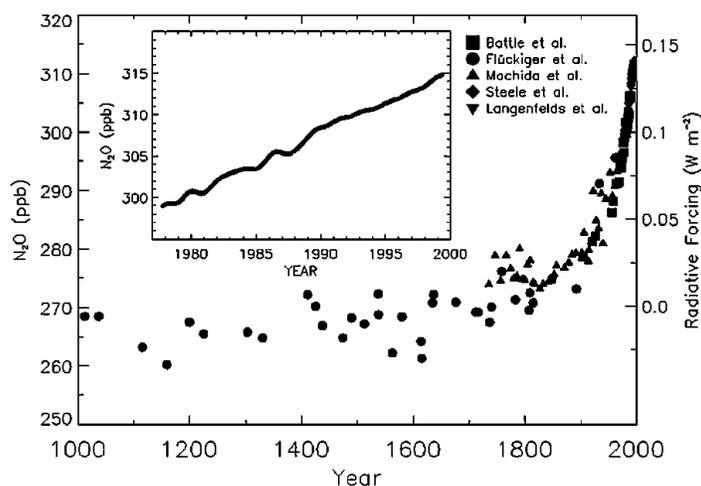
Figure 10. Change in N_2O abundance for the last 1,000 years as determined from ice cores, firn, and whole air samples. Graph is compiled from different data sets as referenced in IPCC. Radiative forcing, approximated by a linear scale, is plotted on the right axis. Deseasonalised global averages are plotted in the inset. Taken from IPCC (55).

Soils

Soils contribute 70 % and 20 % to the global N_2O and NO emissions, respectively (18). Soils exposed to intense agriculture account for 50 % of the anthropogenic N_2O emissions (116). Nitrification, denitrification and acidic decomposition of NO_2^- are the major processes that contribute to NO and N_2O emissions from soil. Emission of NO and

N_2O is affected by N-content, temperature, soil texture, water content (i.e. oxygenation) and pH (19, 42). These different factors are thought to influence the pathways that mediate NO and N_2O turnover. However, in studies with whole soils the assignment of NO and N_2O formation to nitrification and denitrification is usually problematic, because of the coupled nature of the two processes, acetylene as an inhibitor affects both processes and micro-environmental concentrations remain unknown (19, 42, 60, 82).

Oceans

Measurements of NO in seawater are rare, because concentrations are low and turnover is fast due to its reactivity. However, Zafiriou et al. (140) found that surface water of the central equatorial Pacific is a NO source to the atmosphere. Here, NO is formed by photolysis of NO_2^- during daytime and reaches concentrations in the picomolar range. Moreover, NO is formed by microbial processes in the O_2 minimum zone of the eastern tropical North Pacific (133). Here, maximum NO turnover and concentration coincide with low O_2 concentrations (10 – 100 μM) and some nitrification activity overlying the O_2 minimum zone. In contrast, NO turnover and concentrations are low in the core of the O_2 minimum zone. The exact source of NO remained unidentified, but it was hypothesized that nitrifiers produce NO under reduced O_2 concentrations and that denitrifiers establish rather low NO concentrations in the core of the O_2 minimum zone. This study was performed before the discovery of anammox and crenarchaeal ammonium oxidation, which changed the concepts for the marine N-cycle (33). Thus, linking marine NO production to anammox and NH_4^+-oxidizing Crenarchaeota would be of interest for future studies. Furthermore, NO may be produced by diatoms, which use NOS-derived NO as signalling molecule in a stress surveillance system (128). Thus, NO production by diatoms might occur especially during bloom formation, which has not been investigated so far.

Nitrous oxide in the ocean has been studied since more than 4 decades (22). Commonly, large areas of the ocean are thought to be in equilibrium with the atmosphere, but regions

of O_2 depletion are significant sources of N_2O (30). In O_2 minimum zones, N_2O is generally produced to concentrations in the nanomolar range as O_2 reaches low concentrations (17, 85, 86, 136). Drastic increases of N_2O concentrations were observed in surface water of the Arabian Sea as a result of intensifying anoxia (84). High N_2O accumulation was explained with frequent, turbulence-induced aeration of suboxic surface water. These O_2 perturbations may lead to increased formation of intermediates by processes that produce N_2O. Likewise, O_2 fluctuations, induced by the El Nino-Southern oscillation, have been proposed to affect N_2O emission from the O_2 minimum zone of the eastern South Pacific (17). Responsible processes for N_2O formation in the sea cannot unequivocally be determined. The correlation between excess N_2O and O_2 depletion (i.e. both in relation to the expected saturation under atmospheric conditions) or between excess N_2O and increased NO_3^- concentrations is generally used as an indicator for nitrification (30, 132). However, problems may arise if denitrification occurs under aerobic conditions or in anoxic micro-niches within particles (136).

Sediments

High resolution concentrations profiles of NO have not been reported in sediments before this thesis. Thus, an aim of this thesis was the development of a NO microsensor suitable for profiling in sediments (chapter 2). Nitrous oxide microsensors are available already (2), however, their use has long been restricted to study denitrification potentials in sediments with the acetylene block technique. More recently, two studies used N_2O microsensors to study N_2O emissions from mangrove and estuary (Weser) sediments without addition of acetylene (79, 87). These studies showed that denitrification and nitrification contributed to N_2O formation in distinct sediment strata if subjected to high nutrient input. In mangrove sediments, N_2O production by nitrification was stimulated by NH_4^+, whereas N_2O production by denitrification was stimulated by NO_3^-. Although denitrification produced more N_2O, nitrification was more important for sediment N_2O emission. Nitrification produced N_2O closer to the surface, which decreased the fraction of N_2O that could be consumed within the sediment (79). In sediments of the Weser

estuary, anaerobic N_2O production was stimulated by NO_3^- addition and salinity changes. Specifically, high N_2O production was shown to be a transient phenomenon. In chapter 3 of this thesis the mechanisms of transient NO and N_2O formation upon perturbations has been studied and modelled in a biofilm displaying nitrifying and denitrifying activity.

Waste water treatment plants

Waste water treatment plants (WWTP) have a high throughput of nitrogen. Thus, sewage treatment is a source for NO and N_2O emission to the atmosphere. Nitric oxide and N_2O formation has been shown for mixed microbial communities from a sewage treatment background under nitrifying and denitrifying conditions (39, 56, 57, 123, 130). Decreased O_2, and increased NO_2^- and NH_4^+ concentrations were major factors that increased NO and N_2O emissions.
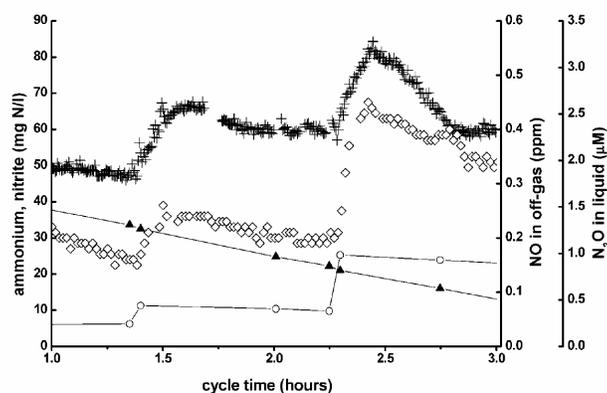
Figure 11. Dynamic NO and N_2O emission of nitrifying biomass exposed to sudden NO_2^- pulses under oxic conditions in the presence of NH_4^+. NO (open diamonds), N_2O (crosses), NO_2^- (open circles), and NH_4^+ (filled triangles). Taken from Kampschreur et al. (56).

Kampschreur et al. (56, 57) found that NO and N_2O emissions change dynamically if exposed to sudden changes of O_2, NO_2^- and NH_4^+ concentrations (Figure 11). Thus, emissions will be underestimated if relying on point samples, because it is a common practice in WWTP to subject sewage to dynamic changes. Nitrifier denitrification was discussed to be the main process responsible for NO and N_2O production.

Nitric oxide and N_2O formation were significantly higher in the nitrification unit of a full-scale reject water treatment, which consisted of a nitrification and an anammox reactor in sequence (57). Microbial communities in sewage are commonly aggregated and display micro-environments, but investigations into NO and N_2O formation by those aggregates relies on the measurement in the head space or in the bulk liquid. In contrast, the study presented in chapter 3 uses NO and N_2O microsensors to investigate an aggregated (biofilm) microbial community with nitrifying and denitrifying activity grown from WWTP sludge. This study elucidates the pathways of NO and N_2O formation under different conditions based on activity measurements with high spatial resolution. Moreover, mechanisms for transient NO and N_2O formation upon changes in O_2 and NO_2^- are inferred from measurements with high temporal resolution.

Humans and animals

Microorganisms are associated to humans and can be found in the mouth, the stomach, intestines, vagina, ear and lungs (27). Air emitted from the human mouth is enriched with NO and N_2O relative to the atmosphere. Nitrous oxide was measured in exhaled air rendering stomach, lung, airway and mouth as possible source areas (11, 80, 99). In contrast, mouth NO production was unequivocally shown by incubating air exclusively in the mouth (29). Furthermore, it has been demonstrated that bacteria located on the rat tongue reduce salivary NO_3^- to NO_2^- (29, 69), which in turn accumulates in saliva (16, 45, 135). Upon swallowing, this NO_2^- enters the blood exerting important physiological functions (as discussed on page 4). Moreover, it has been hypothesized that salivary NO_2^- is chemically reduced to NO in acidic micro-environments within dental plaque (29). In chapter 4 it is shown that dental plaque performs denitrification leading to biological production of NO and N_2O. Microbial communities in dental plaque, as opposed to those on the tongue, are the major site for N_2O production and thus nitrogen conversions in the human mouth.

Nitrous oxide formation by animal-associated microorganisms has been demonstrated in earthworms and aquatic macrofauna due to the activity of ingested soil and sediment, respectively (53, 117). In both cases, the gut represents an anoxic micro-environment that stimulates denitrification. Moreover, for aquatic macrofauna molecular evidence indicated that expression of N_2O reductase lacks behind the expression of other denitrification enzymes leading to accumulation of N_2O during the short gut residence time of sediment of 2 to 3 h (117).

Microbial Biofilms

Definition and characteristics of biofilms

The focus of this thesis was to study the mechanisms of NO formation in microbial biofilms. Biofilms are matrix-enclosed microbial communities that adhere to biotic or abiotic surfaces or float as aggregates in water (47). Biofilms occur on virtually every surface that is exposed to non-sterile water. Hence, biofilms are present in every natural and man-made ecosystem, and thus are important for biogeochemical cycling, biotechnological applications and health-related aspects. Development of biofilms proceeds as a regulated sequence, including (i) the initial, reversible and irreversible adhesion; (ii) the aggregation of cells into microcolonies; (iii) growth with subsequent maturation; and (iv) detachment of cells from the biofilm by active dispersal and passive mechanical processes. The structure of biofilms is influenced by many factors, including nutrient supply, characteristics of the surface, hydrodynamic regime and cell-to-cell signalling events (26). The biofilm mode of growth offers several advantages to microorganisms. Biofilms provide a degree of environmental stability, protection from grazing and toxic substances in the bulk water, division of metabolic labour between cells in close proximity and more micro-niches that can be occupied by microorganisms than in the water phase.

Analysis of biofilms with microsensors

Micro-environments in biofilms develop due to mass transfer resistance of the biofilm matrix and microbial activity, which leads to chemical gradients (stratification) within biofilms (26). Mass transfer in biofilms proceeds by diffusion; however, some biofilms have voids, which allow advective transport. Stratification, micro-environmental concentrations and microbial activity can be studied with microsensors, which allow concentration measurements with high spatial resolution of solutes in biofilms. The shape of microprofiles depends on transport and microbial activity. The liquid above the biofilm is well mixed by advective transport. A boundary layer develops adjacent to the biofilm surface, where transport processes change gradually from advection to diffusion. This causes transport out of and into the biofilm to be driven by diffusion through a diffusive boundary layer. Assuming diffusive conditions, the local transport in each point of a concentration profile can be described by Fick's 1st law

$$J = D\frac{\partial c}{\partial z}, \qquad (6)$$

where J is the flux (mol m^{-2} s^{-1}), D is the diffusion coefficient (m^2 s^{-1}), ∂c is the change in concentration (mol m^{-3}) over a distance ∂z (m). Local conversion rates are equal to transport in steady state. This allows the description of microbial activity in a biofilm layer assuming a constant D, and planar geometry by

$$r = -D\frac{\partial^2 c}{\partial z^2}, \qquad (7)$$

where r is the local conversion rate (mol m^{-3} s^{-1}) at depth z.

Nitrifying biofilms

Biofilm formation of different AOB pure cultures is induced when liquid NO concentrations increase by 10-60 nM depending on the species (101). In contrast, NO concentrations below 10 nM favour AOB to thrive in the planktonic state. Multi-species nitrifying biofilms that developed in sewage treatment reactors have been studied in great detail by combining microsensor measurements with fluorescence in situ hybridisation (FISH) (103). Most of these studies indicated that AOB and NOB are closely associated to each other (Figure 12) and their activity is mainly regulated by the availability of O_2. This close association is thought to minimize the diffusional distance of NO_2^-, which is a product of AOB and a substrate for NOB.
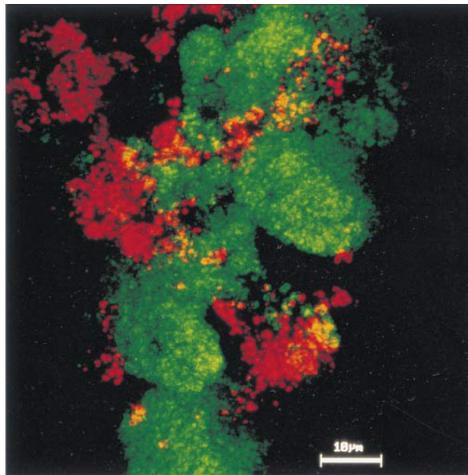
Figure 12. Dense associations of AOB and NOB in nitrifying biofilms. Confocal laser scanning micrograph from a trickling filter of an aquaculture water recirculation system hybridized with probes specific for AOB (Neu23a, green) including *Nitrosomonas europaea* and *Nitrosomonas eutropha* and NOB including *Nitrobacter* spp. (NIT2 and NIT3, red). Taken from Schramm (104).

Cell densities of nitrifiers are highest in the oxic part of the biofilm; however, nitrifiers also inhabit permanently anoxic parts of biofilms and sediments. Moreover, the combined FISH-microsensor approach in nitrifying biofilms of low complexity allowed determination of cell-specific conversion rates and affinity constants of cultured and uncultured nitrifiers in their natural environment. Gieseke et al. (40) observed that NO_2^-

and NO_3^- formation did not account for the uptake of O_2 and NH_4^+ in a nitrifying biofilm form a sequencing batch reactor, which was exposed to varying O_2 concentration during its development. It was suggested that nitrifier denitrification accounted for NO_2^--uptake, resulting in a decreased gross NO_x production rate as opposed to the net rate. In chapter 3 it is shown that high NO_2^- concentrations can induce N-loss by nitrifier denitrification in nitrifying biofilms and that this enhances the formation of NO and N_2O.

Dental biofilms

Dental plaque is an example of both a biofilm and a microbial community (76). Culture-dependent and culture-independent methods estimate 500 to 700 different bacterial species being present in the oral cavity (64, 66). Cultured species account for up to 60 % of the species identified with molecular methods rendering plaque a well characterized microbial community (64). The habitat of dental biofilms comprises the tooth and the gingival tissue (Figure 13). Hence, plaque is distinguished in subgingival and supragingival dental plaque. Supragingival dental plaque is formed on the outwardly visible enamel (the primary mineral is hydroxyapatite, a crystalline calcium phosphate) surface of teeth and is commonly implicated with dental caries. In contrast, subgingival plaque is comprised of a biofilm that forms below the gum line and is commonly implicated in the development of periodontal diseases and root surface caries (64, 106).

Dental caries is the most prevalent chronic disease worldwide, which is defined as the localized destruction of dental hard tissues by demineralization due to acid by-products from bacterial fermentation of dietary carbohydrates (106). Dental caries results from an ecological imbalance in the equilibrium between tooth minerals and microbial biofilms that colonize the tooth. The proportion of acidogenic and acid-tolerating microorganisms (streptococci and lactobacilli) increases in cariogenic biofilms, which leads to locally low pH conditions favoring enamel demineralization, preventing enamel remineralization and leading to the disappearance of microorganisms associated to healthy teeth (76, 106).
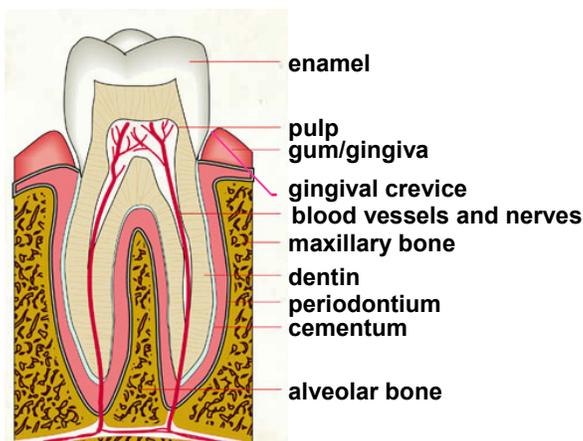
Figure 13. Section through a tooth that shows the architecture and surrounding tissues anchoring the tooth in the gum. Dental plaque can accumulate on the enamel surface or in the gingival crevice. Modified from www.infovisual.info.

Periodontal diseases are disorders of tissues surrounding the teeth that are caused by dental biofilms forming adjacent to the teeth. Periodontal diseases encompass gingivitis; a mild, reversible inflammatory disorder, and periodontitis; a strong inflammatory disorder that extends deeply into tissue leading to tissue, teeth and bone loss (94). Periodontal diseases are associated with a general increase in biofilm around the gingival margin, which elicits an inflammatory host response including an increased flow of gingival crevicular fluid. This creates a nutritionally rich micro-environment in the periodontal pocket supporting the growth of obligatory anaerobic bacteria with proteolytic activity and an increase in local pH (76). Nitric oxide plays a complex, not well understood role in periodontal diseases, because they are inflammatory disorders (15, 59). On the one hand, NO regulates functions of cells involved in inflammatory processes (13). On the other hand, bacterial lipopolysaccharides stimulate production of pro-inflammatory cytokines, which induce production of high, cytotoxic NO concentrations by certain immune cells. Furthermore, high NO levels during inflammation may induce expression of matrix metalloproteinases in neutrophiles (white blood cells), which mediates soft tissue degradation (126).

Periodontal diseases and dental caries are diseases that are not caused by a single pathogen, but by a microbial community in a specific environment. The concept of the 'ecological plaque hypothesis' has been formulated to explain the onset of both diseases as a result of environmental perturbations that select for bacteria in the plaque, which favor environmental conditions detrimental to health (76). These bacteria further shape the environment leading to their manifestation and to selective disadvantages for other bacteria.

Understanding of dental biofilm functions has mainly focused on determining the conditions under which specific bacteria are present in dental plaque and relating this information to physiological investigations of cultured plaque bacteria. Co-culture experiments and genetic manipulation revealed a great deal of interactions between plaque bacteria based on metabolic products, co-aggregation and signaling compounds (64, 66). Direct assessments of dental plaque were mainly restricted to investigating the structure and composition with microscopic techniques. Physiological investigations with dental plaque microbial communities have been done with regard to *in situ* pH levels (131, 141). More recently, quantitative gene expression studies have linked periodontal disease with the presence of hydrogenotrophic microbes (methanogenic Archaea, sulphate-reducing bacteria and acetogenic bacteria) (68, 129). However, also these studies did not perform direct physiological measurements of H_2-uptake, CH_4 or H_2S formation. The study presented in chapter 4 shows direct physiological measurements of N-metabolism in dental plaque. The study shows that dental plaque performs denitrification, which leads to NO and N_2O formation within dental plaque.

Detection of NO in biological systems

Nitric oxide can be detected by a range of methods that are based on *ex situ* or *in situ* measurement of NO reaction products, such as NO_2^- and NO_3^- or NO itself. *Ex situ* methods rely on the measurement of samples taken from the examined biological system,

whereas *in situ* methods detect NO or NO-adducts within the examined system. *Ex situ* methods involve the Griess reaction (105), the oxyhemoglobin reaction (32), gas-chromatographic detection, electron paramagnetic resonance spectroscopy (50) and the chemiluminescence assay employing so called NO_x-analyzers (78). Most data in NO research are collected using *ex situ* methods and should, thus, be analyzed carefully for artifacts or overseen reactions (10).

In situ detection of NO is restricted to the electrochemical oxidation of NO on a polarized electrode (10) and to the imaging of NO using fluorescein-based dyes (63, 70). Until now, only few microbiologists have addressed research questions in microbial ecology with *in situ* methods for NO detection. However, application of electrochemical microsensors for *in situ* measurements of compounds other than NO revealed the existence of stratified micro-environments in microbial habitats like biofilms, sediments and soils, where concentrations of certain compounds might change drastically due to high local conversion rates and limited transport processes (26). *Ex situ* methods are limited in their ability to detect these processes. NO is a versatile and reactive molecule, which makes it very likely to be involved in localized processes of production and consumption. Hence, chapter 2 of this thesis will describe the development and first application of an electrochemical NO microsensor that is suited for *in situ* measurements in stratified microbial communities, such as biofilms and sediments.

NO microsensors

Amperometric sensing of NO is commonly achieved by the oxidation of NO at a working electrode polarized with 0.7 - 0.9 V vs. a reference electrode (Ag/AgCl or Calomel) leading to the anodic reaction.

$$NO + 2\ H_2O - 3e^- \rightarrow NO_3^- + 4\ H^+ \tag{8}$$

The resulting current is proportional to the NO concentration and can be detected as the analytical signal. The alternative electro-reductive approach is undesirable, due to the similar physicochemical properties of O_2 and NO that would lead to interference of O_2 with the measurements (10). Electrodes are reported as single anode-type electrodes or as combined sensors (Figure 14). In combined sensors, reference electrode and sensing electrode are placed together in an internal electrolyte compartment that is separated from the sample by a water repellent membrane, whereas single anode-type electrodes use the aqueous sample as an electrolyte to complete the measuring circuit by submerging an external reference electrode into it. Typical anode materials are carbon fiber (75), platinum (Pt) (67, 109), glassy carbon (91) and gold (9). NO sensing electrodes are usually modified with one or more coatings and membranes to facilitate the selectivity against common interferences.
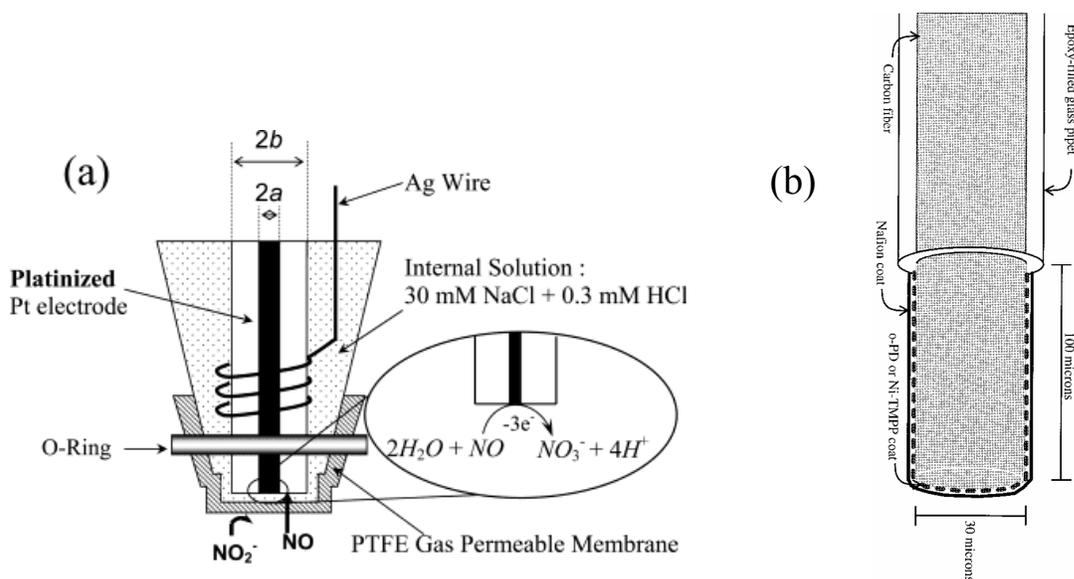
Figure 14. Combined (a) and the single anode-type (b) NO sensors. **(a)** the combined sensor (taken from Lee et al. (67)) has an Ag-wire as reference electrode inserted in an internal electrolyte, which is shielded from the sample by a PTFE membrane. The platinized Pt-disc is 76 µm (2a) and the inner glass barrel is 150 µm (2b), while the outer sleeve is ~1 mm wide. **(b)** The single anode microsensor (taken from Friedemann et al. (36)) is a carbon fiber electrode, which is exposed to the sample medium that is also used as electrolyte to complete the measuring circuit to an external reference electrode (not shown). Selectivity is achieved by coating the carbon fiber with various polymeric films.

Charged interferences like NO_2^- and ascorbate are typically repelled by constructing combined sensors with hydrophobic, gas permeable membranes like chloroprene (108), PTFE (Teflon™) (67), sol-gels (109) or polystyrene (62), or by depositing Nafion™ on single anode-type electrodes (75). The widely used Nafion is a polysulfonated PTFE that carries intrinsic negative charges, thereby acting as a cation exchanger. It can be cast from alcoholic solutions forming a gas permeable, conducting hydrogel (77). In the electro-oxidation of NO, the polyanionic nature of Nafion is believed to stabilize NO^+ as the primary oxidation product, thereby reducing the detected current (75). Non-charged interferences like catecholamines (neurotransmitters, e.g. serotonin) are repelled by non-conducting polymeric phenylendiamine (36). In addition, surface modifications with various polymeric metalloporphyrin films contribute to increased sensitivity (75).

Low detection limit and high sensitivity are required for NO sensors, because NO is usually present at sub-micromolar concentrations. This is mostly achieved by constructing sensors with a big sensing surface. In this respect it must be mentioned that even though in many publications tip diameters in the low micrometer range are stated, the length of the sensing tip is rarely reported. Comparably, sensors with disc surfaces have usually wider diameters starting from 50 μm up to 2 mm. Long microsensors are not applicable for profiling stratified microbial systems like biofilms, because the concentration of the analyte might change along the sensing surface. The obtained signal is then an integrated measure of the concentrations along the electrode. Comparably, wide disc-shaped electrodes are also problematic for profiling applications, since the step size of different measurement points in the profile should not be smaller than 2 times the diameter of the electrode (25). By employing a disc shaped electrode with 100 μm diameter it would be possible to confidently measure NO concentrations at two different depths in a 200 μm thick biofilm. Thus, a major challenge within this thesis was the construction of the NO microsensor that allows the profiling at high spatial resolution with a sensitivity that is still able to detect NO changes relevant in microbial communities.

Aim of the thesis

The aim of this thesis was to develop a NO microsensor suitable for measurements with high spatial and temporal resolution in microbial biofilms and sediments. The application of the microsensor was focused on studying NO formation in biofilms composed of complex microbial communities that carry out reactions of the N-cycle. The specific aims were first, to quantify the micro-environmental NO concentrations to which N-cycling communities are exposed under different conditions and to understand the factors that control NO accumulation; second, to determine the N-cycle pathways that contribute to NO formation; and third, to obtain insights into the regulatory mechanisms that control transient NO accumulation, which is significant for emission of NO and N_2O to the atmosphere. The studied biofilms were chosen to highlight the broad significance of NO formation by N-cycle reactions. The environmental significance was studied focusing on the mechanisms underlying transient NO and N_2O formation under varying conditions in a biofilm, where nitrification and denitrification occur. The significance for humans and human-associated microbial communities was shown in dental biofilms, where NO and N_2O are formed by denitrification.

References

1.   **Ahlers, B., W. Konig, and E. Bock.** 1990. Nitrite Reductase-Activity in Nitrobacter-Vulgaris. Fems Microbiology Letters **67:**121-126.
2.   **Andersen, K., T. Kjaer, and N. P. Revsbech.** 2001. An oxygen insensitive microsensor for nitrous oxide. Sensors and Actuators B-Chemical **81:**42-48.
3.   **Anjum, M. F., T. M. Stevanin, R. C. Read, and J. W. B. Moir.** 2002. Nitric oxide metabolism in Neisseria meningitidis. Journal of Bacteriology **184:**2987-2993.
4.   **Armor, J. N.** 1974. Influence of Ph and Ionic-Strength Upon Solubility of No in Aqueous-Solution. Journal of Chemical and Engineering Data **19:**82-84.
5.   **Arp, D. J., and L. Y. Stein.** 2003. Metabolism of inorganic N compounds by ammonia-oxidizing bacteria. Critical Reviews in Biochemistry and Molecular Biology **38:**471-495.
6.   **Barraud, N., D. J. Hassett, S. H. Hwang, S. A. Rice, S. Kjelleberg, and J. S. Webb.** 2006. Involvement of nitric oxide in biofilm dispersal of Pseudomonas aeruginosa. Journal of Bacteriology **188:**7344-7353.
7.   **Baumann, B., M. Snozzi, A. J. B. Zehnder, and J. R. vanderMeer.** 1996. Dynamics of denitrification activity of Paracoccus denitrificans in continuous culture during aerobic-anaerobic changes. Journal of Bacteriology **178:**4367-4374.
8.   **Beaumont, H. J. E., S. I. Lens, W. N. M. Reijnders, H. V. Westerhoff, and R. J. M. van Spanning.** 2004. Expression of nitrite reductase in Nitrosomonas europaea involves NsrR, a novel nitrite-sensitive transcription repressor. Molecular Microbiology **54:**148-158.
9.   **Bedioui, F., S. Trevin, and J. Devynck.** 1994. The Use of Gold Electrodes in the Electrochemical Detection of Nitric-Oxide in Aqueous-Solution. Journal of Electroanalytical Chemistry **377:**295-298.
10.   **Bedioui, F., and N. Villeneuve.** 2003. Electrochemical nitric oxide sensors for biological samples - Principle, selected examples and applications. Electroanalysis **15:**5-18.
11.   **Bleakley, B. H., and J. M. Tiedje.** 1982. Nitrous-Oxide Production by Organisms Other Than Nitrifiers or Denitrifiers. Applied and Environmental Microbiology **44:**1342-1348.
12.   **Bock, E., I. Schmidt, R. Stuven, and D. Zart.** 1995. Nitrogen Loss Caused by Denitrifying Nitrosomonas Cells Using Ammonium or Hydrogen as Electron-Donors and Nitrite as Electron-Acceptor. Archives of Microbiology **163:**16-20.
13.   **Bogdan, C.** 2001. Nitric oxide and the immune response. Nature Immunology **2:**907-916.
14.   **Bredt, D. S., and S. H. Snyder.** 1994. Nitric-Oxide - a Physiological Messenger Molecule. Annual Review of Biochemistry **63:**175-195.
15.   **Brennan, P. A., G. J. Thomas, and J. D. Langdon.** 2003. The role of nitric oxide in oral diseases. Archives of Oral Biology **48:**93-100.

16. **Carossa, S., P. Pera, P. Doglio, S. Lombardo, P. Colagrande, L. Brussino, G. Rolla, and C. Bucca.** 2001. Oral nitric oxide during plaque deposition. European Journal of Clinical Investigation **31:**876-879.

17. **Castro-Gonzalez, M., and L. Farias.** 2004. N2O cycling at the core of the oxygen minimum zone off northern Chile. Marine Ecology-Progress Series **280:**1-11.

18. **Conrad, R.** 1995. Soil Microbial Processes and the Cycling of Atmospheric Trace Gases. Philosophical Transactions of the Royal Society of London Series a-Mathematical Physical and Engineering Sciences **351:**219-230.

19. **Conrad, R.** 1996. Soil microorganisms as controllers of atmospheric trace gases (H-2, CO, CH4, OCS, N2O, and NO). Microbiological Reviews **60:**609-&.

20. **Corker, H., and R. K. Poole.** 2003. Nitric oxide formation by Escherichia coli - Dependence on nitrite reductase, the NO-sensing regulator FNR, and flavohemoglobin Hmp. Journal of Biological Chemistry **278:**31584-31592.

21. **Costa, E., J. Perez, and J. U. Kreft.** 2006. Why is metabolic labour divided in nitrification? Trends in Microbiology **14:**213-219.

22. **Craig, H., and L. I. Gordon.** 1963. Nitrous Oxide in the Ocean and the Marine Atmosphere. Geochimica Et Cosmochimica Acta **27:**949-955.

23. **Crutzen, P. J.** 1979. Role of No and No2 in the Chemistry of the Troposphere and Stratosphere. Annual Review of Earth and Planetary Sciences **7:**443-472.

24. **Cutruzzola, F.** 1999. Bacterial nitric oxide synthesis. Biochimica Et Biophysica Acta-Bioenergetics **1411:**231-249.

25. **de Beer, D.** 1998. Use of Microelectrodes to measure in situ microbial activities in biofilm, sediments and microbial mats, Molecular Microbial Ecology, vol. 8.1.3. Kluwer Academic Publishers.

26. **de Beer, D., and P. Stoodley.** 2006. Microbial Biofilms. *In* M. Dworkin (ed.), The Prokaryotes, vol. 2. Springer.

27. **Dethlefsen, L., M. McFall-Ngai, and D. A. Relman.** 2007. An ecological and evolutionary perspective on human-microbe mutualism and disease. Nature **449:**811-818.

28. **Dixon, R., and D. Kahn.** 2004. Genetic regulation of biological nitrogen fixation. Nature Reviews Microbiology **2:**621-631.

29. **Duncan, C., H. Dougall, P. Johnston, S. Green, R. Brogan, C. Leifert, L. Smith, M. Golden, and N. Benjamin.** 1995. Chemical Generation of Nitric-Oxide in the Mouth from the Enterosalivary Circulation of Dietary Nitrate. Nature Medicine **1:**546-551.

30. **Elkins, J. W., S. C. Wofsy, M. B. McElroy, C. E. Kolb, and W. A. Kaplan.** 1978. Aquatic Sources and Sinks for Nitrous-Oxide. Nature **275:**602-606.

31. **Fang, F. C.** 2004. Antimicrobial reactive oxygen and nitrogen species: Concepts and controversies. Nature Reviews Microbiology **2:**820-832.

32. **Feelisch, M., and E. A. Noack.** 1987. Correlation between Nitric-Oxide Formation During Degradation of Organic Nitrates and Activation of Guanylate-Cyclase. European Journal of Pharmacology **139:**19-30.

33. **Francis, C. A., J. M. Beman, and M. M. M. Kuypers.** 2007. New processes and players in the nitrogen cycle: the microbial ecology of anaerobic and archaeal ammonia oxidation. Isme Journal **1:**19-27.

34. **Freitag, A., and E. Bock.** 1990. Energy-Conservation in Nitrobacter. Fems Microbiology Letters **66:**157-162.

35. **Freitag, A., M. Rudert, and E. Bock.** 1987. Growth of Nitrobacter by Dissimilatoric Nitrate Reduction. Fems Microbiology Letters **48:**105-109.

36. **Friedemann, M. N., S. W. Robinson, and G. A. Gerhardt.** 1996. o-phenylenediamine-modified carbon fiber electrodes for the detection of nitric oxide. Analytical Chemistry **68:**2621-2628.

37. **Gardner, A. M., R. A. Helmick, and P. R. Gardner.** 2002. Flavorubredoxin, an inducible catalyst for nitric oxide reduction and detoxification Escherichia coli. Journal of Biological Chemistry **277:**8172-8177.

38. **Gardner, P. R., A. M. Gardner, L. A. Martin, and A. L. Salzman.** 1998. Nitric oxide dioxygenase: An enzymic function for flavohemoglobin. Proceedings of the National Academy of Sciences of the United States of America **95:**10378-10383.

39. **Garrido, J. M., J. L. Campos, R. Mendez, and J. M. Lema.** 1997. Nitrous oxide production by nitrifying biofilms in a biofilm airlift suspension reactor. Water Science and Technology **36:**157-163.

40. **Gieseke, A., L. Bjerrum, M. Wagner, and R. Amann.** 2003. Structure and activity of multiple nitrifying bacterial populations co-existing in a biofilm. Environmental Microbiology **5:**355-369.

41. **Gilberthorpe, N. J., and R. K. Poole.** 2008. Nitric oxide homeostasis in Salmonella typhimurium - Roles of respiratory nitrate reductase and flavohemoglobin. Journal of Biological Chemistry **283:**11146-11154.

42. **Godde, M., and R. Conrad.** 2000. Influence of soil properties on the turnover of nitric oxide and nitrous oxide by nitrification and denitrification at constant temperature and moisture. Biology and Fertility of Soils **32:**120-128.

43. **Gomes, C. M., A. Giuffre, E. Forte, J. B. Vicente, L. M. Saraiva, M. Brunori, and M. Teixeira.** 2002. A novel type of nitric-oxide reductase - Escherichia coli flavorubredoxin. Journal of Biological Chemistry **277:**25273-25276.

44. **Goretski, J., O. C. Zafiriou, and T. C. Hollocher.** 1990. Steady-State Nitric-Oxide Concentrations During Denitrification. Journal of Biological Chemistry **265:**11535-11538.

45. **Govoni, M., E. A. Jansson, E. Weitzberg, and J. O. Lundberg.** 2008. The increase in plasma nitrite after a dietary nitrate load is markedly attenuated by an antibacterial mouthwash. Nitric Oxide-Biology and Chemistry **19:**333-337.

46. **Gow, A. J., C. R. Farkouh, D. A. Munson, M. A. Posencheg, and H. Ischiropoulos.** 2004. Biological significance of nitric oxide-mediated protein modifications. American Journal of Physiology-Lung Cellular and Molecular Physiology **287:**L262-L268.

47. **Hall-Stoodley, L., J. W. Costerton, and P. Stoodley.** 2004. Bacterial biofilms: From the natural environment to infectious diseases. Nature Reviews Microbiology **2:**95-108.

48. **Hausladen, A., R. Rafikov, M. Angelo, D. J. Singel, E. Nudler, and J. S. Stamler.** 2007. Assessment of nitric oxide signals by triiodide chemiluminescence. Proceedings of the National Academy of Sciences of the United States of America **104:**2157-2162.

49. **Hendriks, J., A. Oubrie, J. Castresana, A. Urbani, S. Gemeinhardt, and M. Saraste.** 2000. Presented at the 11th European Bioenergetics Conference (EBEC), Brighton, England, Sep 09-14.

50. **Henry, Y., and A. Guissani.** 2000. Contribution of spin-trapping EPR techniques for the measurement of NO production in biological systems. Analusis **28:**445-454.

51. **Hess, D. T., A. Matsumoto, S. O. Kim, H. E. Marshall, and J. S. Stamler.** 2005. Protein S-nitrosylation: Purview and parameters. Nature Reviews Molecular Cell Biology **6:**150-166.

52. **Hooper, A. B.** 1968. A Nitrite-Reducing Enzyme from Nitrosomonas Europaea - Preliminary Characterization with Hydroxylamine as Electron Donor. Biochimica Et Biophysica Acta **162:**49-&.

53. **Horn, M. A., A. Schramm, and H. L. Drake.** 2003. The earthworm gut: An ideal habitat for ingested N2O-producing microorganisms. Applied and Environmental Microbiology **69:**1662-1669.

54. **Ignarro, L. J., J. M. Fukuto, J. M. Griscavage, N. E. Rogers, and R. E. Byrns.** 1993. Oxidation of Nitric-Oxide in Aqueous-Solution to Nitrite but Not Nitrate - Comparison with Enzymatically Formed Nitric-Oxide from L-Arginine. Proceedings of the National Academy of Sciences of the United States of America **90:**8103-8107.

55. **IPCC.** 2001. Climate Change 2001: The Scientific Basis.

56. **Kampschreur, M. J., N. C. G. Tan, R. Kleerebezem, C. Picioreanu, M. S. M. Jetten, and M. C. M. Loosdrecht.** 2008. Effect of dynamic process conditions on nitrogen oxides emission from a nitrifying culture. Environmental Science & Technology **42:**429-435.

57. **Kampschreur, M. J., W. R. L. van der Star, H. A. Wielders, J. W. Mulder, M. S. M. Jetten, and M. C. M. van Loosdrecht.** 2008. Dynamics of nitric oxide and nitrous oxide emission during full-scale reject water treatment. Water Research **42:**812-826.

58. **Kartal, B., M. M. M. Kuypers, G. Lavik, J. Schalk, H. den Camp, M. S. M. Jetten, and M. Strous.** 2007. Anammox bacteria disguised as denitrifiers: nitrate reduction to dinitrogen gas via nitrite and ammonium. Environmental Microbiology **9:**635-642.

59. **Kendall, H. K., R. I. Marshall, and P. M. Bartold.** 2001. Nitric oxide and tissue destruction. Oral Diseases **7:**2-10.

60. **Kester, R. A., W. deBoer, and H. J. Laanbroek.** 1997. Production of NO and N2O by pure cultures of nitrifying and denitrifying bacteria during changes in aeration. Applied and Environmental Microbiology **63:**3872-3877.

61. **Kharitonov, V. G., A. R. Sundquist, and V. S. Sharma.** 1994. Kinetics of Nitric-Oxide Autoxidation in Aqueous-Solution. Journal of Biological Chemistry **269:**5881-5883.

62. **Kitamura, Y., T. Uzawa, K. Oka, Y. Komai, H. Ogawa, N. Takizawa, H. Kobayashi, and K. Tanishita.** 2000. Microcoaxial electrode for in vivo nitric oxide measurement. Analytical Chemistry **72:**2957-2962.
63. **Kojima, H., N. Nakatsubo, K. Kikuchi, S. Kawahara, Y. Kirino, H. Nagoshi, Y. Hirata, and T. Nagano.** 1998. Detection and imaging of nitric oxide with novel fluorescent indicators: Diaminofluoresceins. Analytical Chemistry **70:**2446-2453.
64. **Kolenbrander, P. E., R. N. Andersen, D. S. Blehert, P. G. Egland, J. S. Foster, and R. J. Palmer.** 2002. Communication among oral bacteria. Microbiology and Molecular Biology Reviews **66:**486-+.
65. **Konneke, M., A. E. Bernhard, J. R. de la Torre, C. B. Walker, J. B. Waterbury, and D. A. Stahl.** 2005. Isolation of an autotrophic ammonia-oxidizing marine archaeon. Nature **437:**543-546.
66. **Kuramitsu, H. K., X. S. He, R. Lux, M. H. Anderson, and W. Y. Shi.** 2007. Interspecies interactions within oral microbial communities. Microbiology and Molecular Biology Reviews **71:**653-+.
67. **Lee, Y., B. K. Oh, and M. E. Meyerhoff.** 2004. Improved planar amperometric nitric oxide sensor based on platinized platinum anode. 1. Experimental results and theory when applied for monitoring NO release from diazeniumdiolate-doped polymeric films. Analytical Chemistry **76:**536-544.
68. **Lepp, P. W., M. M. Brinig, C. C. Ouverney, K. Palm, G. C. Armitage, and D. A. Relman.** 2004. Methanogenic Archaea and human periodontal disease. Proceedings of the National Academy of Sciences of the United States of America **101:**6176-6181.
69. **Li, H., C. Duncan, J. Townend, K. Killham, L. M. Smith, P. Johnston, R. Dykhuizen, D. Kelly, M. Golden, N. Benjamin, and C. Leifert.** 1997. Nitrate-reducing bacteria on rat tongues. Applied and Environmental Microbiology **63:**924-930.
70. **Lim, M. H., D. Xu, and S. J. Lippard.** 2006. Visualization of nitric oxide in living cells by a copper-based fluorescent probe. Nature Chemical Biology **2:**375-380.
71. **Lipschultz, F., O. C. Zafiriou, S. C. Wofsy, M. B. McElroy, F. W. Valois, and S. W. Watson.** 1981. Production of No and N2o by Soil Nitrifying Bacteria. Nature **294:**641-643.
72. **Lloyd, D.** 1993. Aerobic Denitrification in Soils and Sediments - from Fallacies to Facts. Trends in Ecology & Evolution **8:**352-356.
73. **Lundberg, J. O., E. Weitzberg, J. A. Cole, and N. Benjamin.** 2004. Opinion - Nitrate, bacteria and human health. Nature Reviews Microbiology **2:**593-602.
74. **Lundberg, J. O., E. Weitzberg, and M. T. Gladwin.** 2008. The nitrate-nitrite-nitric oxide pathway in physiology and therapeutics. Nature Reviews Drug Discovery **7:**156-167.
75. **Malinski, T., and Z. Taha.** 1992. Nitric-Oxide Release from a Single Cell Measured Insitu by a Porphyrinic-Based Microsensor. Nature **358:**676-678.
76. **Marsh, P. D.** 2003. Are dental diseases examples of ecological catastrophes? Microbiology-Sgm **149:**279-294.

77. **Mauritz, K. A., and R. B. Moore.** 2004. State of understanding of Nafion. Chemical Reviews **104:**4535-4585.

78. **McMurtry, M. S., D. H. Kim, T. Dinh-Xuan, and S. L. Archer.** 2000. Measurement of nitric oxide, nitrite and nitrate using a chemiluminescence assay: an update for the year 2000. Analusis **28:**455-465.

79. **Meyer, R. L., D. E. Allen, and S. Schmidt.** 2008. Nitrification and denitrification as sources of sediment nitrous oxide production: A microsensor approach. Marine Chemistry **110:**68-76.

80. **Mitsui, T., and T. Kondo.** 1998. Effects of mouth cleansing on the levels of exhaled nitrous oxide in young and older adults. Science of the Total Environment **224:**177-180.

81. **Mohan, S. B., and J. A. Cole.** 2007. The Dissimilatory Reduction of Nitrate to Ammonia by Anaerobic Bacteria. *In* H. Bothe, S. J. Ferguson, and W. E. Newton (ed.), The Biology of the Nitrogen Cycle, 1st ed. Elsevier, Amsterdam.

82. **Morkved, P. T., P. Dorsch, and L. R. Bakken.** 2007. The N2O product ratio of nitrification and its dependence on long-term changes in soil pH. Soil Biology & Biochemistry **39:**2048-2057.

83. **Morley, N., E. M. Baggs, P. Dorsch, and L. Bakken.** 2008. Production of NO, N2O and N-2 by extracted soil bacteria, regulation by NO2- and O-2 concentrations. Fems Microbiology Ecology **65:**102-112.

84. **Naqvi, S. W. A., D. A. Jayakumar, P. V. Narvekar, H. Naik, V. Sarma, W. D'Souza, S. Joseph, and M. D. George.** 2000. Increased marine production of N2O due to intensifying anoxia on the Indian continental shelf. Nature **408:**346-349.

85. **Naqvi, S. W. A., T. Yoshinari, D. A. Jayakumar, M. A. Altabet, P. V. Narvekar, A. H. Devol, J. A. Brandes, and L. A. Codispoti.** 1998. Budgetary and biogeochemical implications of N2O isotope signatures in the Arabian Sea. Nature **394:**462-464.

86. **Nicholls, J. C., C. A. Davies, and M. Trimmer.** 2007. High-resolution profiles and nitrogen isotope tracing reveal a dominant source of nitrous oxide and multiple pathways of nitrogen gas formation in the central Arabian Sea. Limnology and Oceanography **52:**156-168.

87. **Nielsen, M., A. Gieseke, D. de Beer, and N. P. Revsbech.** 2009. Nitrate, nitrite, and nitrous oxide transformations in sediments along a salinity gradient in the Weser Estuary. Aquatic Microbial Ecology **55:**39-52.

88. **Nunoshiba, T., T. Derojaswalker, J. S. Wishnok, S. R. Tannenbaum, and B. Demple.** 1993. Activation by Nitric-Oxide of an Oxidative-Stress Response That Defends Escherichia-Coli against Activated Macrophages. Proceedings of the National Academy of Sciences of the United States of America **90:**9993-9997.

89. **Otte, S., N. G. Grobben, L. A. Robertson, M. S. M. Jetten, and J. G. Kuenen.** 1996. Nitrous oxide production by Alcaligenes faecalis under transient and dynamic aerobic and anaerobic conditions. Applied and Environmental Microbiology **62:**2421-2426.

90. **Otte, S., J. G. Kuenen, L. P. Nielsen, H. W. Paerl, J. Zopfi, H. N. Schulz, A. Teske, B. Strotmann, V. A. Gallardo, and B. B. Jorgensen.** 1999. Nitrogen,

carbon, and sulfur metabolism in natural Thioploca samples. Applied and Environmental Microbiology **65:**3148-3157.

91.   **Pallini, M., A. Curulli, A. Amine, and G. Palleschi.** 1998. Amperometric nitric oxide sensors: a comparative study. Electroanalysis **10:**1010-1016.

92.   **Palumbo, A.** 2005. Nitric oxide in marine invertebrates: A comparative perspective. Comparative Biochemistry and Physiology a-Molecular & Integrative Physiology **142:**241-248.

93.   **Park, J. Y., and Y. N. Lee.** 1988. Solubility and Decomposition Kinetics of Nitrous-Acid in Aqueous-Solution. Journal of Physical Chemistry **92:**6294-6302.

94.   **Pihlstrom, B. L., B. S. Michalowicz, and N. W. Johnson.** 2005. Periodontal diseases. Lancet **366:**1809-1820.

95.   **Poole, R. K.** 2004. Nitric oxide and nitrosative stress tolerance in bacteria. Biochemical Society Transactions **33:**176-180.

96.   **Poth, M., and D. D. Focht.** 1985. N-15 Kinetic-Analysis of N2o Production by Nitrosomonas-Europaea - an Examination of Nitrifier Denitrification. Applied and Environmental Microbiology **49:**1134-1141.

97.   **Raghoebarsing, A. A., A. Pol, K. T. van de Pas-Schoonen, A. J. P. Smolders, K. F. Ettwig, W. I. C. Rijpstra, S. Schouten, J. S. S. Damste, H. J. M. Op den Camp, M. S. M. Jetten, and M. Strous.** 2006. A microbial consortium couples anaerobic methane oxidation to denitrification. Nature **440:**918-921.

98.   **Rock, J. D., M. J. Thomson, R. C. Read, and J. W. B. Moir.** 2007. Regulation of denitrification genes in Neisseria meningitidis by nitric oxide and the repressor NsrR. Journal of Bacteriology **189:**1138-1144.

99.   **Russow, R., H. U. Neue, I. Wolf, and C. Plath.** 2002. Presented at the 3rd International Symposium on Non-CO2 Greenhouse Gases, Maastricht, Netherlands, Jan 21-23.

100. **Schmidt, I., C. Hermelink, K. de Pas-Schoonen, M. Strous, H. J. O. den Camp, J. G. Kuenen, and M. S. M. Jetten.** 2002. Anaerobic ammonia oxidation in the presence of nitrogen oxides (NOx) by two different lithotrophs. Applied and Environmental Microbiology **68:**5351-5357.

101. **Schmidt, I., P. J. M. Steenbakkers, H. J. M. op den Camp, K. Schmidt, and M. S. M. Jetten.** 2004. Physiologic and proteomic evidence for a role of nitric oxide in biofilm formation by Nitrosomonas europaea and other ammonia oxidizers. Journal of Bacteriology **186:**2781-2788.

102. **Schmidt, I., R. J. M. van Spanning, and M. S. M. Jetten.** 2004. Denitrification and ammonia oxidation by Nitrosomonas europaea wild-type, and NirK- and NorB-deficient mutants. Microbiology-Sgm **150:**4107-4114.

103. **Schramm, A.** 2003. In situ analysis of structure and activity of the nitrifying community in biofilms, aggregates, and sediments. Geomicrobiology Journal **20:**313-333.

104. **Schramm, A., L. H. Larsen, N. P. Revsbech, N. B. Ramsing, R. Amann, and K. H. Schleifer.** 1996. Structure and function of a nitrifying biofilm as determined by in situ hybridization and the use of microelectrodes. Applied and Environmental Microbiology **62:**4641-4647.

105. **Schulz, K., S. Kerber, and M. Kelm.** 1999. Reevaluation of the Griess method for determining NO/NO2- in aqueous and protein-containing samples. Nitric Oxide-Biology and Chemistry **3:**225-234.

106. **Selwitz, R. H., A. I. Ismail, and N. B. Pitts.** 2007. Dental caries. Lancet **369:**51-59.

107. **Shaw, L. J., G. W. Nicol, Z. Smith, J. Fear, J. I. Prosser, and E. M. Baggs.** 2006. Nitrosospira spp. can produce nitrous oxide via a nitrifier denitrification pathway. Environmental Microbiology **8:**214-222.

108. **Shibuki, K.** 1990. An Electrochemical Microprobe for Detecting Nitric-Oxide Release in Brain-Tissue. Neuroscience Research **9:**69-76.

109. **Shin, J. H., S. W. Weinman, and M. H. Schoenfisch.** 2005. Sol-gel derived amperometric nitric oxide microsensor. Analytical Chemistry **77:**3494-3501.

110. **Simon, J.** 2002. Enzymology and bioenergetics of respiratory nitrite ammonification. Fems Microbiology Reviews **26:**285-309.

111. **Singel, D. J., and J. S. Stamler.** 2005. Chemical physiology of blood flow regulation by red blood cells: The role of nitric oxide and S-nitrosohemoglobin. Annual Review of Physiology **67:**99-145.

112. **Spiro, S.** 2008. Metalloregulatory proteins and nitric oxide signalling in bacteria. Biochemical Society Transactions **36:**1160-1164.

113. **Spiro, S.** 2007. Regulators of bacterial responses to nitric oxide. Fems Microbiology Reviews **31:**193-211.

114. **Stamler, J. S., S. Lamas, and F. C. Fang.** 2001. Nitrosylation: The prototypic redox-based signaling mechanism. Cell **106:**675-683.

115. **Starkenburg, S. R., D. J. Arp, and P. J. Bottomley.** 2008. Expression of a putative nitrite reductase and the reversible inhibition of nitrite-dependent respiration by nitric oxide in Nitrobacter winogradskyi Nb-255. Environmental Microbiology **10:**3036-3042.

116. **Stein, L. Y., and Y. L. Yung.** 2003. Production, isotopic composition, and atmospheric fate of biologically produced nitrous oxide. Annual Review of Earth and Planetary Sciences **31:**329-356.

117. **Stief, P., M. Poulsen, L. P. Nielsen, H. Brix, and A. Schramm.** 2009. Nitrous oxide emission by aquatic macrofauna. Proceedings of the National Academy of Sciences of the United States of America **106:**4296-4300.

118. **Straub, K. L., M. Benz, B. Schink, and F. Widdel.** 1996. Anaerobic, nitrate-dependent microbial oxidation of ferrous iron. Applied and Environmental Microbiology **62:**1458-1460.

119. **Strous, M., J. A. Fuerst, E. H. M. Kramer, S. Logemann, G. Muyzer, K. T. van de Pas-Schoonen, R. Webb, J. G. Kuenen, and M. S. M. Jetten.** 1999. Missing lithotroph identified as new planctomycete. Nature **400:**446-449.

120. **Strous, M., J. J. Heijnen, J. G. Kuenen, and M. S. M. Jetten.** 1998. The sequencing batch reactor as a powerful tool for the study of slowly growing anaerobic ammonium-oxidizing microorganisms. Applied Microbiology and Biotechnology **50:**589-596.

121. **Strous, M., and M. S. M. Jetten.** 2004. Anaerobic oxidation of methane and ammonium. Annual Review of Microbiology **58:**99-117.

122. **Strous, M., E. Pelletier, S. Mangenot, T. Rattei, A. Lehner, M. W. Taylor, M. Horn, H. Daims, D. Bartol-Mavel, P. Wincker, V. Barbe, N. Fonknechten, D. Vallenet, B. Segurens, C. Schenowitz-Truong, C. Medigue, A. Collingro, B. Snel, B. E. Dutilh, H. J. M. Op den Camp, C. van der Drift, I. Cirpus, K. T. van de Pas-Schoonen, H. R. Harhangi, L. van Niftrik, M. Schmid, J. Keltjens, J. van de Vossenberg, B. Kartal, H. Meier, D. Frishman, M. A. Huynen, H. W. Mewes, J. Weissenbach, M. S. M. Jetten, M. Wagner, and D. Le Paslier.** 2006. Deciphering the evolution and metabolism of an anammox bacterium from a community genome. Nature **440:**790-794.

123. **Tallec, G., J. Garnier, G. Billen, and M. Gousailles.** 2006. Nitrous oxide emissions from secondary activated sludge in nitrifying conditions of urban wastewater treatment plants: Effect of oxygenation level. Water Research **40:**2972-2980.

124. **Teske, A., E. Alm, J. M. Regan, S. Toze, B. E. Rittmann, and D. A. Stahl.** 1994. Evolutionary Relationships among Ammonia-Oxidizing and Nitrite-Oxidizing Bacteria. Journal of Bacteriology **176:**6623-6630.

125. **Trujillo, M., M. Naviliat, M. N. Alvarez, G. Peluffo, and R. Radi.** 2000. Peroxynitrite biochemistry: formation, reactions and detection. Analusis **28:**518-527.

126. **Ugar-Cankal, D., and N. Ozmeric.** 2006. A multifaceted molecule, nitric oxide in oral and periodontal diseases. Clinica Chimica Acta **366:**90-100.

127. **van Wonderen, J. H., B. Burlat, D. J. Richardson, M. R. Cheesman, and J. N. Butt.** 2008. The nitric oxide reductase activity of cytochrome c nitrite reductase from Escherichia coli. Journal of Biological Chemistry **283:**9587-9594.

128. **Vardi, A., F. Formiggini, R. Casotti, A. De Martino, F. Ribalet, A. Miralto, and C. Bowler.** 2006. A stress surveillance system based on calcium and nitric oxide in marine diatoms. Plos Biology **4:**411-419.

129. **Vianna, M. E., S. Holtgraewe, I. Seyfarth, G. Conrads, and H. P. Horz.** 2008. Quantitative analysis of three hydrogenotrophic microbial groups, methanogenic archaea, sulfate-reducing bacteria, and acetogenic bacteria, within plaque biofilms associated with human periodontal disease. Journal of Bacteriology **190:**3779-3785.

130. **von Schulthess, R., D. Wild, and W. Gujer.** 1994. Presented at the 17th Biennial Conference of the International-Association-on-Water-Quality, Budapest, Hungary, Jul 24-30.

131. **Vroom, J. M., K. J. De Grauw, H. C. Gerritsen, D. J. Bradshaw, P. D. Marsh, G. K. Watson, J. J. Birmingham, and C. Allison.** 1999. Depth penetration and detection of pH gradients in biofilms by two-photon excitation microscopy. Applied and Environmental Microbiology **65:**3502-3511.

132. **Walter, S., H. W. Bange, U. Breitenbach, and D. W. R. Wallace.** 2006. Nitrous oxide in the North Atlantic Ocean. Biogeosciences **3:**607-619.

133. **Ward, B. B., and O. C. Zafiriou.** 1988. Nitrification and Nitric-Oxide in the Oxygen Minimum of the Eastern Tropical North Pacific. Deep-Sea Research Part a-Oceanographic Research Papers **35:**1127-1142.

134. **Webb, A. J., N. Patel, S. Loukogeorgakis, M. Okorie, Z. Aboud, S. Misra, R. Rashid, P. Miall, J. Deanfield, N. Benjamin, R. MacAllister, A. J. Hobbs, and A. Ahluwalia.** 2008. Acute blood pressure lowering, vasoprotective, and antiplatelet properties of dietary nitrate via bioconversion to nitrite. Hypertension **51:**784-790.

135. **Xu, J. L., X. Xu, and W. Verstraete.** 2001. Quantitative measurement of the nitrate reductase activity in the human oral cavity. Food and Chemical Toxicology **39:**393-400.

136. **Yoshida, N., H. Morimoto, M. Hirano, I. Koike, S. Matsuo, E. Wada, T. Saino, and A. Hattori.** 1989. Nitrification Rates and N-15 Abundances of N2o and No-3 in the Western North Pacific. Nature **342:**895-897.

137. **Yung, Y. L., and M. B. McElroy.** 1979. Fixation of Nitrogen in the Prebiotic Atmosphere. Science **203:**1002-1004.

138. **Zacharia, I. G., and W. M. Deen.** 2005. Diffusivity and solubility of nitric oxide in water and saline. Annals of Biomedical Engineering **33:**214-222.

139. **Zafiriou, O. C., Q. S. Hanley, and G. Snyder.** 1989. Nitric-Oxide and Nitrous-Oxide Production and Cycling During Dissimilatory Nitrite Reduction by Pseudomonas-Perfectomarina. Journal of Biological Chemistry **264:**5694-5699.

140. **Zafiriou, O. C., M. McFarland, and R. H. Bromund.** 1980. Nitric-Oxide in Seawater. Science **207:**637-639.

141. **Zaura, E., and J. M. ten Cate.** 2004. Dental plaque as a biofilm: A pilot study of the effects of nutrients on plaque pH and dentin demineralization. Caries Research **38:**9-15.

142. **Zumft, W. G.** 1997. Cell biology and molecular basis of denitrification. Microbiology and Molecular Biology Reviews **61:**533-+.

143. **Zumft, W. G.** 2005. Nitric oxide reductases of prokaryotes with emphasis on the respiratory, heme-copper oxidase type. Journal of Inorganic Biochemistry **99:**194-215.

Chapter 2

Nitric Oxide Microsensor for High Spatial Resolution Measurements in Biofilms and Sediments

Frank Schreiber, Lubos Polerecky, and Dirk de Beer

Microsensor Research Group, Max-Planck-Institute for Marine Microbiology, Celsiusstrasse 1, D-28359 Bremen, Germany

Abstract

Nitric oxide (NO) is a ubiquitous biomolecule that is known as a signaling compound in eukaryotes and prokaryotes. In addition, NO is involved in all conversions of the biogeochemical nitrogen cycle: denitrification, nitrification, and the anaerobic oxidation of ammonium (Anammox). Until now, NO has not been measured with high spatial resolution within microbial communities, such as biofilms, sediments, aggregates or microbial mats, because the available sensors are not robust enough and their spatial resolution is insufficient. Here we describe the fabrication and application of a novel Clark-type NO microsensor with an internal reference electrode and a guard anode. The NO microsensor has a spatial resolution of 60-80 μm, a sensitivity of 2 pA μM^{-1}, and a detection limit of ~30 nM. Hydrogen sulfide (H$_2$S) was found to be a major interfering compound for the electrochemical detection of NO. The application of the novel NO microsensor to nitrifying biofilms and marine sediments revealed dynamic NO concentration profiles with peaks in the oxic parts of the samples. The local concentrations suggested that NO may be an important bioactive compound in natural environments. The consumption and production of NO occurs in separate regions of stratified microbial communities and indicates that it is linked to distinct biogeochemical cycles.

Introduction

Nitric oxide (NO) is a gaseous compound that is present in various biological systems. In eukaryotes NO is synthesized by different cell types *via* the enzyme NO synthase (NOS) and acts as an important signaling molecule and as an antimicrobial agent (6). Similarly, in certain prokaryotes NO can be synthesized by NOS. In contrast to eukaryotes, NO synthesis in prokaryotes is not involved in cell signaling but was shown to be involved in the biosynthetic nitration of tryptophanyl moieties (18) and the cytoprotection against oxidative stress (16).

In addition, NO is produced and consumed during the microbial conversions of the nitrogen cycle. During denitrification NO is an intermediate within the sequential, respiratory reduction of NO_3^- or NO_2^- to N_2O or N_2 (43). In the respiratory chain NO is generated by the enzyme nitrite reductase (Nir) and further reduced by the enzyme nitric oxide reductase (Nor) to N_2O. In contrast to the well studied mechanisms of NO production and consumption during denitrification, the mechanisms of NO production during nitrification are still under debate. Nitrification is the oxygen-dependent two-step process of the oxidation of NH_4^+ by ammonia oxidizing bacteria (AOB) to NO_2^- and the subsequent oxidation of NO_2^- to NO_3^- by nitrite oxidizing bacteria (NOB). Studies on pure cultures, soils, and sewage sludge showed that considerable amounts of NO and N_2O are produced by AOB in the presence of low O_2 concentrations (9). Isotope-labeling studies attributed this N-loss to a denitrifying activity of AOB, termed nitrifier denitrification (29), that is carried out by Nir and Nor for which the genes were detected in several AOB (7, 8). In addition, the recent first genome sequence of a bacterium that mediates the anaerobic oxidation of ammonia (Anammox) suggested NO as the most likely intermediate of this process because Nir was also detected in its genome (36). Understanding the liberation of microbial-derived NO into the atmosphere is of environmental concern since it is involved in a complex set of reactions in the troposphere that has effects on ozone distribution and global warming (10).

Despite the lack of biochemical understanding of the conversions of the nitrogen cycle, the links and controls of the nitrogen conversions in natural settings are the subject of ongoing debate (13). The interactions of these conversions have been successfully studied by the use of microsensors for NO_3^-, NO_2^-, and N_2O in stratified microbial communities, such as biofilms, aggregates, and sediments (31, 33). Until now, the role of NO in the interaction of the different processes of the nitrogen cycle in stratified microbial communities has not been investigated because no suitable microsensors were available to date. Microsensors for environmental applications must fulfill four major requirements: (i) they must be sensitive enough to detect the concentration changes in the sample, (ii) the spatial resolution must be small enough to detect the concentration

changes at the small scale (micrometers) at which they might occur in microbial communities, (iii) the sensors must be robust enough to withstand insertion into rough samples, e.g., sediments, and (iv) the sensor must be selective against possible interfering compounds that might be present in complex natural samples.

Until now, NO microsensors were mainly produced for the sensitive detection of NO release from mammalian cells in cultures or for the implantation on a fixed position in mammalian tissues (3). The two different sensor designs that were described can be divided into (i) single-anode electrodes with an external reference electrode placed in the sample and (ii) a Clark-type combined sensor design, whereby the sensing anode and the reference electrode are placed in an internal electrolyte that is separated from the sample by a gas-permeable membrane. To achieve adequate sensitivity to NO and prevent interference with NO_2^-, most single-anode-type NO microsensors rely on exposed carbon fiber electrodes coated with a selective Nafion membrane. Due to the length of the exposed electrode (up to several millimeters), this design is not suitable for most environmental applications, where a spatial resolution in the micrometer range is required (14, 40, 41). Furthermore, the sensitive Nafion membrane is easily destroyed when inserting the sensor into environmental samples, such as coarse sediments. In contrast, most Clark-type NO microsensors would be robust enough to withstand penetration of such samples, but to achieve high sensitivity for these sensors, wide tip openings have to be employed (23, 34, 35). However, microbial conversions in biofilms occur within very small scales, and confined sensor openings need to be employed in order to study the fluxes and conversion rates of the compounds in these systems (11).

In this study, we describe the construction of a robust, Clark-type NO microsensor that can measure at high spatial resolution and that is yet sensitive enough to detect concentration changes of NO that are relevant in environmental settings. Furthermore, we report on the sensitivity of the sensor toward interfering compounds that might be present in natural systems and that have not been considered in previous studies by medical

physiologists. Subsequently, the novel Clark-type NO microsensor was applied in natural stratified microbial communities, i.e., a nitrifying biofilm and marine sediments.

Experimental Section

Chemicals and preparation of NO solutions

KI, NaNO$_2$, H$_2$SO$_4$, NaOH, KMnO$_4$, HCl, KCl, Na$_2$HPO$_4$, NaH$_2$PO$_4$, NH$_4$Cl, ascorbate, NH$_2$OH, CS$_2$, dimethylsulfide (DMS), sodium methanethiolate, Na$_2$S, and H$_2$O$_2$ were obtained from Sigma or Merck. N$_2$, N$_2$O, H$_2$, and CH$_4$ were obtained from Messer (Sulzbach, Germany). NO solutions were prepared as described previously (12). Briefly, concentrated H$_2$SO$_4$ was slowly added to a N$_2$-flushed 1/1 mixture of saturated NaNO$_2$ and KI. Evolved NO gas was passed through 10 M NaOH to remove traces of NO$_2$ and captured in a Hungate tube fitted with a butyl rubber stopper containing 3 mL of double-distilled H$_2$O. The excess NO that escaped from this reservoir was led into a wash bottle containing 0.4 M KMnO$_4$ in 1.2 M NaOH for neutralization. Saturation of the NO solution was verified by mass spectrometry of the headspace gas that was completely comprised of NO.

NO microsensor fabrication

The sensor was composed of a carbon fiber sensing anode, a Ag/AgCl reference electrode, and a Pt guard anode placed inside an outer glass casing filled with an internal electrolyte (Figure 1). The carbon fiber sensing anode consisted of a carbon fiber that was sealed with epoxy resin into a pulled glass capillary. The glass capillary (Schott 8533, Schott AG, Mainz, Germany) was pulled in a propane flame to an o.d. of 80 μm. The carbon fiber (d = 30 μm, World Precision Instruments, Inc., Sarasota, FL) was inserted from the back and protruded slightly from the tip of the glass capillary. The tip of the glass capillary was dipped into freshly mixed, liquid epoxy resin (105 resin and 206

hardener, West System Inc., Bay City, MI). The resin went up between the carbon fiber and glass by capillary force and was then left to cure for 2 days to seal the carbon fiber in the glass. Then the carbon fiber was polished with a diamond lapping film (Ultra prep, Buehler, Lake Bluff, IL) which was attached to a rotary table in successive steps from 9 to 3 µm to achieve a planar sensing surface.

30 µm

Ag/AgCl reference cathode

glass sealing

epoxy sealing

Pt-guard-anode

internal electrolyte

glass casing

carbon fiber anode

membrane (5 -10 µm)

100 - 200 µm

30 -40 µm
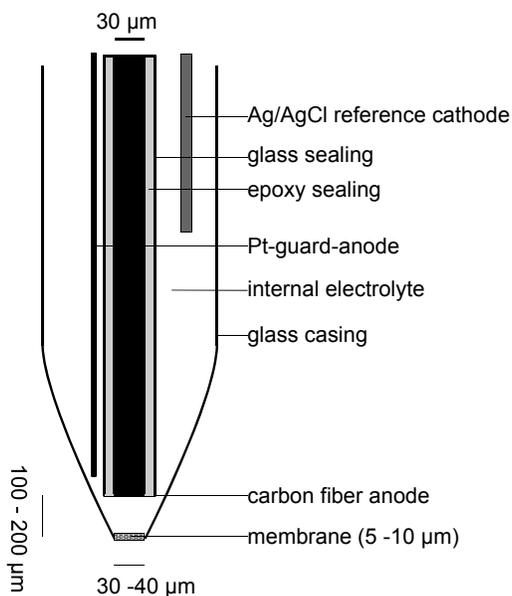
Figure 1. Schematic drawing of the Clark-type NO microsensor. The drawing shows the carbon fiber sensing anode, the Pt guard anode, the Ag/AgCl reference electrode, all placed inside a glass casing. The glass casing is filled with an internal electrolyte (100 mM sodium phosphate, 100 mM KCl pH 7.2) that is separated by a silicone membrane from the sample. Drawing is not to scale.

Afterward, the planar carbon fiber surface was modified by deposition of nickel(II) tetrakis(3-methoxy-4-hydroxyphenyl)porphyrin (Ni-TMPP; Frontier Scientific Europe Ltd., Lancashire, U.K.) using differential pulse amperometry (DPA) (12). The electrochemical cell comprised the carbon fiber working electrode, a Ag/AgCl reference electrode (Metrohm AG, Herisau, Switzerland), and a platinum counter electrode connected to the control unit (µAutolab Type III, Eco Chemie B.V., Utrecht, The Netherlands). Before each plating session 0.5 mM Ni-TMPP was freshly prepared in 0.1 M NaOH. A resting potential of 0 V for 1s and a polymerization potential of 1 V for 1 s was applied for DPA plating. Currents were recorded at the end of each potential pulse to

monitor Ni-TMPP plating. Plating was performed for 30 s because after that no change in current could be observed which indicated the end of film growth.

The guard anode was prepared from a Pt wire (d = 100 μm, stretched Pt; Ögussa, Vienna, Austria). The Pt wire was inserted into a slim glass capillary with the tip protruding ~10 cm and was electrochemically etched in concentrated KCN (1-7 V) to a diameter of ~30 μm. The Ag/AgCl reference electrode was prepared by electroplating of a Ag wire (d = 300 μm, Gold- und Silberschneideanstalt AG, Pforzheim, Germany) in a 1 M HCl solution. The outer casing was prepared by pulling glass (Schott AG, Mainz, Germany) to a conical shape. The glass was opened at the tip with fine tweezers to obtain an opening of 30–40 μm. The tip was closed with a 5 μm thick gas-permeable silicone membrane (Dow Corning 92-009, Dow Corning Corp., Midland, MI) that cured for 1 day. The tip of the sensing anode was placed at approximately 100-200 μm distance from the silicone membrane. The tip of the guard anode was placed ~200 μm behind the tip of the sensing anode. Glass beads (30–60 μm) were added from the back to avoid sedimentation of particles between the sensing anode and the silicone membrane. Thereafter, the casing was filled with an internal electrolyte (100 mM KCl buffered with 100 mM sodium phosphate pH 7.2) and the reference electrode was inserted into the electrolyte.

Characterization of NO microsensor performance

The NO microsensor was connected to a sensitive picoammeter and polarized at +750 mV (sensing anode vs reference and guard anode vs reference) until a stable zero current was obtained. Amperometric responses were recorded with a data acquisition system (DAQCard-AI-16XE-50; National Instruments, Austin, TX) connected to a computer with a data acquisition software (μ-Profiler, Max-Planck-Innovation GmbH, München, Germany). Electrode signals at specific NO concentrations were recorded in 1 s intervals, whereas every single recording was an average of 2000 readings obtained at a sampling frequency of 10 kHz. Calibrations were obtained by adding increasing amounts of NO stock solutions to 100 mL of deoxygenated 100 mM sodium phosphate buffer (pH 7.4)

under weak continuous stirring. Sensor noise was calculated as the standard deviation of 10 subsequent recordings of the sensor signal.

The selectivity of the NO microsensor was assed by exposing it to common interfering compounds ($NaNO_2$, ascorbate, H_2O_2) and a variety of oxidizable compounds that are able to penetrate a silicone membrane and may occur in nitrifying biofilms or marine sediments (H_2S, N_2O, NH_2OH, NH_4Cl, H_2, CH_4, sodium methanethiolate, CS_2, DMS). H_2S was introduced as Na_2S. The actual H_2S concentration was calculated based on its equilibrium constant and pH (27).

Application of NO microsensors

NO microsensors were used to study nitrifying biofilms and marine sediments. Nitrifying biofilms were grown in a gently aerated flow cell (~800 mL) using Tygon tubing as a substratum for biofilm growth. The inoculum was obtained from a sewage treatment plant (Seehausen, Bremen) and was fed with nitrifying media at a flow rate of 1 mL min^{-1}. The medium for nitrifying bacteria consisted of 10 mM NH_4Cl and trace elements at final concentrations of 3 μM Na_2EDTA, 1.5 μM $FeSO_4$, 77 nM H_3BO_4, 100 nM $MnCl_2$, 160 nM $CoCl_2$, 20 nM $NiCl_2$, 2.4 nM $CuCl_2$, 100 nM $ZnSO_4$, and 30 nM Na_2MoO_4 in tap water at pH 7.4. For microsensor measurements, small pieces of the biofilm-covered substratum were transferred into a smaller flow cell (~80 mL) that was placed in an aquarium. The aquarium served as a reservoir for medium that was recirculated through the small flow cell at a flow rate of 3 mL s^{-1} to create a constant flow of ~0.2 cm s^{-1} above the biofilm. Biofilm samples adjusted for the flow conditions for at least 2 h.

NO measurements in marine sediments were performed in marine sediments from Janssand, an intertidal sandflat situated landward of the island Spiekeroog, North Sea, Germany (53° 44' 07" N, 007° 41' 57" E) (5). For laboratory measurements, intact sediment cores were retrieved approximately 25 m away from the low water line toward the upper sandflat in July 2006 and stored with overlying seawater from the site for 3

days at 4 °C. Measurements were performed within 1 day at 19 °C with a continuous air flow directed on the overlying water in the core to induce a constant water flow above the sediment surface. In addition, NO microprofiles were measured during low tide directly on the exposed sandflat during a field campaign in October 2006. The investigated area was similar to the area where the cores were taken for laboratory measurements. During the measurements the sediment was completely exposed to air but was saturated with seawater.

Calibrations of the NO microsensor were performed as described above, at the same temperatures and in the same media as used for subsequent measurements. Vertical NO concentration profiles were measured with the NO microsensor mounted on a three-axis micromanipulator (MM 33; Märzhäuser, Wetzlar, Germany). The vertical axis was motorized for micropositioning (VT-80 linear stage, Micos, Germany, equipped with a 3564-K-024-BC motor, Faulhaber Group, Schönaich, Germany) and controlled by μ-Profiler software. The microsensor tip was adjusted manually to the sample surface by using a dissection microscope (Stemi SV 6; Carl Zeiss AG, Oberkochen, Germany). In addition, microprofiles of O_2(30) and H_2S (17) concentrations were measured. The microprofiles were fitted and analyzed with a diffusion-reaction model (4) to calculate the local conversion rates, which was done with a program written in Matlab. The NO diffusion coefficient D was(38) 2.21×10^{-9} m^2 s^{-1}. The effective diffusion coefficient D_{eff} in biofilms was calculated according to $D_{eff} = \varphi^2 D$, where $\varphi = 0.9$ is the porosity of biofilms (11).

Results and Discussion

Sensor performance and characteristics

The NO microsensor responded to increasing amounts of NO that have been added to a deoxygenated buffer solution (Figure 2A). The response was linear within the

investigated range between 40 nM and 4 µM NO, with a sensitivity of 2.22 pA µM^{-1} (Figure 2B). The sensor signal was very stable, with fluctuations of ~0.022 pA. Accepting a signal-to-noise ratio of not less than 3, the sensor had a lower detection limit of ~30 nM. The response time (t_{90}) was ~1s upon a change of 60 nM NO (Figure 2A, inset), the temperature sensitivity was 5–10% °C^{-1}, and the sensor was not sensitive to stirring.
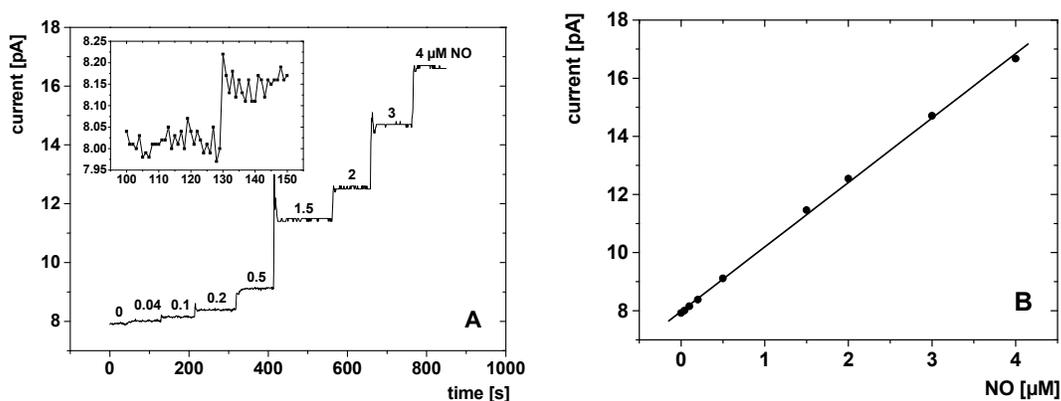
Figure 2. Performance of the Clark-type NO microsensor. **(A)** Dynamic amperometric response of the NO microsensor to increasing amounts of NO added to the calibration solution. Final concentrations [µM] are shown on the signal plateaus. The inset magnifies the response to an increase from 0.04 µM to 0.1 µM NO. **(B)** Resulting calibration plot for the NO microsensor.

In the constructed NO microsensor the sensing anode and reference electrode are situated in an internal electrolyte (Clark-type design) and, hence, are separated from the sample by a gas-permeable membrane. This feature makes the novel NO microsensor ideal for the application in environmental samples, as the sensing surface is protected from mechanical disturbances by hard sample particles, and the confined tip opening of the sensor casing of 30–40 µm allows measurements with high spatial resolution (60–80 µm), estimated as approximately twice the outer diameter of the sensor tip (11). Although the sensor signal is limited by transport through the confined tip and the silicone membrane, the detection limit of the NO microsensor is still very low (~30 nM). These characteristics compare favorably with those reported previously for different sensor

designs. For example, previous designs optimized for small spatial resolution and high sensitivity employed coated sensing anodes that were in direct contact with the sample and, thus, not sufficiently robust for environmental applications (26, 28). On the other hand, the reported Clark-type NO sensors, optimized for robustness, had tip openings that were too wide (> 100 μm) and decreased the spatial resolution to a level that is not sufficient for the measurement in biofilms (23, 34, 35).

Sensitivity of the constructed NO microsensor was ~2.22 pA μM^{-1}. This is considerably lower than that reported for sensors using long single-anodes exposed directly to the solution (14, 40) or for Clark-type microsensors with wide tip openings and wide sensing surfaces(23, 35), which had sensitivities in the nanoamp per micromolar range. However, as reported by Kitamura et al. (22), the use of a planar sensing surface with a tip diameter of 10 μm leads to reduced sensitivity of 0.8 pA μM^{-1}, which is in the same range as that reported here for a sensing surface with a diameter of 30 μm. In contrast, Patel et al. (28) and Malinski and Taha (26) reported sensitivities in the nanoamp per micromolar range even though the sensors had sensing surfaces similar in size to the NO microsensor of this study.

To understand the wide range of sensitivities reported for sensing surfaces that are similar in size but arranged in different sensor designs (combined vs bare single-anode), we developed a simple model describing the physical transport of NO molecules toward the sensing surfaces in these geometrical arrangements (see the Supplementary Information). For a combined sensor, the sensing surface is enclosed in a protective casing with a confined opening (Figure 1), and the NO flux towards the electrochemically active sensing surface is limited by one-dimensional diffusion through the membrane and electrolyte. Considering the dimensions of the constructed sensor (Figure 1), maximum sensitivity of 2.28 pA μM^{-1} is calculated by the model, which is similar to the actually measured sensitivity. On the other hand, the physical transport toward a bare single-anode is three-dimensional, which allows for greater NO fluxes toward the sensing surface. Indeed, assuming diffusive transport, sensitivity in the range of ~120 pA μM^{-1}

was calculated for a sensing surface with the same diameter. According to the model the sensitivity of bare single-anodes might be further increased to the nanoamp per micromolar range by stirring the medium, as flow enhances transport of the NO molecules by decreasing the diffusive boundary around the sensing surface. However, this stirring sensitivity is undesirable because the flow may vary between calibration and measurement.

The use of an outer casing leads to increased robustness and a lower sensitivity. In addition, it shields the sensing electrode from electromagnetic interferences. Thus, the combined sensor design results in a superior signal-to-noise ratio, leading to increased resolution and decreased lower detection limit. The use of carbon instead of Pt as the sensing electrode material might contribute to improved stability. In contrast to metal surfaces, the carbon surface does not adsorb oxygen and does not form oxides (42) that may lead to fluctuations of background currents due to unstable polarization of the sensing surface. Furthermore, the use of a guard anode helped to reduce fluctuations in the background currents. We detected ~2-fold increased fluctuations of the background current upon disconnecting the guard anode after it was polarized for several hours (Figure S3). A possible explanation is the occurrence of inorganic and organic micro-pollutants in the electrolyte that may be oxidizable at the high oxidation potential of 750 mV. The guard anode might oxidize these compounds and thus prevent the compounds from reaching the sensing anode.

Interference with NO detection

The interference with NO detection was investigated at environmentally relevant or higher concentrations of substances that have been already reported to interfere with NO detection (NO_2^-, ascorbate, H_2O_2). Since the silicone membrane would allow any gas to enter the sensor, additionally, the interference with other potentially oxidizable gaseous compounds (N_2O, H_2, NH_3 derived from NH_4Cl, H_2S) and with selected volatile organic sulfur compounds (vosc; CS_2, DMS, and sodium methanethiolate) was investigated. As

expected, the NO sensor was not affected by ions such as NO_2-, ascorbate, or NH_4^+ because the silicone membrane effectively selects for gaseous compounds (Table 1). Furthermore, the NO sensor did not show any significant responses to N_2O, H_2, CH_4, H_2O_2, NH_3, NH_2OH, CS_2 and DMS. Sodium methanethiolate addition resulted in a considerable interference of 3.5% at 97 µM. Since sodium methanethiolate is typically present in the nanomolar concentration range (25) it will not interfere with *in situ* NO detection. However, H_2S is a seriously interfering substance, leading to increased currents (Figure 3). The slope of the signal versus concentration plot at H_2S concentrations between 0.6 and 2.44 µM was 3.53 pA µM^{-1}, which gives an interference of 158% (interference = [H_2S sensitivity / NO sensitivity] × 100); however, at lower H_2S concentrations (0–0.61 µM) the interference was only 85%.

Table 1. Interferences of various compounds with the Clark-type NO microsensor.

	Tested concentration[a]	Sensitivity	Interference[b]
	[µM]	[pA µM^{-1}]	[%]
N_2O	50	0.0002	< 0.1
NO_2^-	200	0.0004	< 0.1
Ascorbic Acid	500	0.000007	< 0.1
NH_4Cl (NH_3)[c]	10000 (100)	(0.001)	(0.2)
NH_2OH	240	0.006	0.3
CH_4	300	0.003	0.4
H_2O_2	11	0.007	1.1
H_2	20	0.009	1.4
Dimethylsulfide	9.7	0.0003	< 0.1
Na-methanethiolate	97.8	0.03	3.5
CS_2	874	0	0
H_2S	0.61[d]	1.9	85.6

[a] Concentrations of the tested compounds were chosen based on the environmental occurrence or a higher concentration. [b] Interference of compound X [%] = (X sensitivity / NO sensitivity) × 100. [c] Resulting [NH_3] calculated from the pH (7.4) and equilibrium constant. [d] For H_2S the response to a lower concentration than that of environmental relevance is shown, because the interference is so strong.

H_2S is a highly reduced gaseous compound that can pass the silicone membrane and is oxidized at the anode to elemental sulfur. The sulfur deposits did not seem to interfere with NO detection, since the interference of H_2S with the sensor was reversible and did not permanently damage the sensor. After short-term exposure to H_2S the sensor was still able to detect NO without loss of sensitivity (data not shown). Furthermore, we investigated H_2S interference at Ni-TMPP-plated and nonplated bare carbon fiber anodes without glass casing. Both plated and nonplated anodes were sensitive to H_2S. Plating with Ni-TMPP led to increased H_2S sensitivity (1.9-2.9-fold) and to slightly increased interference with H_2S (1.2-3.3-fold). However, regardless of the Ni-TMPP plating, H_2S sensitivity was always higher than NO sensitivity (3–40-fold). Further investigations are needed to clarify how commonly used electrode materials and sensing surface modifications in NO microsensors influence H_2S interference with NO detection. To our knowledge, for all NO sensors that have been reported for the application of NO detection in medical physiology, H_2S was never considered as an interfering compound. However, H_2S has been a fairly well-established messenger molecule for mammalian cells (21). Thus, our findings may have important implications in this research field.
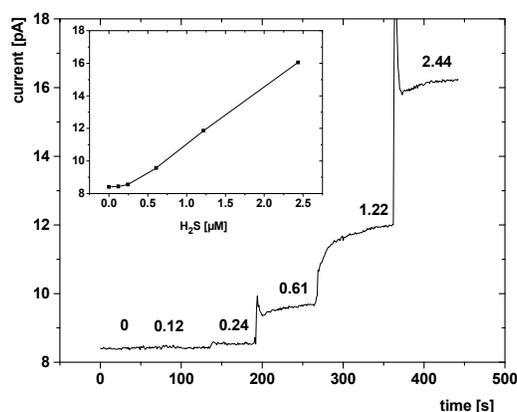
Figure 3. Dynamic amperometric response curve of the Clark-type NO microsensor to increasing amounts of H_2S added to the calibration solution as Na_2S. Final H_2S concentrations [μM] are shown on signal plateaus. The inset shows the resulting signal-vs-concentration curve.

The interference of NO detection with H_2S restricts the use of the sensor in environmental samples toward oxidized parts of the microbial communities. In addition, H_2S should be separately monitored with the H_2S microsensor. Since the conventional H_2S microsensor for environmental application has a lower detection limit of ~1 µM(17), only the occurrence of elevated H_2S concentrations may be determined independently, whereas uncontrolled interference of H_2S with NO detection might occur at sub-micromolar concentrations.

NO microprofiles in nitrifying biofilms

Vertical NO microprofiles were measured in nitrifying biofilms (Figure 4). The concentration measurements in a certain spot of the biofilm were reproducible; however, the maximum NO concentrations varied considerably across the biofilm (ranging from 1 to 2.3 µM; Figure 4A & B), reflecting the heterogeneity of a natural, multispecies biofilm. In addition to NO, O_2 microprofiles were measured in nitrifying biofilms (Figure 4C). The zone of O_2 consumption was located within the upper 300 µm of the biofilm and O_2 became depleted below 300 µm. NO was produced in the micro-oxic zone of the biofilm between 150–300 µm depth to concentrations of ~1 µM at rate of ~136 pmol cm^{-3} s^{-1}, as calculated from the fitted profile with the diffusion-reaction model (Figure 4C). In the top, oxic zone of the biofilm the produced NO is only insignificantly consumed and leaves the biofilm matrix by diffusion, which is indicated by the linear decrease of NO concentrations away from the surface of the biofilm. Furthermore, NO diffuses downward inside the anoxic zone where the fit of the profile indicated a consumption activity of ~31 pmol cm^{-3} s^{-1}. The switch of AOB at micro-oxic conditions to denitrification with concomitant NO production has been reported earlier (19, 24). AOB that are present in the micro-oxic part of the biofilm can use NO_2^- as an electron acceptor. In this metabolism NH_4^+ is activated in the presence of O_2 by the enzyme ammonia monooxygenase to hydroxylamine, which serves as the electron donor for NO_2^- reduction. This nitrifier denitrification was discussed to be a way for NO_2^- detoxification (2) or involved in energy metabolism (32, 39) and is accompanied by the production of NO.
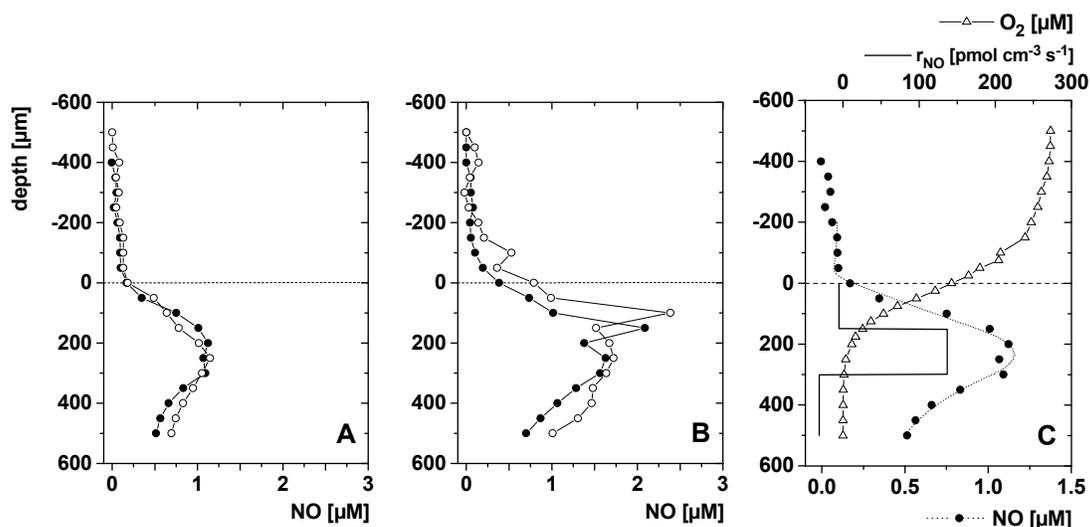
Figure 4. Vertical NO (filled and open circles) and O_2 (open triangles) microprofiles measured in a nitrifying biofilm using NO and O_2 microsensors, respectively. The dashed line represents the biofilm surface. **(A)** and **(B)** show NO microprofiles measured in different spots of the biofilm, whereby filled and open circles in each graph represent repeated measurements in the same spot. **(C)** shows the NO microprofile (filled circles) presented in (A) together with the best fit by a diffusion model (dotted line). The solid line represents the rate of NO production (r_{NO}). Note the different x-axis scaling in (C).

The NO microprofile in the biofilm shows a change in concentration of ~400 nM within 50 μm (depth from 50 to 100 μm). Due to its small spatial resolution and sensitivity to NO concentrations in the nanomolar range, the novel NO microsensor could resolve these concentration changes in microbial biofilms. The low amount of sulfate in the medium excludes H_2S as an interfering species during NO detection.

NO microprofiles in marine sediments

The vertical microprofiles of NO and the simultaneous occurrence of O_2 in marine sediments are shown in Figure 5. NO and O_2 distributions showed differences when measured directly on the field site (*in situ*; Figure 5A) and when measured in sediment cores stored for 3 days (*ex situ*; Figure 5B). In both systems a NO peak could be observed within the oxic zone of the sediment. The maximum concentrations were ~900 nM in collected cores and ~500 nM in the field.
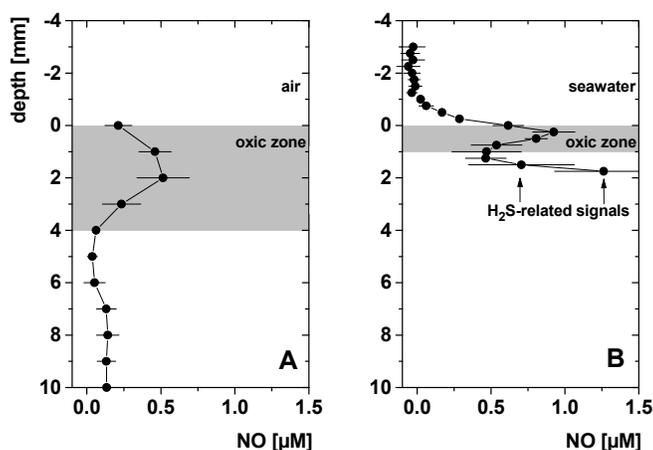
Figure 5. Vertical NO microprofiles measured in marine sediments from an intertidal sandflat (North Sea, Germany). **(A)** NO microprofiles measured directly in the field in exposed sediments during low tide. **(B)** NO microprofiles measured in sediment cores retrieved from the same site after 3 days of storage. The gray area represents the extent of the oxic zone near the sediment surface, as determined by the O_2 microsensor. H_2S related signals in (B) were confirmed by measurements with a H_2S microsensor. Error bars represent the standard deviation calculated from three individual profiles measured at different spots in the sample.

NO is produced in the oxic part and consumed in the anoxic parts of the sediments. Other studies attributed the production of NO to pure cultures of ammonia oxidizers and to the process of nitrification in batch incubations of sediments and soils (19, 20, 24). Together, this suggests that NO is produced by AOB that thrive in oxic or micro-oxic zones of the upper sediment layers. However, an alternative source of NO at the sediment surface might be NO synthesis from NOS by diatoms. NO synthesis has been shown to be involved in cell-cell signaling by bloom-forming, pelagic diatoms (37) and might also occur in benthic diatoms that inhibit the sediment surface. In addition, NO was shown to be produced by green algae and cyanobacteria, when inhibited photosynthesis resulted in the production of NO by the enzyme assimilatory nitrate reductase (1). Furthermore, the NO microprofiles indicate that NO produced in the oxic sediment layers is channeled into the respiratory chain of denitrifying bacteria that occur below the oxic-anoxic interface. The denitrifying bacteria will subsequently reduce NO to N_2O and N_2. This is supported by the view that denitrifying bacteria effectively control the ambient NO concentrations to levels in the low nanomolar range (15).

In cores, H_2S developed in the anoxic parts of the sediment, as confirmed with the H_2S microsensor, resulting in a drastic rise of signals of the NO sensor below the oxic zone. In contrast, due to the more powerful hydrodynamics in the field, H_2S is absent in the top 1 cm of the sediment. Nevertheless, care should be taken when analyzing the results because it cannot be excluded that submicromolar amounts of H_2S might contribute to the signals obtained with the NO microsensor.

The novel NO microsensor was suitable to measure NO concentration changes in marine sediments. The sensitivity in the nanomolar range was sufficient to resolve the ambient NO concentration changes. Concentration changes in sediments are not as confined as in biofilms, and the step size during profiling was 250 μm and 1 mm for *ex situ* and *in situ* measurements, respectively. Thus, the spatial resolution of the NO microsensor was more than sufficient to study these sediments. In addition, the Clark-type NO microsensor was robust enough to penetrate the coarse sediments. The robust glass casing protected the sensing anode against big and hard sediments particles and was sturdy enough not to break upon inserting the sensor into the sediment.

Conclusions

The Clark-type design is a useful design for NO microsensors, especially if high spatial resolution *and* robustness against rough samples are required. The Clark-type design in combination with a guard anode leads to low background currents. The reduced noise contributed to lowering the detection limit and sensor resolution to sufficient levels, even though the sensitivity achieved was relatively low.

H_2S was shown to interfere with NO detection. As H_2S is an established signaling compound in mammalian systems, the application of NO microsensors in biomedical research should regard H_2S as a potential interference for NO detection. This interference should be investigated for each specific sensor design employed.

The Clark-type NO microsensor made it possible for the first time to measure NO microprofiles in nitrifying biofilms and marine sediments. NO concentrations can be confidently quantified in areas were H_2S is not present, namely, in oxic parts of the sample or in anoxic, yet oxidized regions. The NO microprofiles showed dynamic changes of NO concentrations, indicating an active involvement of NO in the cycling of nitrogen in stratified microbial communities.

Acknowledgements

Author Contribution

DdB and FS conceived research and designed the sensor. FS constructed, tested and applied the sensors. LP and FS modeled theoretical sensor currents. FS wrote the manuscript with input of DdB and LP.

References

1.   **Barros, M. P., E. Pinto, T. C. S. Sigaud-Kutner, K. H. M. Cardozo, and P. Colepicolo.** 2005. Rhythmicity and oxidative/nitrosative stress in algae. Biological Rhythm Research **36:**67-82.
2.   **Beaumont, H. J. E., S. I. Lens, W. N. M. Reijnders, H. V. Westerhoff, and R. J. M. van Spanning.** 2004. Expression of nitrite reductase in Nitrosomonas europaea involves NsrR, a novel nitrite-sensitive transcription repressor. Molecular Microbiology **54:**148-158.
3.   **Bedioui, F., and N. Villeneuve.** 2003. Electrochemical nitric oxide sensors for biological samples - Principle, selected examples and applications. Electroanalysis **15:**5-18.
4.   **Berg, P., N. Risgaard-Petersen, and S. Rysgaard.** 1998. Interpretation of measured concentration profiles in sediment pore water. Limnology and Oceanography **43:**1500-1510.
5.   **Billerbeck, M., U. Werner, L. Polerecky, E. Walpersdorf, D. deBeer, and M. Huettel.** 2006. Surficial and deep pore water circulation governs spatial and temporal scales of nutrient recycling in intertidal sand flat sediment. Marine Ecology-Progress Series **326:**61-76.
6.   **Bredt, D. S., and S. H. Snyder.** 1994. Nitric-Oxide - a Physiological Messenger Molecule. Annual Review of Biochemistry **63:**175-195.
7.   **Casciotti, K. L., and B. B. Ward.** 2001. Dissimilatory nitrite reductase genes from autotrophic ammonia-oxidizing bacteria. Applied and Environmental Microbiology **67:**2213-2221.
8.   **Casciotti, K. L., and B. B. Ward.** 2005. Phylogenetic analysis of nitric oxide reductase gene homologues from aerobic ammonia-oxidizing bacteria. Fems Microbiology Ecology **52:**197-205.
9.   **Colliver, B. B., and T. Stephenson.** 2000. Production of nitrogen oxide and dinitrogen oxide by autotrophic nitrifiers. Biotechnology Advances **18:**219-232.
10. **Crutzen, P. J., and J. Lelieveld.** 2001. Human impacts on atmospheric chemisty. Annual Review of Earth and Planetary Sciences **29:**17-45.
11. **deBeer, D.** 1998. Use of Microelectrodes to measure in situ microbial activities in biofilm, sediments and microbial mats, Molecular Microbial Ecology, vol. 8.1.3. Kluwer Academic Publishers.
12. **Diab, N., J. Oni, and W. Schuhmann.** 2005. Electrochemical nitric oxide sensor preparation: A comparison of two electrochemical methods of electrode surface modification. Bioelectrochemistry **66:**105-110.
13. **Francis, C. A., J. M. Beman, and M. M. M. Kuypers.** 2007. New processes and players in the nitrogen cycle: the microbial ecology of anaerobic and archaeal ammonia oxidation. Isme Journal **1:**19-27.
14. **Friedemann, M. N., S. W. Robinson, and G. A. Gerhardt.** 1996. o-phenylenediamine-modified carbon fiber electrodes for the detection of nitric oxide. Analytical Chemistry **68:**2621-2628.

15. **Goretski, J., O. C. Zafiriou, and T. C. Hollocher.** 1990. Steady-State Nitric-Oxide Concentrations During Denitrification. Journal of Biological Chemistry **265:**11535-11538.

16. **Gusarov, I., and E. Nudler.** 2005. NO-mediated cytoprotection: Instant adaptation to oxidative stress in bacteria. Proceedings of the National Academy of Sciences of the United States of America **102:**13855-13860.

17. **Jeroschewski, P., C. Steuckart, and M. Kuhl.** 1996. An amperometric microsensor for the determination of H2S in aquatic environments. Analytical Chemistry **68:**4351-4357.

18. **Kers, J. A., M. J. Wach, S. B. Krasnoff, J. Widom, K. D. Cameron, R. A. Bukhalid, D. M. Gibson, B. R. Crane, and R. Loria.** 2004. Nitration of a peptide phytotoxin by bacterial nitric oxide synthase. Nature **429:**79-82.

19. **Kester, R. A., W. deBoer, and H. J. Laanbroek.** 1997. Production of NO and N2O by pure cultures of nitrifying and denitrifying bacteria during changes in aeration. Applied and Environmental Microbiology **63:**3872-3877.

20. **Kester, R. A., M. E. Meijer, J. A. Libochant, W. de Boer, and H. J. Laanbroek.** 1997. Contribution of nitrification and denitrification to the NO and N2O emissions of an acid forest soil, a river sediment and a fertilized grassland soil. Soil Biology & Biochemistry **29:**1655-1664.

21. **Kimura, H., Y. Nagai, K. Umemura, and Y. Kimura.** 2005. Physiological roles of hydrogen sulfide: Synaptic modulation, neuroprotection, and smooth muscle relaxation. Antioxidants & Redox Signaling **7:**795-803.

22. **Kitamura, Y., T. Uzawa, K. Oka, Y. Komai, H. Ogawa, N. Takizawa, H. Kobayashi, and K. Tanishita.** 2000. Microcoaxial electrode for in vivo nitric oxide measurement. Analytical Chemistry **72:**2957-2962.

23. **Lee, Y., B. K. Oh, and M. E. Meyerhoff.** 2004. Improved planar amperometric nitric oxide sensor based on platinized platinum anode. 1. Experimental results and theory when applied for monitoring NO release from diazeniumdiolate-doped polymeric films. Analytical Chemistry **76:**536-544.

24. **Lipschultz, F., O. C. Zafiriou, S. C. Wofsy, M. B. McElroy, F. W. Valois, and S. W. Watson.** 1981. Production of No and N2o by Soil Nitrifying Bacteria. Nature **294:**641-643.

25. **Lomans, B. P., A. J. P. Smolders, L. M. Intven, A. Pol, H. denCamp, and C. vanderDrift.** 1997. Formation of dimethyl sulfide and methanethiol in anoxic freshwater sediments. Applied and Environmental Microbiology **63:**4741-4747.

26. **Malinski, T., and Z. Taha.** 1992. Nitric-Oxide Release from a Single Cell Measured Insitu by a Porphyrinic-Based Microsensor. Nature **358:**676-678.

27. **Millero, F. J., T. Plese, and M. Fernandez.** 1988. The Dissociation of Hydrogen-Sulfide in Seawater. Limnology and Oceanography **33:**269-274.

28. **Patel, B. A., M. Arundell, K. H. Parker, M. S. Yeoman, and D. O'Hare.** 2006. Detection of nitric oxide release from single neurons in the pond snail, Lymnaea stagnalis. Analytical Chemistry **78:**7643-7648.

29. **Poth, M., and D. D. Focht.** 1985. N-15 Kinetic-Analysis of N2o Production by Nitrosomonas-Europaea - an Examination of Nitrifier Denitrification. Applied and Environmental Microbiology **49:**1134-1141.

30. **Revsbech, N. P.** 1989. An Oxygen Microsensor with a Guard Cathode. Limnology and Oceanography **34:**474-478.
31. **Revsbech, N. P., N. Risgaard-Petersen, A. Schramm, and L. P. Nielsen.** 2006. Nitrogen transformations in stratified aquatic microbial ecosystems. Antonie Van Leeuwenhoek International Journal of General and Molecular Microbiology **90:**361-375.
32. **Schmidt, I., E. Bock, and M. S. M. Jetten.** 2001. Ammonia oxidation by Nitrosomonas eutropha with NO2 as oxidant is not inhibited by acetylene. Microbiology-Sgm **147:**2247-2253.
33. **Schramm, A.** 2003. In situ analysis of structure and activity of the nitrifying community in biofilms, aggregates, and sediments. Geomicrobiology Journal **20:**313-333.
34. **Shibuki, K.** 1990. An Electrochemical Microprobe for Detecting Nitric-Oxide Release in Brain-Tissue. Neuroscience Research **9:**69-76.
35. **Shin, J. H., S. W. Weinman, and M. H. Schoenfisch.** 2005. Sol-gel derived amperometric nitric oxide microsensor. Analytical Chemistry **77:**3494-3501.
36. **Strous, M., E. Pelletier, S. Mangenot, T. Rattei, A. Lehner, M. W. Taylor, M. Horn, H. Daims, D. Bartol-Mavel, P. Wincker, V. Barbe, N. Fonknechten, D. Vallenet, B. Segurens, C. Schenowitz-Truong, C. Medigue, A. Collingro, B. Snel, B. E. Dutilh, H. J. M. Op den Camp, C. van der Drift, I. Cirpus, K. T. van de Pas-Schoonen, H. R. Harhangi, L. van Niftrik, M. Schmid, J. Keltjens, J. van de Vossenberg, B. Kartal, H. Meier, D. Frishman, M. A. Huynen, H. W. Mewes, J. Weissenbach, M. S. M. Jetten, M. Wagner, and D. Le Paslier.** 2006. Deciphering the evolution and metabolism of an anammox bacterium from a community genome. Nature **440:**790-794.
37. **Vardi, A., F. Formiggini, R. Casotti, A. De Martino, F. Ribalet, A. Miralto, and C. Bowler.** 2006. A stress surveillance system based on calcium and nitric oxide in marine diatoms. Plos Biology **4:**411-419.
38. **Zacharia, I. G., and W. M. Deen.** 2005. Diffusivity and solubility of nitric oxide in water and saline. Annals of Biomedical Engineering **33:**214-222.
39. **Zart, D., I. Schmidt, and E. Bock.** 2000. Significance of gaseous NO for ammonia oxidation by Nitrosomonas eutropha. Antonie Van Leeuwenhoek International Journal of General and Molecular Microbiology **77:**49-55.
40. **Zhang, X. J., L. Cardosa, M. Broderick, H. Fein, and J. Lin.** 2000. An integrated nitric oxide sensor based on carbon fiber coated with selective membranes. Electroanalysis **12:**1113-1117.
41. **Zhang, X. J., Y. Kislyak, H. Lin, A. Dickson, L. Cardosa, M. Broderick, and H. Fein.** 2002. Nanometer size electrode for nitric oxide and S-nitrosothiols measurement. Electrochemistry Communications **4:**11-16.
42. **Zhang, X. J., J. Lin, L. Cardoso, M. Broderick, and V. Darley-Usmar.** 2002. A novel microchip nitric oxide sensor with sub-nM detection limit. Electroanalysis **14:**697-703.
43. **Zumft, W. G.** 1997. Cell biology and molecular basis of denitrification. Microbiology and Molecular Biology Reviews **61:**533-+.

Supplementary Information

Theoretical maximum of sensitivity for a combined NO-microsensor operating at a constant potential

The theoretically maximum sensitivity for the combined NO microsensor (Figure 1) is estimated by calculating the maximum flux of NO molecules towards the sensing electrode at a given NO bulk concentration c_{bulk}, assuming that the concentration of the reduced NO molecules at the sensing surface is zero (Figure S1).
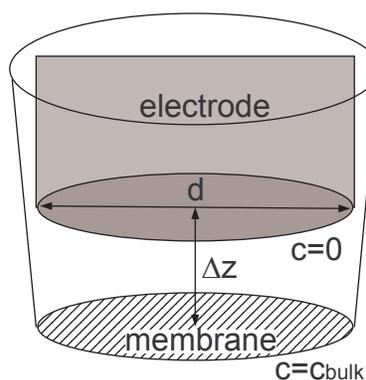
Figure S1.

Molecules that enter the sensor through the membrane are transported by diffusion over a distance Δz to the planar sensing surface (diameter d). Using Fick's 1st law of diffusion, the flux of the NO molecules is

$$J = -D \, \Delta c / \Delta z, \tag{S1}$$

where $D = 2.21 \times 10^{-9}$ m^2 s^{-1} is the molecular diffusion coefficient of NO in the aqueous electrolyte and Δc is the concentration difference between the bulk medium and the sensing surface, i.e., $\Delta c = c_{bulk}$. The diffusion of NO through the silicone membrane can be assumed to be equal to that in water because similar diffusion coefficients in both were

reported earlier (2, 3). Considering that the reaction of one NO molecule at the sensing surface donates 3 electrons to the measuring circuit ($NO + 2 H_2O - 3e^- \rightarrow NO_3^- + 4 H^+$), the current through the electrode can be written as

$$I = 3\, A\, J\, N_A\, C_{e^-}, \tag{S2}$$

where $N_A = 6.022 \times 10^{23}$ mol^{-1} is Avogadro's constant, $C_{e^-} = -1.6022 \times 10^{-19}$ C is the charge of electron and $A = \pi\, (d/2)^2$ is the area of the sensing surface. Since the sensor sensitivity is defined as $S = dI/dc_{bulk}$, it can be written as

$$S = \frac{3}{4}\pi D N_A C_{e^-} \frac{d^2}{\Delta z}, \tag{S3}$$

as follows from equations (S1–S2). Using the values of $d = 30$ µm, $\Delta z = 200$ µm (Figure S1), the maximum sensitivity of the combined sensor determined by the physical transport limitation of NO molecules towards the sensing electrode is 2.28 pA µM^{-1}.

Theoretical maximum of sensitivity for a bare single-anode NO-microsensor operating a at constant potential

In contrast to the combined sensor, the current that can be theoretically reached at a bare single-anode microsensor is not limited by the one-dimensional diffusive transport of NO molecules through the membrane and electrolyte, but by the three-dimensional transport of NO molecules from the bulk solution toward the sensing electrode surface. To estimate this flux under constant-potential operation, we assume that the concentration of the NO molecules at the electrode surface is zero and that the transport is diffusive (diffusion coefficient of NO in water of $D = 2.21 \times 10^{-9}$ m^2 s^{-1}). To allow analytical expression, we further assume that the sensing area of the electrode is a sphere of radius r_0 instead of the planar circular area of radius r_0 (Figure S2).
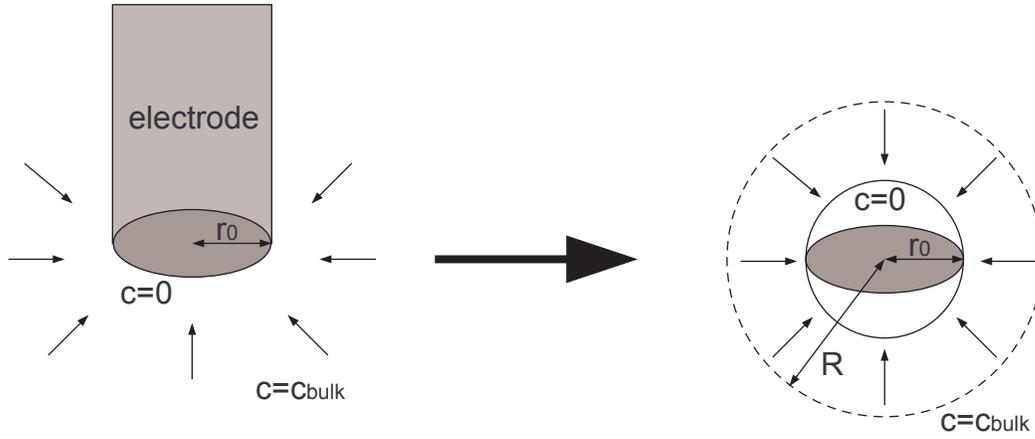
Figure S2.

Consequently, the steady-state concentration field around the sensing surface is spherically symmetric, i.e., dependent only on the radial distance r, and fulfills the differential equation

$$D\frac{1}{r}\frac{\partial}{\partial r}r^2\frac{\partial c}{\partial r}=0,\qquad\qquad\text{(S4)}$$

which is the diffusion equation expressed in spherical coordinates. The general solution for this differential equation is

$$c(r)=\frac{A}{r}+B,\qquad\qquad\text{(S5)}$$

where A and B are constants determined from the boundary conditions. The 1st boundary condition is derived from the assumption that the concentration at the spherical sensing surface is zero, i.e.,

$$c(r_0) = 0\,\mu M = \frac{A}{r_0} + B. \tag{S6}$$

The 2nd boundary condition is derived from the assumption that the concentration in the bulk solution is c_{bulk}, i.e.,

$$c(r \rightarrow \infty) = B = c_{bulk}. \tag{S7}$$

Using the general solution (S5), the radial flux can be calculated as

$$J_r = -D\frac{\partial c}{\partial r} = D\frac{A}{r^2}. \tag{S8}$$

Thus, the NO flux at the sensing surface can be expressed as

$$J_r(r_0) = D\frac{A}{r_0^2} = -D\frac{B}{r_0}. \tag{S9}$$

Considering that each NO molecule oxidized at the sensing surface results in the donation of 3 electrons to the electrochemical circuit, the current through the electrode can be written as

$$I = 3\,A_{eff}\,J\,N_A\,C_{e-}, \tag{S10}$$

where $N_A = 6.022 \times 10^{23}$ mol^{-1} is Avogadro's constant, $C_{e-} = -1.6022 \times 10^{-19}$ C is the charge of electron, and $A_{eff} = 4\pi r_0^2$ is the area of the effective sensing surface. The sensor sensitivity is defined as $S = dI/dc_{bulk}$. Thus, combining Eqs. (S6–S10), the maximum sensor sensitivity of a bare single-anode sensor can be approximated as

$$S = 12\,\pi\,D\,N_A\,C_{e-}\,r_0, \tag{S11}$$

which is equal to 120.3 pA µM^{-1} when r_0 = 15 µm (Figure S2) is used. Thus the sensitivity of a bare single-anode sensor is ~54 times greater than that for a combined sensor (see above), when the transport of NO molecules towards the sensing surface is diffusive in the entire volume of the bulk medium.

If the bulk medium is stirred, the same model as above can be applied but the concept of a diffusive boundary layer (1) needs to be additionally taken into account. This is done by considering that the radial distance R at which the concentration around the sensing surface reaches the bulk value c$_{bulk}$ is decreased from infinity (as in the unstirred medium above) to a finite value. This condition leads to the modification of equation (S7) representing the second boundary condition, namely

$$c(R) = \frac{A}{R} + B = c_{bulk} .$$
(S12)

Combining equation (S8), (S10) and (S12), the maximum sensor sensitivity of a bare single-anode sensor in a stirred medium can be approximated as

$$S = 12\pi D N_A C_{e-} r_0 \frac{R}{R - r_0} ,$$
(S13)

which is by a factor of $R/(R-r_0)$ greater than the sensitivity in an unstirred medium. When the diffusive boundary layer is thin, such as during vigorous stirring of the medium, R may become close to r_0 and the enhancement factor may increase considerably. For example, sensitivity may increase twice to ~240 pA µM^{-1} when R = 30 µm is used, whereas it can increase 8.5 times to ~1 nA µM^{-1} for R = 17 µm.

Influence of the guard anode on fluctuations of the background current
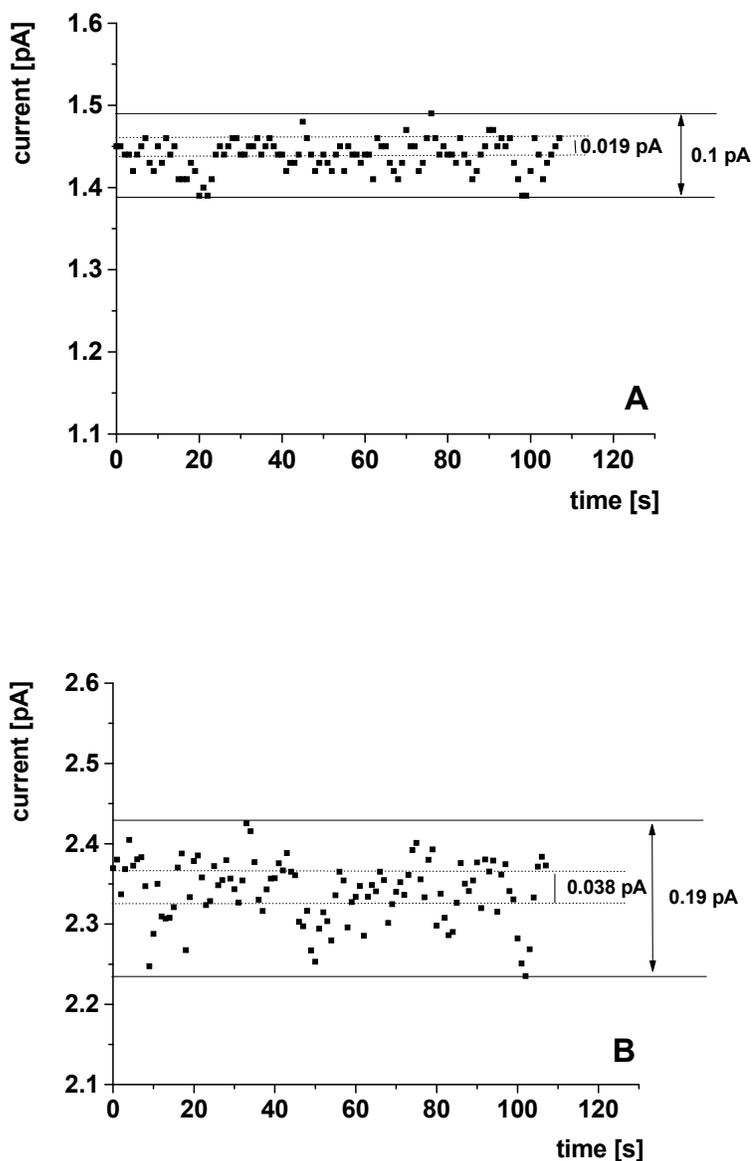
Figure S3. Fluctuations of a background current of a combined NO microsensor (A) with and (B) without a connected guard anode. The sensor was connected with the guard anode for ~1 month beforehand and currents were recorded after disconnecting the guard anode and after reconnecting the guard anode again. Solid lines represent maximum difference between 107 subsequent recordings, while dotted lines represent their standard deviation.

Supplementary References

1. **Dade, W. B., Hogg, A.J. & Boudreau, B.P.** 2001. Physics of Flow above the sediment-water interface. *In* B. P. J. Boudreau, B.B. (ed.), The Benthic Boundary Layer: Transport Processes and Biogeochemistry. Oxford University Press, Oxford.
2. **Mowery, K. A., and M. E. Meyerhoff.** 1999. The transport of nitric oxide through various polymeric matrices. Polymer **40:**6203-6207.
3. **Zacharia, I. G., and W. M. Deen.** 2005. Diffusivity and solubility of nitric oxide in water and saline. Annals of Biomedical Engineering **33:**214-222.

Chapter 3

Mechanisms of Transient Nitric Oxide and Nitrous Oxide Production in a Complex Biofilm

Frank Schreiber, Birte Loeffler, Lubos Polerecky, Marcel M. M. Kuypers, and Dirk de Beer

Max-Planck-Institute for Marine Microbiology, Bremen, Celsiusstr. 1, D-28359 Bremen, Germany

Abstract

Nitric oxide and N_2O are formed during N-cycling in complex microbial communities in response to fluctuating O_2 and NO_2^- concentrations. Until now, the formation of NO and N_2O in microbial communities has been measured with low spatial and temporal resolution, which hampered elucidation of the turnover pathways and their regulation. In this study, we combined microsensor measurements with metabolic modeling to investigate the functional response of a complex biofilm with nitrifying and denitrifying activity to variations in O_2 and NO_2^-. In steady state, NO and N_2O formation was detected if NH_4^+ was present under oxic conditions and if NO_2^- was present under anoxic conditions. Thus, NO and N_2O are produced by ammonia oxidizing bacteria (AOB) under oxic conditions and by heterotrophic denitrifiers under anoxic conditions. Nitric oxide and N_2O formation by AOB occurred at fully oxic conditions if NO_2^- concentrations were high. Modeling showed that steady state NO concentrations are controlled by the affinity of NO-consuming processes to NO. Transient accumulation of NO and N_2O occurred upon O_2 removal from, or NO_2^- addition to the medium only if NH_4^+ was present under oxic conditions or if NO_2^- was already present under anoxic conditions. This showed that AOB and heterotrophic denitrifiers need to be metabolically active to respond with instantaneous NO and N_2O production upon perturbations. Transiently-accumulated NO and N_2O decreased rapidly after their formation, indicating a direct effect of NO on the metabolism. By fitting model results to measurements, the kinetic relationships in the model were extended with dynamic parameters to predict transient NO release from perturbed ecosystems.

Introduction

Nitric oxide (NO) and nitrous oxide (N_2O) are produced and consumed by catabolic reactions of bacteria involved in the biogeochemical N-cycle. These reactions are fostered by increased anthropogenic N-input into the environment leading to a steadily increasing atmospheric N_2O concentration. This is of environmental concern, since the

infrared radiative forcing potential of N$_2$O is ~200 times that of CO$_2$, which makes N$_2$O a potent greenhouse gas (41). Moreover, NO and N$_2$O are involved in a set of catalytic reactions that transform ozone to molecular oxygen (O$_2$) in the stratosphere (12).

Denitrification and nitrification are generally considered to be the two main processes responsible for the formation of NO and N$_2$O (41). Heterotrophic denitrification is the respiratory, sequential reduction of nitrate (NO$_3^-$) or nitrite (NO$_2^-$) *via* NO and N$_2$O to N$_2$ (44). The key enzymes in denitrification are nitrite reductase (Nir), nitric oxide reductase (Nor) and nitrous oxide reductase (Nos). Nitric oxide levels in heterotrophic denitrifiers are well regulated, independent of NO$_3^-$ and NO$_2^-$ concentrations, and are in the range of low nanomolar concentrations (18). Nitric oxide consumption in heterotrophic denitrifiers might be mediated by widespread NO detoxifying enzymes, such as flavohemoglobins (Hmp or Fhp) and Flavorubredoxin (NorVW), or respiratory NorB that can reduce NO to N$_2$O (36).

Nitrification is the aerobic oxidation of ammonium (NH$_4^+$) performed by different groups of microorganisms. Ammonium oxidation to NO$_2^-$ (Aox) is performed by ammonia-oxidizing bacteria (AOB) or archaea (2, 26). In a next step, NO$_2^-$ is oxidized to NO$_3^-$ (Nox) by nitrite-oxidizing bacteria (NOB). Several studies have demonstrated the production of NO and N$_2$O by pure cultures of AOB (25, 31, 40), but the mechanism is not completely understood. Generally two different pathways are inferred. First, the activity of hydroxylamine oxidoreductase (HAO) converts hydroxylamine (NH$_2$OH) to NO$_2^-$ and releases small amounts of NO and N$_2$O (19). Second, the activity of nitrifier-encoded Nir and Nor reduces NO$_2^-$ to NO and N$_2$O in a process termed nitrifier denitrification (7, 34, 38). In both pathways, O$_2$ and NH$_4^+$ are required to form NH$_2$OH, the electron donor for NO$_2^-$ reduction.

Nitric oxide and N$_2$O turnover have also been studied in complex microbial communities. Studies in soils and nitrifying granules revealed that denitrification and nitrification are

the contributing microbial pathways. Commonly, NO and N_2O accumulation increased with decreased O_2 and with increased NO_2^- and NH_4^+ concentrations (10, 11, 23).

Change in environmental conditions leads to transient production of NO and N_2O in pure cultures of AOB and heterotrophic denitrifiers (5, 25), as well as in mixed microbial communities (23, 32). This transient production can lead to high concentrations and might thus contribute significantly to NO and N_2O emissions from various habitats. Despite the importance of transient NO and N_2O formation, the coupling and regulation of the responsible pathways remain poorly understood in complex microbial communities. This is primarily due to the fact that the experiments on release of NO and N_2O from natural samples commonly rely on analysis of the headspace volume or the bulk solution, which have no spatial and low temporal resolution. However, local conversion rates and limited transport in aggregated or attached microbial communities lead to stratification and to micro-environments that are different from the bulk solution. Thus, high spatial resolution measurements of NO, N_2O, and O_2, are required to distinguish between the contribution of aerobic (Aox) and anaerobic (heterotrophic denitrification) processes to NO and N_2O emission from stratified ecosystems where nitrification and denitrification co-occurs. In addition, high temporal resolution measurements during system perturbation are a powerful method for unraveling complex sets of processes and to obtain insights into the coupling of different pathways.

The objective of this study was to assign NO and N_2O production to nitrifying or denitrifying processes occurring in a complex biofilm. Furthermore, we aimed to quantify the influence of O_2, and NO_2^- fluctuations and of metabolic state on the dynamics of the transient NO and N_2O formation. We conducted microsensor measurements with high spatial and temporal resolution to characterize *in situ* micro-environmental conditions, quantify the rates of the relevant processes and follow NO and N_2O formation upon perturbations. Furthermore, we developed a novel metabolic model that allowed numerical simulations of the measured NO transitions. Based on this model, we propose

mechanisms that explain transient turnover of NO and N$_2$O by AOB and associated heterotrophic denitrifiers in the studied biofilm.

Materials and Methods

Biofilm growth

Biofilms were grown in an aerated flow cell (~ 800 mL) using tygon tubing as a surface for biofilm growth. The inoculum was obtained from a sewage treatment plant (Seehausen, Bremen) and was fed with medium at a flow rate of 1 mL min^{-1}. Biofilms with a thickness of 0.4-0.7 mm developed within 2-3 months in a medium consisting of 10 mM NH$_4$Cl and trace elements at final concentrations of 3 μM Na$_2$-EDTA, 1.5 μM FeSO$_4$, 77 nM H$_3$BO$_4$, 100 nM MnCl$_2$, 160 nM CoCl$_2$, 20 nM NiCl$_2$, 2.4 nM CuCl$_2$, 100 nM ZnSO$_4$, and 30 nM Na$_2$MoO$_4$ in tap water at pH 7.4. One month prior to the measurements, the medium was changed to a phosphate buffered artificial freshwater medium containing 17 mM NaCl, 2 mM MgCl$_2$, 0.9 mM CaCl$_2$, 6.7 mM KCl and 1.5 mM KH$_2$PO4/K$_2$HPO$_4$ pH 7.5, supplemented with 400 μM NH$_4$Cl and trace elements as stated before. For microsensor measurements, small pieces of the biofilm-covered tubing were transferred into a smaller flow cell (~ 80 mL) placed in an aquarium. The aquarium served as a reservoir for 1.7 L of aerated artificial freshwater medium (with or without NH$_4$Cl) that re-circulated through the small flow cell at a flow rate of 3 mL s^{-1} to create a constant flow of ~ 0.2 cm s^{-1} above the biofilm.

Experimental design

After biofilms adjusted to the conditions in the small flow cell for one to two days, steady state microprofiles of O$_2$, pH, NH$_4^+$, NO$_2^-$, NO$_3^-$, N$_2$O, and NO were measured in the presence of 400 or 0 μM NH$_4$Cl and at varying O$_2$ and NO$_2^-$ concentrations in the overlying water. The metabolic response of the biofilms was studied by changing the

conditions in the aquarium in the following sequence; (i) starting condition with O_2 at air saturation, (ii) switching to low O_2 (~3% air saturation) by purging the medium with N_2, (iii) addition of 3 mM $NaNO_2$ with O_2 at air saturation, and (iv) switching to low O_2 (~3 % air saturation) in the presence of 3 mM $NaNO_2$. The response to the addition of 3 mM $NaNO_2$ at low O_2 was investigated in separate experiments. Transient concentration changes of NO, N_2O and O_2 were monitored inside the biofilm upon switching the conditions until a new steady state was reached. The re-circulated media was sampled regularly to test for NO_3^- and NO_2^- accumulation from NH_4^+, stability of NH_4^+ concentrations, pH, and temperature. Nitrate and NO_2^- accumulated only in the presence of NH_4^+, and reached maximum concentrations of approximately 30 μM and 5 μM, respectively. Ammonium did not decrease below 370 μM. The temperature was 25 - 26 °C, and the pH was 7.2 - 7.3.

Microsensor measurements

Concentrations of O_2, N_2O, and NO were measured with amperometric microsensors, whereas liquid-ion-exchange (LIX) microsensors were used for pH, NH_4^+, NO_2^-, and NO_3^- measurements. Microsensors were prepared and calibrated as previously described (1, 13, 14, 35, 39). Vertical concentration profiles were measured with the microsensor mounted on a 3-axis micromanipulator (MM 33; Märzhäuser, Wetzlar, Germany). The vertical axis was motorized for μ-positioning (VT-80 linear stage, Micos, Germany, equipped with a 3564-K-024-BC motor, Faulhaber Group, Schönaich, Germany), and measurements were controlled by μ-Profiler software (www.microsen-wiki.net). The microsensor tip was adjusted manually to the sample surface with the help of a dissection microscope (Stemi SV 6; Carl Zeiss AG, Oberkochen, Germany).

Diffusive fluxes across the liquid-biofilm interface were calculated from the concentration gradients multiplied by the molecular diffusion coefficient, D, as previously described. Values used for D were 2.34×10^{-9} m^2 s^{-1} for O_2, 1.98×10^{-9} m^2 s^{-1}

for NH$_4^+$, 1.86 × 10^{-9} m^2 s^{-1} for NO$_2^-$, 1.92 × 10^{-9} m^2 s^{-1} for NO$_3^-$, 2.36 × 10^{-9} m^2 s^{-1} for N$_2$O, and 2.21 × 10^{-9} m^2 s^{-1} for NO (8, 30, 43).

Metabolic modeling of NO production

We developed an N-cycle model that couples processes involved in the production and consumption of NO, O$_2$, and NO$_2^-$ in the biofilm (Figure 4). We assumed that NH$_4^+$ was aerobically converted to NO$_2^-$ by NH$_4^+$ oxidation (Aox), and NO$_2^-$ subsequently converted to NO$_3^-$ by NO$_2^-$ oxidation (Nox). Anaerobic conditions favor NO$_2^-$ consumption by heterotrophic denitrification (hD). This results in the formation of NO, which is consumed in a sequential step by heterotrophic denitrification (hD-NO). Nitrifier denitrification by NH$_4^+$-dependent AOB (niD) produced NO aerobically from NO$_2^-$. Subsequently, NO is consumed by nitrifier denitrification (niD-NO). In addition, the model incorporated chemical NO oxidation with O$_2$ to NO$_2^-$ (chem) and O$_2$ consumption by heterotrophic respiration (hR).

This model was implemented numerically in Matlab (Mathworks Inc., USA, the code is available at www.microsen-wiki.net) to describe the kinetic, metabolic, and mass-transfer control of NO, O$_2$ and NO$_2^-$ in the biofilm. We assumed that the biofilm was laterally homogeneous and transport was governed by diffusion. Thus, the dynamics of a solute with concentration C (mol m^{-3}) in and above the biofilm was described by a one-dimensional diffusion-reaction equation

$$\frac{\partial C}{\partial t} = D_C \frac{\partial^2 C}{\partial z^2} + R_C . \tag{1}$$

Here, C denotes concentration of NO, NO$_2^-$, or O$_2$, D_C is the corresponding diffusion coefficient in water (in m^2 s^{-1}), which was assumed to be constant throughout the biofilm, and R_C (mol m^{-3} s^{-1}) is the net reaction rate at which the solute is produced or consumed. Both C and R_C were explicit functions of time, t, and depth, z, with $z > 0$ and $z < 0$

corresponding to the biofilm and overlying water, respectively. Based on the scheme in Figure 4, the net reaction rates R_C for NO, O_2, and NO_2^- were stochiometrically balanced and expressed as

$$R_{NO} = 8R^{niD} - 4R^{niD-NO} + R^{hD} - 1R^{hD-NO} - 4R^{chem} \tag{2a}$$

$$R_{O_2} = -1R^{niD} - 1R^{niD-NO} - 3R^{Aox} - 1R^{Nox} - 1R^{hR} - 1R^{chem} \tag{2b}$$

$$R_{NO_2^-} = -6R^{niD} + 2R^{Aox} - R^{hD} - 2R^{Nox} + 4R^{chem} . \tag{2c}$$

Each individual rate was an explicit function of the concentrations of the solutes involved in the process and is described in detail in the Supplement (Table S1).

Kinetic control of the reaction rates R^i was described by the Michaelis-Menten law,

$$R^i(C) = v_{max}^i \cdot \frac{C}{K_C^i + C} = v_{max}^i \cdot M(C, K_C^i) , \tag{3}$$

where K_C^i (mol m^{-3}) is the affinity constant of the process i to substrate C, v_{max}^i (mol m^{-3} s^{-1}) is the maximum rate of the process i, and M denotes the Michaelis-Menten function describing the relationship between affinity and concentration without v_{max}. The affinity constants were obtained from the literature and the maximum rates were derived from the measured steady state fluxes at the liquid-biofilm interface (as in Table 1 and 2) divided by the biofilm thickness. The maximum rates of NO-consuming processes (niD-NO under oxic conditions and hD-NO under anoxic conditions) were determined by assuming that both processes were coupled to the respective production process. This allowed subtraction of the net NO production rate from the rate of the NO-producing process, which was determined from NO_2^- consumption.

Metabolic control of the reaction rates was implemented by combining information available from pure culture studies with postulated mechanisms based on data presented

in this work. First, maximum activity of NO production (R^{hD}) and NO consumption by heterotrophic denitrification (R^{hD-NO}) occurred at micro-oxic to anoxic conditions, i.e., at O$_2$ below a certain threshold concentration $\Theta^i_{O_2}$. This was implemented by multiplying the maximum reaction rates, v^{hD}_{max} and v^{hD-NO}_{max}, with a threshold function

$$T(C,\Theta^i_C,\delta^i_C) = \frac{1}{1+\exp^{\frac{C-\Theta^i_C}{\delta^i_C}}} \,, \tag{4}$$

where δ^i_C represents the width of the concentration interval over which the threshold function changes, from 1 to 0 (see Figure S1). Furthermore, NO production by nitrifier denitrification (R^{niD}) was allowed only at low O$_2$ or high NO$_2^-$ concentrations, which was achieved by multiplying the corresponding v^{niD}_{max} value with an extended threshold function (see Figure S2)

$$\widetilde{T}\left(NO_2^-,O_2,\Theta^{niD}_{NO_2^-},\Theta^{niD}_{O_2},\delta^{niD}_{NO_2^-},\delta^{niD}_{O_2}\right) = \frac{1-T(NO_2^-,\Theta^{niD}_{NO_2^-},\delta^{niD}_{NO_2^-})}{T(O_2,\Theta^{niD}_{O_2},\delta^{niD}_{O_2})+T(NO_2^-,\Theta^{niD}_{NO_2^-},\delta^{niD}_{NO_2^-})} \,. \tag{5}$$

Threshold values were chosen by biological reasoning and by matching the concentration dynamics observed in the measurements.

Second, our experimental data suggested that after the O$_2$ concentration has decreased below a certain threshold, and when NO$_2^-$ was simultaneously present in sufficient amounts, the rate of NO production by heterotrophic denitrification, R^{hD}, increased slowly with time (Figure 2D). This mechanism was implemented by further multiplying the v^{hD}_{max} value with the dynamic function

$$Dyn(t,t_0,\Delta t) = 1 - \exp^{\frac{-(t-t_0)}{\Delta t}} \,, \tag{6}$$

where t_0 is the time at which O_2 decreased below a threshold value $\Theta_{O2}^{hD} - 2\delta_{O2}^{hD}$ while NO_2^- was simultaneously present above 1 μM. The value of $\Delta t = 400$ s was estimated by fitting the measured dynamic increase of NO in the presence of NO_2^- after the conditions in the overlying water were switched from oxic to suboxic (Figure 2D). In contrast, the dynamic increase of heterotrophic denitrification towards its maximum rate was accelerated to $\Delta t = 4$ s if NO was present above $\Theta_{NO}^{hD} = 0.32$ μM. This assumption is based on reported evidence that NO serves as a signal for the expression of denitrification genes (45, 46).

Third, a shift mechanism (Sh) was implemented to model the instantaneous increase in NO concentration after NO_2^- was added under oxic conditions (Figure 3A). Reasoning for this mechanism was based on the assumption that HAO function is impaired by NO_2^-, leading to the release of NO that is reported to be an HAO-bound intermediate (2). This was implemented by removing a fraction, f, of the NO_2^- production rate by Aox from $R_{NO_2^-}$ in Eq. (2c) and adding it to the total net NO production rate R_{NO} in Eq. (2a) as a function

$$Sh(t,t_0,\Delta t) = f \cdot R_{Aox}.\exp^{\frac{-(t-t_0)}{\Delta t}}. \tag{7}$$

Here, t_0 is the time when NO_2^- reached a threshold concentration of $\Theta_{NO_2^-}^{Sh} = 200$ μM. The fraction of the shifted R^{Aox} decreased exponentially with time, resembling an adjustment of AOB metabolism after perturbation. The values of $f = 0.55$ and $\Delta t = 200$ s were estimated from the experimental data (Figure 3A).

The time-dependent diffusion-reaction equations (1) were solved for all solutes using boundary conditions: (i) solute concentrations were fixed to the concentrations in the overlying water, C_w, at the top of the diffusive boundary layer (DBL), i.e., $C(-z_{DBL}) = C_w$,

and (ii) the diffusive flux at the base of the biofilm was set to zero, i.e., $\partial C/\partial z(z_B) = 0$, where z_{DBL} and z_B denote the thickness of the DBL and the biofilm, respectively. Experimental perturbations that resulted in O$_2$ decrease and NO$_2^-$ increase in the medium were implemented by varying C$_w$ over time. Experiments performed in the absence of NH$_4^+$ were modeled by excluding all processes from NO, NO$_2^-$ and O$_2$ turnover that require NH$_4^+$ as electron donor, namely, Aox, nitrifier denitrification (niD), and NO consumption by nitrifier denitrification (niD-NO).

All parameters of the model are listed in Table S1 in the Supplement. When available, they were adjusted within a biologically reasonable range of values reported in the literature; otherwise, they were adjusted to match the experimental data presented in this work. In the paper, the model is used to interpret and discuss the experimental findings.

Results

Performance of the biofilm in steady state

For all compounds, the micro-profiles showed either production or consumption within the entire biofilm. Stratified zones of production and consumption were not apparent (Figures 1 and S4). Thus, the overall performance of the biofilm was estimated from the fluxes across the liquid-biofilm interface (Table 1). Maximum potentials of aerobic NH$_4^+$ oxidation (Aox), aerobic NO$_2^-$ oxidation (Nox), nitrifier denitrification, and heterotrophic denitrification were determined by creating the conditions such that only the process of interest occurred, and coupled processes were inhibited (Table 2).

The biofilm was fully oxic when the medium was aerated (Figure S4A). In the presence of O$_2$, NH$_4^+$ was completely converted to NO$_3^-$ with minor accumulation of NO$_2^-$ (Figure S4D) indicating that Aox and Nox occurred at similar rates (Table 1 and 2). The coupling between Aox and Nox was not affected by addition of 3 mM NO$_2^-$. This was indicated by

a similar 1:2:1 stoichiometry of NH_4^+, O_2, and NO_3^- fluxes in both, the absence and presence of NO_2^- (Table 1). However, in the presence of NH_4^+ and O_2, addition of NO_2^- induced nitrifier denitrification. Nitrifier denitrification was indicated by the fact that the gross NO_2^- uptake, calculated from net NO_2^- uptake from the medium and NO_2^- production by Aox, exceeded the maximum NO_2^- consumption potential of Nox (Table 2). The remaining NO_2^- was reduced by AOB, with a rate that was ~20 % of the NO_2^- production rate of Aox. Consumption of NH_4^+ and O_2 was slightly elevated in the presence of NO_2^- (Table 1). In the absence of NH_4^+, the potential for heterotrophic processes was detectable, which were probably performed at the expense of reduced organic carbon present in the biofilm. Under oxic conditions, heterotrophic respiration of O_2 accounted for ~15 % of the total O_2 consumption. In the absence of O_2, nitrite consumption by heterotrophic denitrification was ~50 % of the NO_2^- consumption by NOB (Table 1 and 2).

Table 1. Fluxes of measured solutes through the liquid-biofilm interface determined from micro-profiles in a biofilm with the medium containing 400 μM NH_4Cl.

	Flux [nmol cm^{-2} h^{-1}][a]			
	5 μM NO_2^- [b]		3 mM NO_2^- [b]	
Solute	100 % O_2 [c]	< 3 % O_2 [c]	100 % O_2 [c]	< 3% O_2 [c]
NO	0.066 ± 0.024 (7)	1 ± 0.26 (10)	1.56 ± 0.49 (10)	0.92 ± 0.22 (7)
N_2O	2.53 ± 1.16 (7)	1.55 ± 0.36 (10)	4.72 ± 0.71 (7)	5.35 ± 2.68 (4)
O_2	-404 ± 44 (7)	-27 ± 9 (3)	-455 ± 56 (11)	-18 ± 8 (4)
NH_4^+	-168 ± 31 (6)	24 ± 11 (6)	-218 ± 28 (3)[d]	-48 ± 22 (3)[d]
NO_3^-	210 ± 30 (6)	21 ± 9 (3)	208 ± 37 (4)	-7 ± 2 (4)
NO_2^-	9.6 ± 3.6 (9)	-13.9 ± 5.5 (6)	-43 ± 15 (3)[d]	-67 ± 39 (3)[d]

[a]Fluxes are presented as mean ± standard error (number of profiles indicated in parentheses). Negative and positive values indicate net uptake and release of the solute, respectively. [b]Nitrite concentration in the medium; [c]Values are given as % air saturation in the medium; [d]Measured at 250 μM NO_2^- instead of 3 mM NO_2^- because the sensitivity of the NO_2^- sensor was too low at 3 mM. However, 250 μM did not limit the uptake.

The effects of NO_2^- and O_2 on the formation of NO and N_2O in NH_4^+-containing medium are summarized in Table 1 and Figure 1. In the presence of NH_4^+ and high NO_2^-, NO, and N_2O were produced regardless of the O_2 concentration in the medium. In contrast, at low NO_2^-, NO production was observed only under anoxic conditions, whereas N_2O production was low regardless of O_2. Nitrous oxide concentrations in the biofilm were an order of magnitude higher than NO concentrations, with NO ranging from < 0.02 to 0.35 µM and N_2O from 0.35 to 5.4 µM. In the presence of high NO_2^-, the yields were 0.007 mol NO per mol NH_4^+ and 0.022 mol N_2O per mol NH_4^+. At low NO_2^-, the N_2O yield was reduced to 0.015 mol N_2O per mol NH_4^+ (Table 1). In the absence of NH_4^+ and NO_2^-, NO and N_2O fluxes were negligible regardless of O_2. However, in the absence of NH_4^+ and presence of NO_2^-, NO and N_2O were produced, but only under anoxic conditions (Figure S6). The resulting fluxes were in the same range as those observed in the presence of NH_4^+ and NO_2^- under anoxic conditions.

Table 2. Maximum activities of selected processes in the biofilm under different conditions.

Process[a]	Measured parameter	Condition $NH_4^{+\,[b]}$/$NO_2^{-\,[b]}$/O_2 [c]	J[d]	Calculation	Rate of process[e]
hR	O_2	0 / 0 / 100	- 52	-	$J_{O_2}^{hR} = -52$
Nox	O_2	0 / 200 / 100	- 154	$J_{O_2}^{Nox} = J_{O_2} - J_{O_2}^{hR} = 0.5 J_{NO_2^-}^{Nox}$	$J_{NO_2^-}^{Nox} = -204$
Aox	NH_4^+	400 / 5 / 100	- 218	$J_{NH_4^+} = J_{NO_2^-}^{Aox}$	$J_{NO_2^-}^{Aox} = +218$
niD	NO_2^-	400 / 250 / 100	-43	$J_{NO_2^-}^{niD} = J_{NO_2^-} - J_{NO_2^-}^{Aox} - J_{NO_2^-}^{Nox}$	$J_{NO_2^-}^{niD} = -57$
hD	NO_2^-	0 / 250 /3	-102	-	$J_{NO_2^-}^{hD} = -102$

[a] see Figure 4 or text for explanation of the abbreviations; [b] [µM]; [c] [%] air saturation; [d] J - Flux [nmol cm^{-2} h^{-1}] through the liquid-biofilm interface presented as the net areal uptake rate of a certain solute by the biofilm or [e] as a gross areal rate caused by a process. Processes and compounds are indicated by superscript and subscript notations, respectively. Negative and positive values indicate consumption and production, respectively.
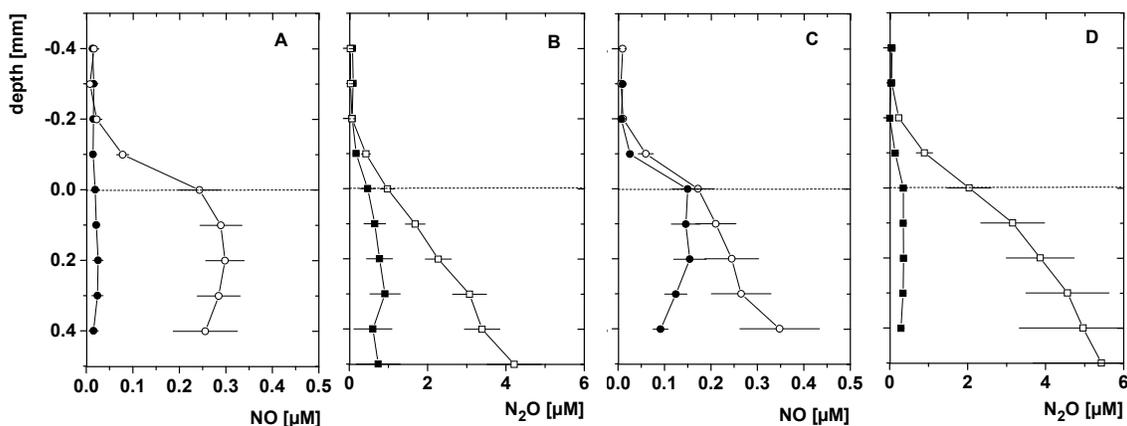
Figure 1. Averaged steady state microprofiles of NO **(A and C)** and N_2O **(B and D)** in a complex biofilm. Microprofiles were measured in artificial freshwater medium containing 400 µM NH_4Cl with 5 µM NO_2^- (filled symbols) or with 3 mM NO_2^- (open symbols) and during aeration **(A and B)** or N_2-purging **(C and D)** of the medium. The dashed line represents the biofilm surface. Horizontal bars represent standard errors (number of profiles is given in Table 2).

Transient NO and N_2O formation in response to O_2 and NO_2^- changes

Upon the start of N_2-purging, O_2 decreased gradually in the biofilm until anoxic conditions were reached. The transient phase lasted ~7 min in the presence of NH_4^+ and ~12 min in the absence of NH_4^+ (Figure S3). During this transition, highly dynamic concentration changes of NO and N_2O were detected with microsensors positioned in the biofilm at 200 µm depth (Figure 2 A-D). Decreasing O_2 concentrations in the presence of NH_4^+ caused a transient accumulation of NO and N_2O, which decreased to a new steady state after anoxic conditions were reached (Figure 2A-B). Although the accumulation was more pronounced at high NO_2^- concentration, the final steady state levels were on average comparable to those observed at low NO_2^- (see also Figure 1C). Control measurements showed that in the absence of NH_4^+ and NO_2^-, NO and N_2O were neither produced nor consumed during the decrease of O_2 concentration (Figure 2C). In contrast, the absence of NH_4^+ at high NO_2^- concentration resulted in slow formation of NO and N_2O, starting shortly before anoxic conditions were reached (Figure 2D).
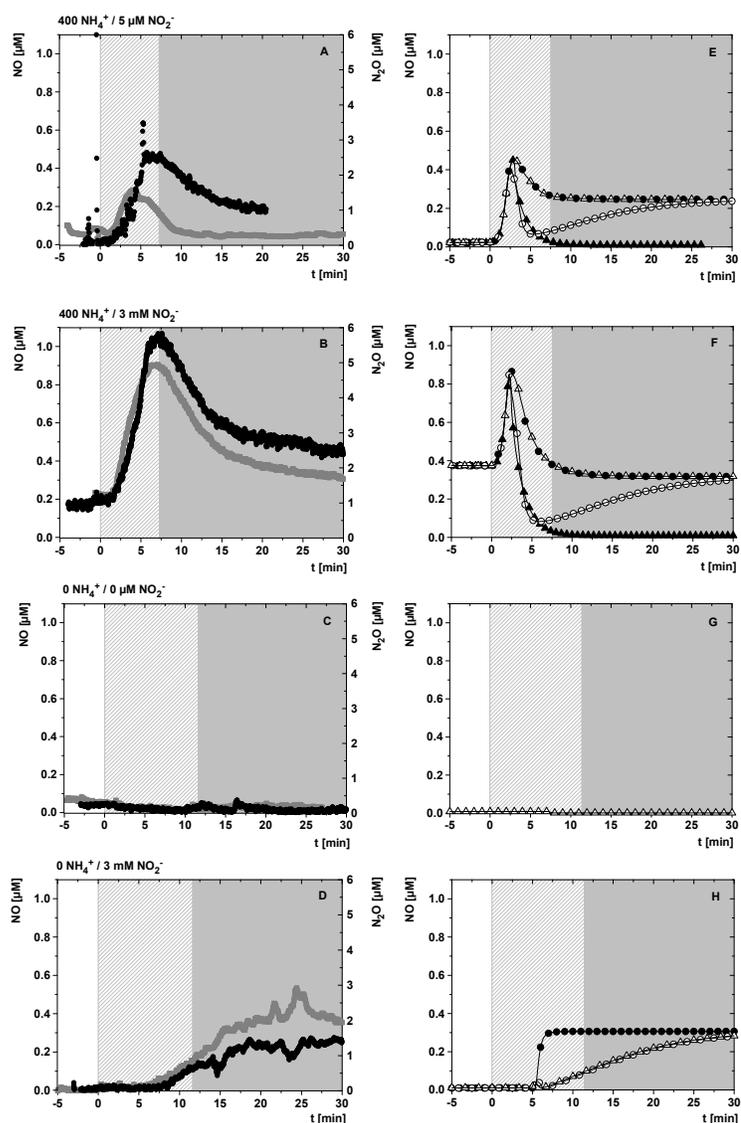
Figure 2. (A-D) Time series of measured NO (black line) and N₂O (grey line) concentrations with microsensors inserted in the biofilm at 200 μm depth. Purging of the medium with N₂ started at t = 0 min. **(E-H)** Time series of NO derived from the model shown in Figure 4. In each row, the boundary conditions and perturbations were implemented in the model such that they corresponded to the conditions applied during the measurement. Different stages of the model are shown, including (i) the model governed by kinetics and thresholds only (T and $\widetilde{T}$; equations 4 and 5; filled circles), (ii) the model implementing the dynamic function (Dyn, equation 6) on heterotrophic denitrification (open circles), (iii) the model implementing the dynamic function controlled by NO concentration (open triangles), (iv) and the model implementing NO loss by diffusion after stopping all processes when the peak NO concentration was reached (filled triangles). White background indicates oxic, shaded areas the transient phase from oxic to anoxic, and grey areas indicate anoxic conditions. The medium composition with respect to NH₄⁺ and NO₂⁻ is depicted at the top-left of each row.

When NO_2^- was added under oxic conditions, NO concentration increased within less than a minute from below the detection limit to 1.2 μM, after which it decreased within 20 min to a new steady state. This was observed only if NH_4^+ was present (Figure 3A). In the absence of O_2, concentrations of NO increased upon the addition of NO_2^-. The presence of NH_4^+ did not influence the final NO steady state concentrations, but affected the kinetics of its formation. The presence of NH_4^+, which resulted in low concentrations of NO_2^- and NO_3^- in the medium, caused an instantaneous increase of NO from slightly elevated levels, whereas NO formed slowly in the absence of NH_4^+ (Figure 3B).
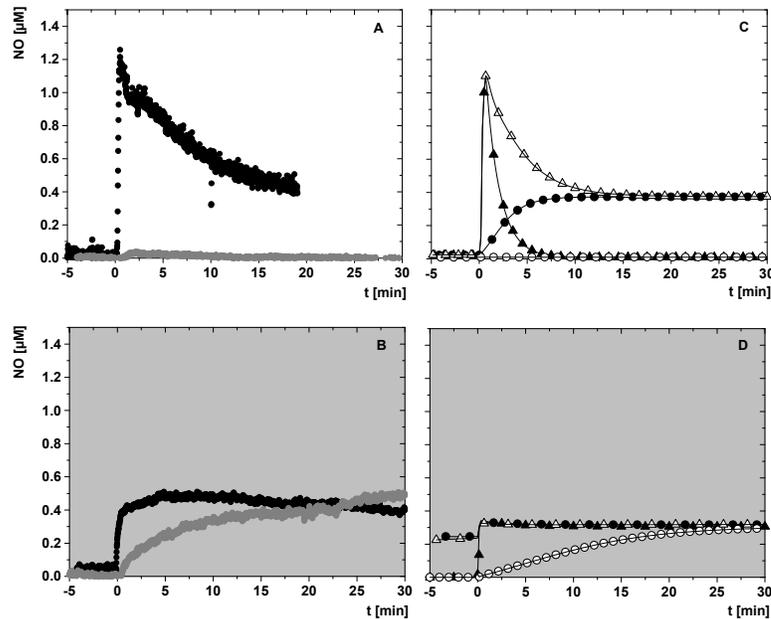
Figure 3. (A – B) Time series of NO measured with a microsensor inserted in the biofilm at 200 μm depth. 3 mM NO_2^- were added at t = 0 min to the medium containing 400 μM NH_4^+ and ~ 5/30 μM NO_2^-/NO_3^- (black line) or to the medium that did not contain NH_4^+ and NO_2^-/NO_3^- (grey line). White and grey backgrounds indicate oxic and anoxic conditions, respectively. **(C – D)** Time series of NO derived from the model (see Figure 4). In each row, the boundary conditions and perturbations were implemented in the model such that they corresponded to the conditions applied during the measurement. Different symbols depict different stages of the model. In panel **(C)**, this includes the model governed by kinetics and thresholds only (filled circles), the model additionally implementing a shift function (Sh) that resulted in the production of NO instead of NO_2^- by Aox (open triangles), the model implementing NO loss by diffusion after stopping all processes when the peak NO concentration was reached (filled triangles), and the control condition where all NH_4^+-dependent processes were switched off (open circles). In panel **(D)**, this includes the model governed by kinetics and thresholds only (filled circles), with the dynamic function added (open triangles), and the model in the absence of NH_4^+-dependent processes governed by kinetics and thresholds only (closed triangles) or with the dynamic function included (open circles).

Discussion

Regulation of steady state NO and N$_2$O production by ammonium oxidation under oxic conditions and by heterotrophic denitrification under anoxic conditions

Nitric oxide and N$_2$O formation within a complex N-cycling community could be mediated by processes, such as aerobic NH$_4^+$ oxidation (Aox), aerobic NO$_2^-$ oxidation (Nox), heterotrophic denitrification or anaerobic oxidation of NH$_4^+$ (anammox) (17, 24, 41). Measuring the *in situ* activities and micro-environmental conditions enabled us to assign concomitant NO and N$_2$O formation to active processes.
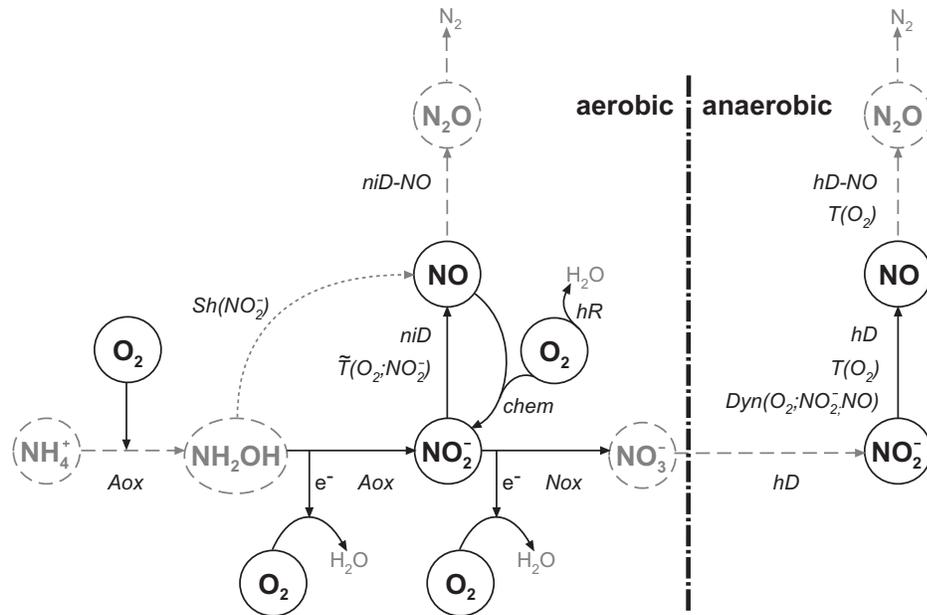
Figure 4. Schematic representation of the metabolic model of NO turnover in a complex biofilm. Pathways and compounds marked by solid black lines were calculated by the numerical model, whereas those marked with grey dashed lines were not calculated. Italic text next to the arrows indicates the pathways: Aox – Ammonium oxidation; Nox – Nitrite oxidation; niD – NO production by nitrifier denitrification; niD-NO NO consumption by nitrifier denitrification; hD – NO production by heterotrophic denitrification; hD-NO – NO consumption by heterotrophic denitrification; hR – heterotrophic oxygen respiration; chem. – chemical NO oxidation. Additional mechanisms that influence the rate of the respective pathway, with the compounds that affect those mechanisms in parentheses are indicated by T – threshold, $\tilde{T}$ – extended threshold, Dyn – dynamic function, and Sh – Shift function (see text and equations 4, 5, 6 and 7 for details).

Ammonium oxidation in steady state. AOB require NH_4^+ and O_2 to form NO and N_2O either *via* the HAO pathway or by nitrifier denitrification. The present data showed that NO and N_2O formation under oxic conditions depended on the presence of NH_4^+. Nitric oxide and N_2O formation did not occur upon addition of NO_2^- when NH_4^+ was absent (Figures 3A, S6A and S6B). These experiments showed that under oxic conditions, NO and N_2O were formed by AOB, but not by NOB or (aerobic) heterotrophic denitrifiers. Previous studies emphasized the dependence of nitrifier denitrification on reduced O_2 and elevated NO_2^- concentrations (3, 23, 25, 31, 34). Our experiments showed that nitrifier denitrification and simultaneous NO and N_2O formation occurs at high NO_2^- concentrations even if O_2 concentrations are high (Figures 1A, 3A and S4A). This was previously observed for *Nitrosomonas europaea* and *Nitrosospira spp.* (40). Moreover, it has been shown that denitrifying enzymes (NirK and NorB) in *N. europaea* are expressed under fully oxic conditions (3, 4).

In the model, NO production by nitrifier denitrification was kinetically controlled by O_2 and NO_2^-. The resulting steady state NO concentration was kinetically controlled by the affinity of NO consumption by nitrifier denitrification to NO. However, NO production was only measured at high NO_2^- concentrations *or* under micro-oxic conditions. This indicates that NO accumulation under those conditions was controlled by NO production. To limit NO production in the model to high NO_2^- and low O_2 conditions, we implemented an extended threshold function ($\tilde{T}$ equation 5, Figure S2). This allowed an independent influence of O_2 and NO_2^- on NO production with a restricted maximum rate, excluding additive effects when both conditions were present at the same time.

Heterotrophic denitrification in steady state. Earlier studies have reported the ability of AOB pure cultures to produce NO under anoxic conditions (25, 37) and reported that in a nitrifying mixed culture, NH_4^+ affected anaerobic NO formation in a concentration-dependent manner (23). Conversely, we found that under anoxic conditions, NO and N_2O formation did not depend on the presence of NH_4^+, and was only observed when NO_2^- and NO_3^- were present. This showed that heterotrophic denitrifiers, but not O_2-depending

AOB, were responsible for NO and N$_2$O formation under anoxic conditions. The dependence of NO and N$_2$O formation on NO$_2^-$ was confirmed under anoxic conditions in the absence of NH$_4^+$ (Figures S6C and D). In the presence of NH$_4^+$, nitrification lead to accumulation of approximately 5 μM NO$_2^-$ and 30 μM NO$_3^-$ in the medium prior to N$_2$-purging. Nitrate and NO$_2^-$ served as electron acceptors for heterotrophic denitrification under subsequent anoxic conditions. This explains the formation of NO and N$_2$O under anoxic conditions by heterotrophic denitrification in the presence of NH$_4^+$ but not in its absence. Anammox could drive NH$_4^+$ oxidation and NO$_2^-$ reduction under anoxic conditions, and could account for NO and N$_2$O formation. However, the biofilms grew under oxic conditions, which hamper growth of anammox bacteria (42). Furthermore, NO$_2^-$ -uptake of the biofilm under anoxic conditions was similar in the presence and the absence of NH$_4^+$ (Table 1 & 2), indicating that anammox did not contribute to additional NO$_2^-$ reduction.

In the model, Michaelis-Menten kinetic dependence of heterotrophic denitrification on NO$_2^-$ allowed NO production in the presence of NO$_2^-$, while threshold functions for O$_2$ restricted the process to anoxic conditions. The measured steady state NO concentrations can be modeled (Figures 2 and 3) by kinetically controlling its accumulation with low K$_m$-values for the NO consumption pathways, as has been described elsewhere (6). As a result, steady state NO concentrations under anoxia were more or less independent of NO$_2^-$ concentrations, even though NO$_2^-$ concentrations varied over ~3 orders of magnitude, corresponding to observations in pure culture studies (18). In addition, the K$_m$-value of heterotrophic denitrifiers for NO$_2^-$ was very low in the model, which resulted in a minor increase of NO production due to the additional NO$_2^-$. In contrast, measured N$_2$O, the sequential product of NO reduction, showed a marked increase in the presence of high NO$_2^-$ concentrations. Thus, in heterotrophic denitrifiers, accumulation of NO may not occur at high NO$_2^-$ concentrations due to efficient reduction of NO to N$_2$O.

Furthermore, the model showed that chemical NO consumption under oxic conditions was always several orders of magnitude lower than the biological rate, and contributed

insignificantly to the total NO loss. Chemical production of NO from acidic decomposition of NO_2^- did not play a role, because the pH measured in the biofilms did not drop below 6.5 (Figures S5A and B).

A recently described model was able to assign NO accumulation in a nitrifying reactor to nitrifier denitrification by implementing kinetic control, and by modeling different production scenarios independent from each other (22). In our model, the use of threshold functions affected by O_2 and NO_2^- concentrations in addition to Michaelis-Menten kinetics enabled us to consider all possible NO-producing pathways simultaneously under varying conditions.

Perturbations of active ammonia oxidation and heterotrophic denitrification causes instantaneous NO and N₂O formation

The time series measurements showed that NO and N_2O reached transient maxima within the biofilm upon decreasing O_2 and adding NO_2^-. This phenomenon was also observed in studies with pure cultures of AOB and heterotrophic denitrifiers (5, 25), as well as with mixed microbial communities (23, 32). However, these observations are not completely understood. We observed transient maxima of NO and N_2O only when either Aox or heterotrophic denitrification was actively performed before O_2 and NO_2^- changed. We conclude that the instantaneous formation of NO and N_2O is caused by perturbation of the active pathways on the enzyme level, resulting in an imbalance of the fine-tuned mechanisms that maintain NO homeostasis. Nitric oxide and N_2O dynamics following perturbation were similar, demonstrating that they are sequentially produced by AOB and heterotrophic denitrifiers. The model can be extended to N_2O concentrations if K_m-values for N_2O reduction are available.

Heterotrophic denitrification in transient states. Nitrite additions were followed by instantaneous NO formation, but only if NO_2^- and NO_3^- were present at low concentrations and if O_2 was absent before the perturbation (Figure 3B). Under such

conditions, only heterotrophic denitrification can cause NO formation. The instantaneous formation of NO upon NO$_2^-$ addition shows that NO producing and consuming enzymes are directly affected by NO$_2^-$ and that *de novo* synthesis of enzymes cannot explain the dynamics. For example, it was demonstrated previously that NO$_2^-$ can directly inhibit Nor (28, 29), which would lead to accumulation of NO. In addition, kinetics of NO$_2^-$ and NO-reducing enzymes might allow NO accumulation depending on the NO$_2^-$ concentration. Instantaneous NO production was modeled by assuming that full expression of heterotrophic denitrification potential requires the absence of O$_2$ and the presence of NO$_2^-$ (45). Under conditions allowing full expression of heterotrophic denitrification, kinetics explained the instantaneous increase of NO upon addition of NO$_2^-$ in the model (Figures 3B black line and 3D filled circles).

In contrast, measured NO increased slowly if the conditions before the perturbation did not allow full expression of denitrification (i.e., the presence of O$_2$ or absence of NO$_2^-$; Figures 2D black line and 3B grey line). We assumed that in these cases, removal of O$_2$ (Figure 2D) or addition of NO$_2^-$ (Figure 3B) results in the expression of denitrification enzymes. The subsequent slow NO increase was modeled by implementing a dynamic function (Dyn; equation 6) in addition to the kinetic control (Figures 2H and 3D open circles). Modeling without the dynamic function resulted in an instantaneous increase of NO for transients upon O$_2$ removal and NO$_2^-$ addition (Figures 2H filled circles and 3D filled triangles), because in this case, the expression of heterotrophic denitrification was assumed to be constitutive. This shows that the requirements for the expression of enzymes for heterotrophic denitrification, and their slow expression when all conditions are met, needs to be included when modeling transient NO accumulation.

Ammonium oxidation in transient states. The measurements showed that NO formed instantaneously if O$_2$ was removed or NO$_2^-$ was added, but only if NH$_4^+$ was available to allow active Aox before the perturbation. AOB form NO and N$_2$O *via* the HAO pathway or by nitrifier denitrification (2). Both pathways might contribute to NO and N$_2$O formation, but cannot be separated from each other by our experiments. Our model

showed that the instantaneous transient increases of NO concentrations caused by AOB upon NO_2^- addition (Figure 3A) cannot be explained solely with NO production by nitrifier denitrification. Here, NO increased slowly to steady state because of the delayed diffusion of NO_2^- into the biofilm matrix (Figure 3C filled circles). The transients upon NO_2^- addition were satisfactorily modeled by implementing a shift function (Sh; equation 7), which resulted in the production of NO instead of NO_2^- from NH_4^+ when NO_2^- concentrations increased above a certain threshold ($\Theta_{NO_2^-}^{Sh}$ = 200 µM) (Figure 3C open triangles). The successful use of this function supports our hypothesis that NO formation by AOB occurs if their active metabolism is disturbed by NO_2^- that possibly impairs the smooth functioning of HAO (2).

AOB-dependent transient increase of NO during O_2 decrease in the model resulted from a micro-oxic threshold imposed on NO production by nitrifier denitrification ($\Theta_{O_2}^{niD}$ = 40 µM) (Figure 2E and F, filled circles). The increase of NO during micro-oxic conditions was not counteracted by NO consumption due to nitrifier denitrification (niD-NO) because O_2 disappeared before the K_m-value for NO (0.6 µM) was reached. Rather, the onset of anoxia resulted in the decline of NO production by nitrifier denitrification (niD) because of kinetic limitations by the substrate O_2. The modeled results suggests that nitrifier denitrification metabolism is fully expressed under oxic conditions as reported by (3), resulting in instantaneous NO formation upon reduced O_2 concentrations. This increase cannot be counteracted until NO accumulates to concentrations equal to the K_m-value of the NO consumption pathway.

Direct regulation of NO and N_2O decrease after its transient accumulation

Nitric oxide and N_2O decreased to a new steady state level after they reached peak concentrations upon O_2 and NO_2^- concentrations were changed. Nitric oxide concentrations were always one order of magnitude below N_2O, indicating that regulation of potentially cytotoxic NO (20) is more critical than that of non-toxic N_2O, and that the

K$_m$-value of N$_2$O reduction is higher than that of NO reduction. The decrease of NO within minutes after the accumulation of NO indicates that genetic regulation cannot explain the dynamics. Instead, different metabolic pathways governed NO turnover after the conditions changed, or enzymes were directly affected after the peak was reached, e.g., by inhibition.

NO decrease after O$_2$ removal. The pathways governing NO turnover switched from nitrifier denitrification to heterotrophic denitrification between oxic and anoxic conditions (Figures 2A and B). Directly after nitrifier denitrification stops, heterotrophic denitrification cannot instantaneously start, as the enzymes must be expressed. Therefore, modeling with the dynamic function (Dyn; equation 6) showed a transient NO minimum when reaching anoxia, because NO was lost from the biofilm by diffusion and increased slowly thereafter (Figures 2E and F, filled triangles and open circles). However, we did not measure such a minimum, indicating that NO production continued directly after the transition. Possible explanations are that either nitrifier denitrification continued or the dynamic of expression of heterotrophic denitrification (Dyn, equation 6) was enhanced in the transient phase in response to NO. Modeling showed that the later scenario was not biologically feasible, because the expression of heterotrophic denitrification needed to be enhanced to be 100fold (Δt = 4s instead of 400s) faster than was calculated for the onset denitrification upon reduced O$_2$ (Figures 2E and F, open triangles and Figure 2H open circles). Alternatively, NO production by nitrifier denitrification might continue for a short time at anoxia with oxidizing compounds stored in the form of NH$_2$OH or oxidized cytochromes.

NO decrease after NO$_2^-$ addition. Oxygen concentrations remained stable upon the addition of NO$_2^-$, which prevented switching between Aox and heterotrophic denitrification that could affect NO. Thus, the instantaneous decrease of NO after reaching the peak concentration (Figures 3A and B) might be regulated by direct effects on the enzymes involved in NO turnover within the bacteria that produce NO. This is

supported by earlier studies, which showed that Nir and Nor can be inhibited by high NO concentrations in heterotrophic denitrifiers (9, 15, 27).

The model suggests that the transient NO maximum after the addition of NO_2^- was due to an imbalance of the AOB metabolism (Shift function, equation 7). Moreover, the decrease of the measured concentration from the maximum was slower than the modeled decrease by diffusion only (Figures 3A black line and 3 C filled triangles), indicating that NO production continued during the decrease. The model showed that if nitrifier denitrification is the only NO-producing process under oxic conditions, NO increased slowly after NO_2^- was added (Figure 3 C filled circles). Therefore, we propose that the direct formation of NO instead of NO_2^- continues with a decreasing rate after it becomes active. This implies that NO or NO_2^- concentrations directly affect the enzymes of AOB, resulting in the regulation of the metabolic imbalance.

Significance to NO and N$_2$O formation in the environment

The extent of transient NO and N_2O accumulation upon perturbation strongly indicates that it can significantly contribute to emissions of gaseous N-oxides into the atmosphere, especially from habitats exposed to fluctuations in O_2 and inorganic nitrogen compounds. It is possible that the large uncertainties about the sources in the global N_2O budget (41) are linked to the contribution of fluctuating emissions from ecosystems, which are not normally considered during measurements (e.g., measurements in chambers often impede exposure to environmental fluctuations).

Fluctuations in environmental conditions which affect O_2 and NO_2^- concentrations and thus lead to NO and N_2O production may occur in soils as a result of drying and wetting, or by a variable fertilizer input. Furthermore, estuaries are exposed to a fluctuating N-input through precipitation and fertilizer run-off from land. Large oceanic volumes are influenced by mixing of water masses with different O_2 and NO_2^- concentrations. For example, massive accumulation of N_2O was observed in the upper layer of the Arabian

Sea during severe upwelling-induced hypoxia on the western Indian shelf (33). Under these conditions, the upper layer of the water body is especially exposed to O$_2$ fluctuations caused by O$_2$ input through wave action. Hence, the fact that oceans are still considered a relatively minor source of N$_2$O in the global budget might be an underestimate linked to difficulties in measuring and modeling N$_2$O emissions during frequently-occurring, short-term environmental perturbations in marine waters. Presently, a linear, empirical-derived framework is employed in large-scale N$_2$O emission models (16, 21). The characteristics of the metabolic model, such as thresholds, dynamic function, and shift function, developed in this study to describe transient production mechanisms, may represent an important step towards more mechanism-based modeling.

Conclusions

In conclusion, characterization of micro-environmental conditions is required to determine the source of NO and N$_2$O production in complex, stratified environments. The presence of O$_2$ determines whether NO and N$_2$O are produced by AOB or by heterotrophic denitrifiers. Interestingly, NO and N$_2$O formation by AOB does not require micro-oxic conditions if NO$_2^-$ is present in high concentrations (mM range). On the other hand, NO production, but not N$_2$O production, by heterotrophic denitrifiers is almost independent of NO$_2^-$ concentrations. The high temporal resolution achieved by microsensors allowed the measurement of highly dynamic NO and N$_2$O formation following the change in O$_2$ and NO$_2^-$ concentrations. Interpretation of the results with a metabolic model showed that Aox and heterotrophic denitrification need to be actively performed to respond to perturbations in O$_2$ and NO$_2^-$ with instantaneous NO and N$_2$O production. The resulting transient accumulation is counteracted within minutes by regulating the NO turnover in the biofilm. This occurs either because a different pathway becomes active, or because enzymes involved in the production process are affected directly. At steady state, NO concentrations are regulated by kinetic control of the consumption processes. In a complex environment, massive formation of NO and N$_2$O may occur if a metabolically active N-cycling community is exposed to an external perturbation.

Acknowledgements

Author Contribution

The study was conceived by FS. Measurements were performed by FS and BL (in the frame of a B.Sc. thesis, Bionik, Hochschule Bremen). The data was analyzed by DdB, MMMK, LP and FS. Modeling was performed by LP and FS. The manuscript was written by FS with input of DdB, MMMK, and LP.

References

1. **Andersen, K., T. Kjaer, and N. P. Revsbech.** 2001. An oxygen insensitive microsensor for nitrous oxide. Sensors and Actuators B-Chemical **81:**42-48.
2. **Arp, D. J., and L. Y. Stein.** 2003. Metabolism of inorganic N compounds by ammonia-oxidizing bacteria. Critical Reviews in Biochemistry and Molecular Biology **38:**471-495.
3. **Beaumont, H. J. E., S. I. Lens, W. N. M. Reijnders, H. V. Westerhoff, and R. J. M. van Spanning.** 2004. Expression of nitrite reductase in Nitrosomonas europaea involves NsrR, a novel nitrite-sensitive transcription repressor. Molecular Microbiology **54:**148-158.
4. **Beaumont, H. J. E., B. van Schooten, S. I. Lens, H. V. Westerhoff, and R. J. M. van Spanning.** 2004. Nitrosomonas europaea expresses a nitric oxide reductase during nitrification. Journal of Bacteriology **186:**4417-4421.
5. **Bergaust, L., J. Shapleigh, A. Frostegard, and L. Bakken.** 2008. Transcription and activities of NOx reductases in Agrobacterium tumefaciens: the influence of nitrate, nitrite and oxygen availability. Environmental Microbiology **10:**3070-3081.
6. **Betlach, M. R., and J. M. Tiedje.** 1981. Kinetic Explanation for Accumulation of Nitrite, Nitric-Oxide, and Nitrous-Oxide During Bacterial Denitrification. Applied and Environmental Microbiology **42:**1074-1084.

7. **Bock, E., I. Schmidt, R. Stuven, and D. Zart.** 1995. Nitrogen Loss Caused by Denitrifying Nitrosomonas Cells Using Ammonium or Hydrogen as Electron-Donors and Nitrite as Electron-Acceptor. Archives of Microbiology **163:**16-20.
8. **Broecker, W. S., and T. H. Peng.** 1974. Gas-Exchange Rates between Air and Sea. Tellus **26:**21-35.
9. **Carr, G. J., and S. J. Ferguson.** 1990. Nitric-Oxide Formed by Nitrite Reductase of Paracoccus-Denitrificans Is Sufficiently Stable to Inhibit Cytochrome-Oxidase Activity and Is Reduced by Its Reductase under Aerobic Conditions. Biochimica Et Biophysica Acta **1017:**57-62.
10. **Colliver, B. B., and T. Stephenson.** 2000. Production of nitrogen oxide and dinitrogen oxide by autotrophic nitrifiers. Biotechnology Advances **18:**219-232.
11. **Conrad, R.** 1996. Soil microorganisms as controllers of atmospheric trace gases (H-2, CO, CH4, OCS, N2O, and NO). Microbiological Reviews **60:**609-+.
12. **Crutzen, P. J.** 1979. Role of No and No2 in the Chemistry of the Troposphere and Stratosphere. Annual Review of Earth and Planetary Sciences **7:**443-472.
13. **deBeer, D., A. Schramm, C. M. Santegoeds, and M. Kuhl.** 1997. A nitrite microsensor for profiling environmental biofilms. Applied and Environmental Microbiology **63:**973-977.
14. **Debeer, D., and J. C. Vandenheuvel.** 1988. Response of Ammonium-Selective Microelectrodes Based on the Neutral Carrier Nonactin. Talanta **35:**728-730.
15. **Dhesi, R., and R. Timkovich.** 1984. Patterns of Product Inhibition for Bacterial Nitrite Reductase. Biochemical and Biophysical Research Communications **123:**966-972.
16. **Duce, R. A., J. LaRoche, K. Altieri, K. R. Arrigo, A. R. Baker, D. G. Capone, S. Cornell, F. Dentener, J. Galloway, R. S. Ganeshram, R. J. Geider, T. Jickells, M. M. Kuypers, R. Langlois, P. S. Liss, S. M. Liu, J. J. Middelburg, C. M. Moore, S. Nickovic, A. Oschlies, T. Pedersen, J. Prospero, R. Schlitzer, S. Seitzinger, L. L. Sorensen, M. Uematsu, O. Ulloa, M. Voss, B. Ward, and L. Zamora.** 2008. Impacts of atmospheric anthropogenic nitrogen on the open ocean. Science **320:**893-897.
17. **Freitag, A., M. Rudert, and E. Bock.** 1987. Growth of Nitrobacter by Dissimilatoric Nitrate Reduction. Fems Microbiology Letters **48:**105-109.
18. **Goretski, J., O. C. Zafiriou, and T. C. Hollocher.** 1990. Steady-State Nitric-Oxide Concentrations During Denitrification. Journal of Biological Chemistry **265:**11535-11538.
19. **Hooper, A. B.** 1968. A Nitrite-Reducing Enzyme from Nitrosomonas Europaea - Preliminary Characterization with Hydroxylamine as Electron Donor. Biochimica Et Biophysica Acta **162:**49-&.
20. **James, S. L.** 1995. Role of Nitric-Oxide in Parasitic Infections. Microbiological Reviews **59:**533-&.
21. **Jin, X., and N. Gruber.** 2003. Offsetting the radiative benefit of ocean iron fertilization by enhancing N2O emissions. Geophysical Research Letters **30:**4.
22. **Kampschreur, M. J., C. Picioreanu, N. Tan, R. Kleerebezem, M. S. M. Jetten, and M. C. M. van Loosdrecht.** 2007. Unraveling the source of nitric oxide emission during nitrification. Water Environment Research **79:**2499-2509.

23. **Kampschreur, M. J., N. C. G. Tan, R. Kleerebezem, C. Picioreanu, M. S. M. Jetten, and M. C. M. Loosdrecht.** 2008. Effect of dynamic process conditions on nitrogen oxides emission from a nitrifying culture. Environmental Science & Technology **42:**429-435.

24. **Kartal, B., M. M. M. Kuypers, G. Lavik, J. Schalk, H. den Camp, M. S. M. Jetten, and M. Strous.** 2007. Anammox bacteria disguised as denitrifiers: nitrate reduction to dinitrogen gas via nitrite and ammonium. Environmental Microbiology **9:**635-642.

25. **Kester, R. A., W. deBoer, and H. J. Laanbroek.** 1997. Production of NO and N2O by pure cultures of nitrifying and denitrifying bacteria during changes in aeration. Applied and Environmental Microbiology **63:**3872-3877.

26. **Konneke, M., A. E. Bernhard, J. R. de la Torre, C. B. Walker, J. B. Waterbury, and D. A. Stahl.** 2005. Isolation of an autotrophic ammonia-oxidizing marine archaeon. Nature **437:**543-546.

27. **Koutny, M., and I. Kucera.** 1999. Kinetic analysis of substrate inhibition in nitric oxide reductase of Paracoccus denitrificans. Biochemical and Biophysical Research Communications **262:**562-564.

28. **Kucera, I.** 1992. Oscillations of Nitric-Oxide Concentration in the Perturbed Denitrification Pathway of Paracoccus-Denitrificans. Biochemical Journal **286:**111-116.

29. **Kucera, I., L. Kozak, and V. Dadak.** 1986. The Inhibitory Effect of Nitrite on the Oxidase Activity of Cells of Paracoccus-Denitrificans. Febs Letters **205:**333-336.

30. **Li, Y. H., and S. Gregory.** 1974. Diffusion of Ions in Sea-Water and in Deep-Sea Sediments. Geochimica Et Cosmochimica Acta **38:**703-714.

31. **Lipschultz, F., O. C. Zafiriou, S. C. Wofsy, M. B. McElroy, F. W. Valois, and S. W. Watson.** 1981. Production of No and N2o by Soil Nitrifying Bacteria. Nature **294:**641-643.

32. **Morley, N., E. M. Baggs, P. Dorsch, and L. Bakken.** 2008. Production of NO, N2O and N-2 by extracted soil bacteria, regulation by NO2- and O-2 concentrations. Fems Microbiology Ecology **65:**102-112.

33. **Naqvi, S. W. A., D. A. Jayakumar, P. V. Narvekar, H. Naik, V. Sarma, W. D'Souza, S. Joseph, and M. D. George.** 2000. Increased marine production of N2O due to intensifying anoxia on the Indian continental shelf. Nature **408:**346-349.

34. **Poth, M., and D. D. Focht.** 1985. N-15 Kinetic-Analysis of N2o Production by Nitrosomonas-Europaea - an Examination of Nitrifier Denitrification. Applied and Environmental Microbiology **49:**1134-1141.

35. **Revsbech, N. P.** 1989. An Oxygen Microsensor with a Guard Cathode. Limnology and Oceanography **34:**474-478.

36. **Rodionov, D. A., I. L. Dubchak, A. P. Arkin, E. J. Alm, and M. S. Gelfand.** 2005. Dissimilatory metabolism of nitrogen oxides in bacteria: Comparative reconstruction of transcriptional networks. Plos Computational Biology **1:**415-431.

37. **Schmidt, I., E. Bock, and M. S. M. Jetten.** 2001. Ammonia oxidation by Nitrosomonas eutropha with NO2 as oxidant is not inhibited by acetylene. Microbiology-Sgm **147:**2247-2253.

38. **Schmidt, I., R. J. M. van Spanning, and M. S. M. Jetten.** 2004. Denitrification and ammonia oxidation by Nitrosomonas europaea wild-type, and NirK- and NorB-deficient mutants. Microbiology-Sgm **150:**4107-4114.

39. **Schreiber, F., L. Polerecky, and D. de Beer.** 2008. Nitric oxide microsensor for high spatial resolution measurements in biofilms and sediments. Analytical Chemistry **80:**1152-1158.

40. **Shaw, L. J., G. W. Nicol, Z. Smith, J. Fear, J. I. Prosser, and E. M. Baggs.** 2006. Nitrosospira spp. can produce nitrous oxide via a nitrifier denitrification pathway. Environmental Microbiology **8:**214-222.

41. **Stein, L. Y., and Y. L. Yung.** 2003. Production, isotopic composition, and atmospheric fate of biologically produced nitrous oxide. Annual Review of Earth and Planetary Sciences **31:**329-356.

42. **Strous, M., E. vanGerven, J. G. Kuenen, and M. Jetten.** 1997. Effects of aerobic and microaerobic conditions on anaerobic ammonium-oxidizing (Anammox) sludge. Applied and Environmental Microbiology **63:**2446-2448.

43. **Zacharia, I. G., and W. M. Deen.** 2005. Diffusivity and solubility of nitric oxide in water and saline. Annals of Biomedical Engineering **33:**214-222.

44. **Zumft, W. G.** 1997. Cell biology and molecular basis of denitrification. Microbiology and Molecular Biology Reviews **61:**533-+.

45. **Zumft, W. G.** 2005. Nitric oxide reductases of prokaryotes with emphasis on the respiratory, heme-copper oxidase type. Journal of Inorganic Biochemistry **99:**194-215.

46. **Zumft, W. G.** 2002. Nitric oxide signaling and NO dependent transcriptional control in bacterial denitrification by members of the FNR-CRP regulator family. Journal of Molecular Microbiology and Biotechnology **4:**277-286.

Supplementary Information
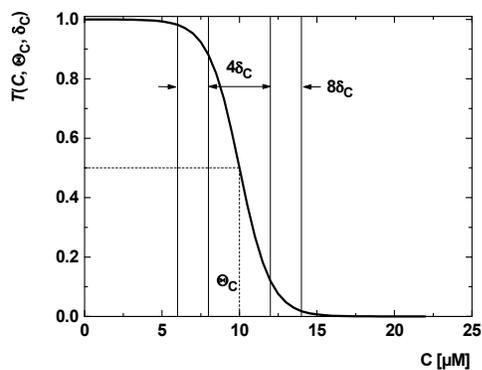
Figure S1. Graphical representation of the threshold function (T, equation 4) that was used to limit the rate of heterotrophic denitrification to low O_2 concentrations.
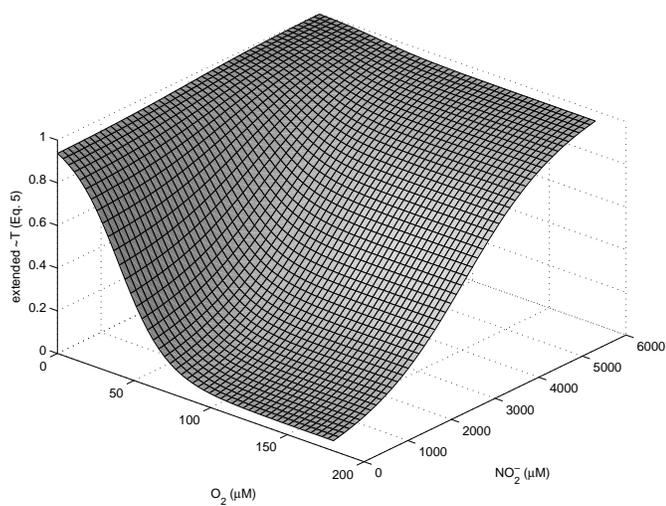
Figure S2. Graphical representation of the extended threshold function ($\widetilde{T}$, equation 5) that was used to limit the rate of NO production by nitrifier denitrification to low O_2 and high NO_2^- concentrations.

Table S1. Processes with stochiometrically balanced chemical formulae, rate expressions and their corresponding parameters that were used in the metabolic model.

hR – heterotrophic respiration

$O_2 + 4e^- + 4H^+ \rightarrow 2H_2O$

$R^{hR} = v_{max}^{hR} \cdot M(O_2, k_{O_2}^{hR})$

Nox – Nitrite oxidation

$2NO_2^- + O_2 \rightarrow 2NO_3^-$

$R^{Nox} = v_{max}^{Nox} \cdot M(O_2, k_{O_2}^{Nox}) \cdot M(NO_2^-, k_{NO_2^-}^{Nox})$

Aox – Ammonia oxidation

$2NH_4^+ + 3O_2 \rightarrow 2NO_2^- + 2H_2O + 4H^+$

$R^{Aox} = v_{max}^{Aox} \cdot M(O_2, k_{O_2}^{Aox})$

niD – nitrifier denitrification; NO production

$2NH_4^+ + 1O_2 + 6NO_2^- + 4H^+ \rightarrow 8NO + 6H_2O$

$R^{niD} = v_{max}^{niD} \cdot M(O_2, k_{O_2}^{niD}) \cdot M(NO_2^-, k_{NO_2^-}^{niD}) \cdot \tilde{T}(NO_2^-, O_2, \Theta_{NO_2^-}^{niD}, \Theta_{O_2}^{niD}, \delta_{NO_2^-}^{niD}, \delta_{O_2}^{niD})$

niD-NO – nitrifier denitrification; NO consumption

$2NH_4^+ + 1O_2 + 4NO \rightarrow 3N_2O + 3H_2O + 2H^+$

$R^{niD-NO} = v_{max}^{niD-NO} \cdot M(O_2, k_{O_2}^{niD-NO}) \cdot M(NO, k_{NO}^{niD-NO}) \cdot T(O_2, \Theta_{O_2}^{niD-NO}, \delta_{O_2}^{niD-NO})$

hD – heterotrophic denitrification; NO production

$NO_2^- + e^- + 2H^+ \rightarrow NO + H_2O$

$R^{hD} = v_{max}^{hD} \cdot M(NO_2^-, k_{NO_2^-}^{hD}) \cdot T(O_2, \Theta_{O_2}^{hD}, \delta_{O_2}^{hD})$

hD-NO – heterotrophic denitrification; NO consumption

$2NO + 2e^- + 2H^+ \rightarrow N_2O + H_2O$

$R^{hD-NO} = v_{max}^{hD-NO} \cdot M(NO, k_{NO}^{hD-NO}) \cdot T(O_2, \Theta_{O_2}^{hD-NO}, \delta_{O_2}^{hD-NO})$

chem. – chemical NO consumption with O_2

$4NO + O_2 + 2H_2O \rightarrow 4NO_2^- + 4H^+$

$R^{chem} = v \cdot NO^2 \cdot O_2$

Process / Stochiometric formula / Rate	Parameter	V_{max} [μM s⁻¹]	K_C (reference) O_2 [μM]	K_C NO_2^- [μM]	K_C NO [μM]	Θ O_2 [μM]	Θ NO_2^- [μM]	δ O_2 [μM]	δ NO_2^- [μM]
hR		0.29; 0.4^b	1 (2)						
Nox		0.74; 0.9^b	42 (4)	15 (5)					
Aox		0.48	9 (4)						
niD		0.06; 0.08^b	9 (4)	21; 10^b (1)		40	3000	15	1000
niD-NO		0.21 (4)	9 (4)		0.6 (es)	280		10	
hD		0.57		0.25 (6)		10		1	
hD-NO		0.85			0.4; 0.15^b (6)	10		1	
chem.		6.3^a (3)							

^{a} $\mu M^{-2}\,s^{-1}$; ^{b} values were adjusted from measured/reported values and used instead; es=estimated
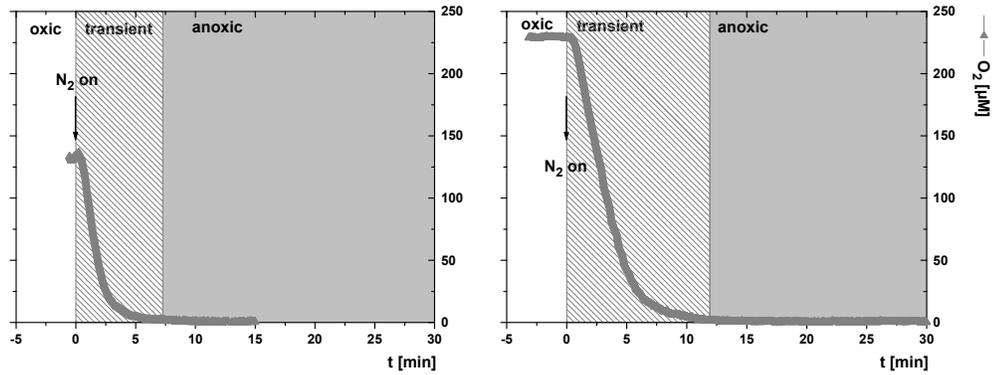
Figure S3. O_2 time series recorded in the biofilm at a depth of 200 μm after the aerated medium was purged with N_2. The medium contained 400 μM NH_4^+ and 5 μM NO_2^- (left graph), and 0 NH_4^+ and 250 μM NO_2^- (right graph).
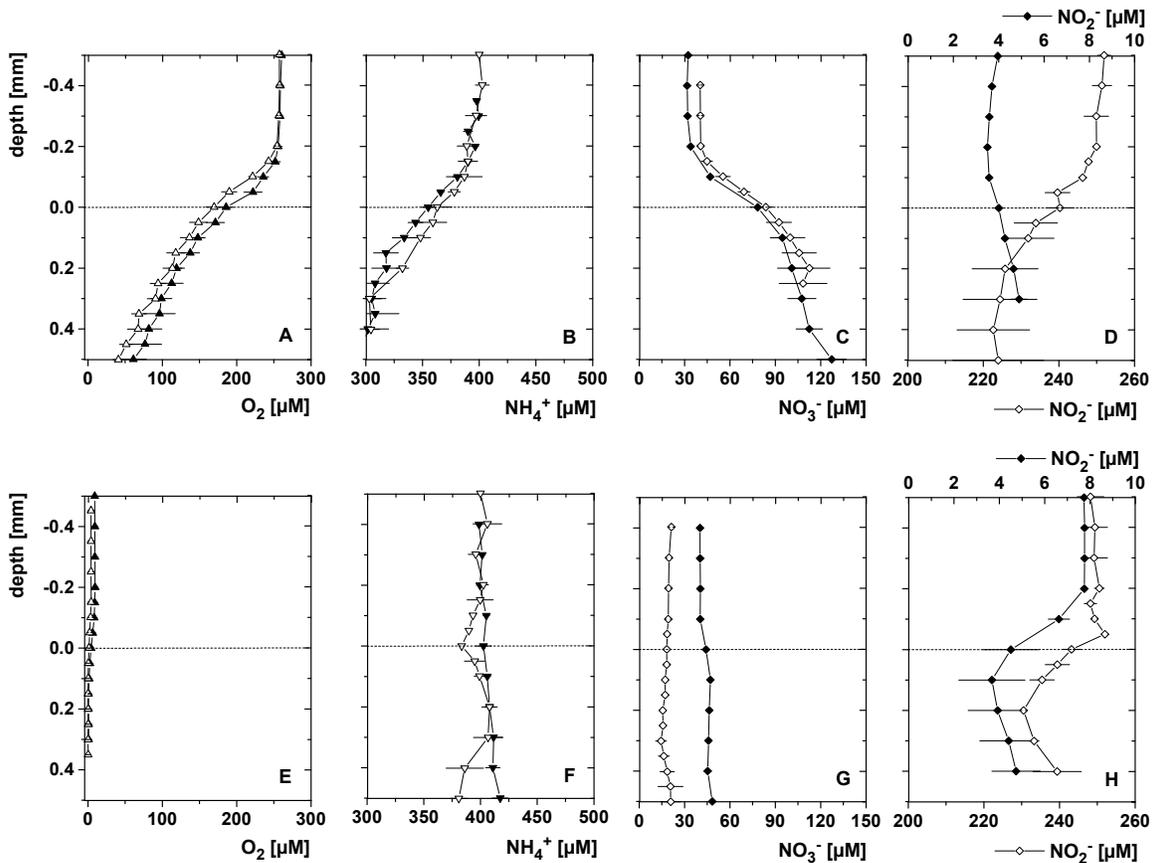
Figure S4. Averaged steady state microprofiles of O_2 **(A and E),** NH_4^+ **(B and F)**, NO_3^- **(C and G)** and NO_2^- **(D and H)** in the biofilm. Microprofiles were measured in an artificial freshwater medium containing 400 μM NH_4Cl with 5 μM NO_2^- (filled symbols) or with 3 mM NO_2^- (open symbols). The medium was aerated **(A-D)** and N_2-purged **(E-H)**. Ammonium and NO_2^- were measured in the presence of 250 μM NO_2^- instead of 3 mM NO_2^-. The dashed line represents the biofilm surface. Horizontal bars represent standard errors (number of measured profiles is given in Table 1).
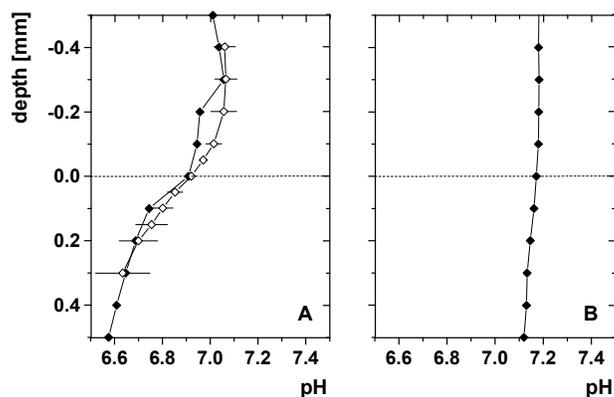
Figure S5. Averaged steady state microprofiles of pH in the biofilm. Microprofiles were measured in a (buffered) artificial freshwater medium containing 400 µM NH$_4$Cl with 5 µM NO$_2^-$ (filled symbols) or with 3 mM NO$_2^-$ (open symbols), and during aeration **(A)** or N$_2$-purging **(B)** of the medium. The dashed line represents the biofilm surface.
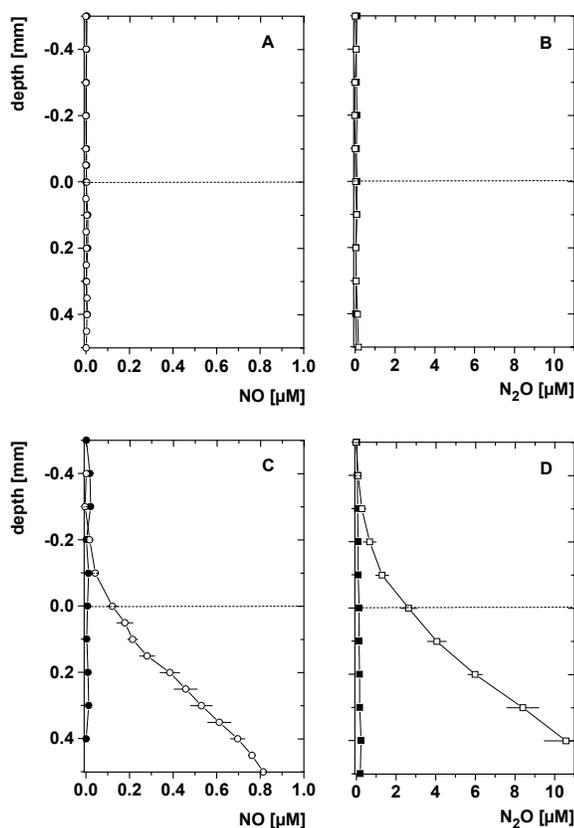
Figure S6. Averaged steady state microprofiles of NO **(A and C)** and N$_2$O **(B and D)** in the biofilm. Microprofiles were measured in an artificial freshwater medium containing 0 µM NH$_4$Cl with 0 µM NO$_2^-$ (filled symbols) or with 3 mM NO$_2^-$ (open symbols), and during aeration **(A and B)** or N$_2$-purging **(C and D)** of the medium. The dashed line represents the biofilm surface. Note different x-scaling as compared to Figure 1.

Supplementary References

1. **Cebron, A., J. Garnier, and G. Billen.** 2005. Nitrous oxide production and nitrification kinetics by natural bacterial communities of the lower Seine river (France). Aquatic Microbial Ecology **41:**25-38.
2. **Devol, A. H.** 1978. Bacterial Oxygen-Uptake Kinetics as Related to Biological Processes in Oxygen Deficient Zones of Oceans. Deep-Sea Research **25:**137-146.
3. **Kharitonov, V. G., A. R. Sundquist, and V. S. Sharma.** 1994. Kinetics of Nitric-Oxide Autoxidation in Aqueous-Solution. Journal of Biological Chemistry **269:**5881-5883.
4. **Peng, Y. Z., and G. B. Zhu.** 2006. Biological nitrogen removal with nitrification and denitrification via nitrite pathway. Applied Microbiology and Biotechnology **73:**15-26.
5. **Sliekers, A. O., S. C. M. Haaijer, M. H. Stafsnes, J. G. Kuenen, and M. S. M. Jetten.** 2005. Competition and coexistence of aerobic ammonium- and nitrite-oxidizing bacteria at low oxygen concentrations. Applied Microbiology and Biotechnology **68:**808-817.
6. **Zafiriou, O. C., Q. S. Hanley, and G. Snyder.** 1989. Nitric-Oxide and Nitrous-Oxide Production and Cycling During Dissimilatory Nitrite Reduction by Pseudomonas-Perfectomarina. Journal of Biological Chemistry **264:**5694-5699.

Chapter 4

Denitrification as a Source for Nitric Oxide and Nitrous Oxide in Human Dental Plaque

Frank Schreiber[a*], Peter Stief [a*], Armin Gieseke[a], Ines Heisterkamp[a], Willy Verstraete[b], Dirk de Beer[a] and Paul Stoodley[c]

[a]*Microsensor Research Group, Max-Planck-Institute for Marine Microbiology, Celsiusstrasse 1, D-28359 Bremen, Germany;* [b]*Laboratory of Microbial Ecology and Technology (LabMET), Ghent University, Coupure Links 653, B-9000 Ghent, Belgium;* [c]*Center for Genomic Sciences, Allegheny General Hospital/Allegheny-Singer Research Institute, Pittsburgh, Pennsylvania, USA; *contributed equally*

Abstract

Dental plaque is a human-associated microbial community (17), which can cause dental caries and periodontal diseases, affecting almost every human being (26, 31). The mouth is a habitat for microorganisms that is characterized by salivary nitrate (NO_3^-) concentrations in the micro- to millimolar range (20), but specific microbial conversions of NO_3^- in dental plaque have never been measured directly. Here we show, using a suite of direct techniques, that denitrification based on salivary NO_3^- leads to nitric oxide (NO), nitrous oxide (N_2O), and dinitrogen (N_2) formation in dental plaque. Incubations with ^{15}N isotopically-labeled NO_3^- and detection of denitrification genes revealed that NO_3^- consumption in dental plaque is mediated by denitrification. Oral N_2O emission rates before and after teeth brushing indicated that dental plaque was the main site for denitrification in the human mouth. Microsensor measurements in dental plaque revealed that NO and N_2O production occurred under aerobic conditions and was regulated by plaque pH. Increases of NO concentrations in dental plaque due to pH decreases were in the range of effective concentrations for NO signaling to vascular, nervous, and immune system cells (5, 10). Due to close proximity of dental plaque to the gum, we hypothesize that pH fluctuations and plaque N-metabolism locally affect blood flow, signaling between nerves, and immune response in the gum.

Introduction

While it is documented that salivary NO_3^- is converted to NO_2^- by bacteria located on the rat tongue (13), other investigators regarded NO_2^- in human saliva as a stable oxidation product of NO synthase-derived NO that is released by gingival cells (2, 9). Detection of NO in air incubated in the mouth has led to the hypothesis that bacterially-derived salivary NO_2^- is chemically reduced to NO in acidic micro-environments (4, 13). However, the underlying processes have never been demonstrated, because NO microsensors that are suited for measurements in dental biofilms were not available. In this study we hypothesized that dental plaque represents a habitat for microbial

denitrification, which drives the biological conversion of NO$_3^-$ to the denitrification intermediates NO$_2^-$, NO and N$_2$O, and to the final product N$_2$. We used a recently developed NO microsensor to demonstrate *in situ* NO formation in dental plaque (30).

Results and Discussion

Dental plaque converted NO$_3^-$ to N$_2$ by denitrification. This was shown by ^{30}N$_2$ formation from ^{15}NO$_3^-$ during incubation of dispersed dental plaque (Figure 1 f). The occurrence of complete denitrification in dental biofilms was corroborated by PCR-detection of genes (NO$_3^-$ reductase, NO reductase, N$_2$O reductase) that are necessary for the respiratory reduction of NO$_3^-$ to N$_2$ (Table 1). These results support the mechanistic model of biological formation of denitrification intermediates from salivary NO$_3^-$ and NO$_2^-$ as depicted in Figure 2.

Table 1. Denitrification genes in dental biofilms of 5 volunteers

Volunteer / gene	NO$_3^-$ reductase	NO$_2^-$ reductase		NO reductase		N$_2$O reductase
	narG	*nirS*	*nirK*	*cnorB*	*qnorB*	*nosZ*
A	+	n.a.	n.a.	-	+	+
B	+	n.a.	n.a.	-	+	+
C	+	n.a.	n.a.	-	+	+
D	+	n.a.	n.a.	-	+	+
E	+	n.a.	n.a.	-	+	n.a.

n.a. – not analyzed, detection of NO$_2^-$ reductase is underway.

Denitrification in dental biofilms occurred under aerobic conditions. This was evident from microprofiles that showed NO$_3^-$-uptake in the presence of O$_2$ (Figure 1 b and c) and because ^{30}N$_2$ production from ^{15}NO$_3^-$ started without delay in air-saturated medium (Figure 1 f). The ability to denitrify in the presence of O$_2$ has been observed for isolated bacterial strains and occasionally for microbial communities (18). Aerobic denitrification guarantees a stable electron accepting process in a NO$_3^-$-rich habitat exposed to frequent

fluctuations in O_2 concentration without energy-demanding expression of new enzyme systems (28). This may perfectly apply to the oral habitat that is characterized by high salivary NO_3^- and fluctuating O_2 concentrations in the mouth.
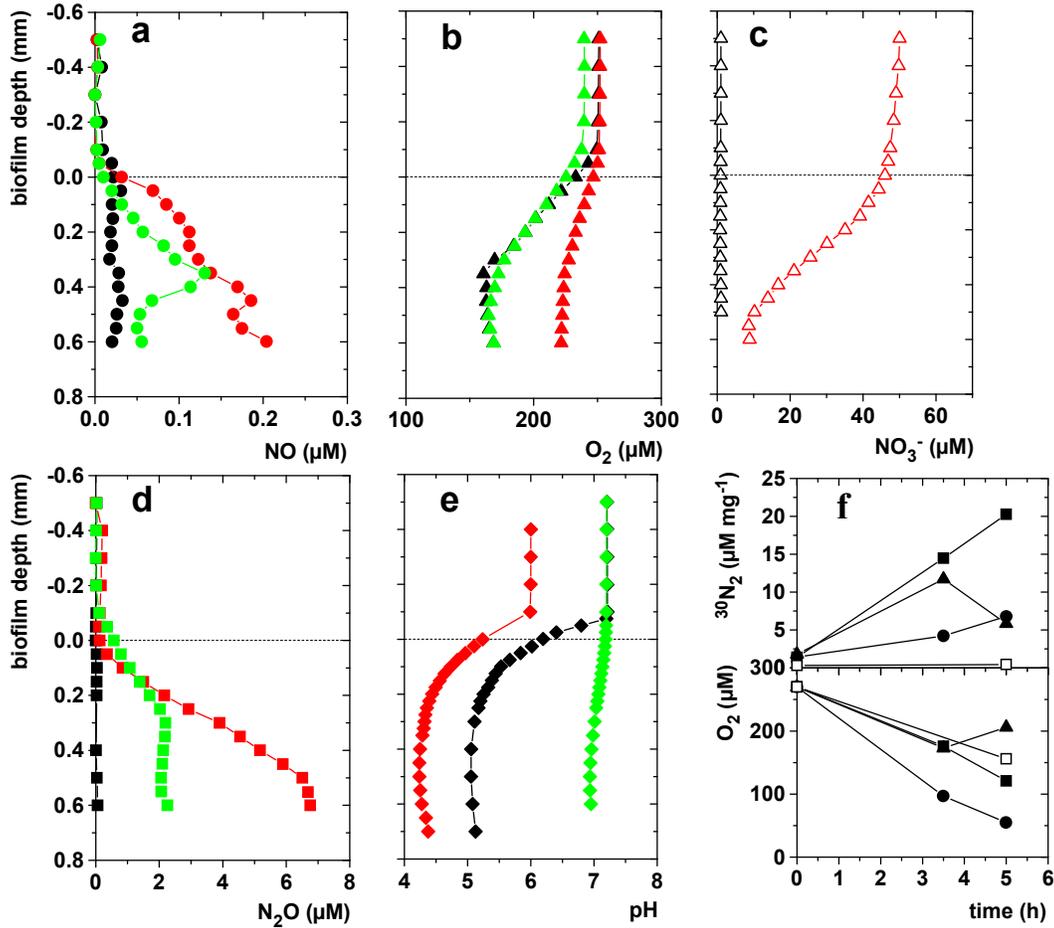
Figure 1. *In situ* concentration microprofiles measured in a dental biofilm outside the mouth **(a-e)**. The medium contained a mineral mix and 2% sucrose in all experiments; (black symbols) non-buffered without $NaNO_3$; (red symbols) non-buffered and supplemented with 760 µM $NaNO_3$; and (green symbols) PBS-buffered (pH 7.2) and supplemented with 760 µM $NaNO_3$. NO_3^- microprofiles were measured in the presence (open red) and the absence (open black) of 50 µM $NaNO_3$ in non-buffered mineral medium with 2% sucrose **(c)**. The horizontal line represents the biofilm surface. **(f)** Production of $^{30}N_2$ (in µM mg^{-1} protein) and O_2 consumption of dental biofilms from incubations in phosphate-buffered saline containing 50 µM Na$^{15}NO_3$ and 2% sucrose. Each symbol type represents $^{30}N_2$ and O_2 measurements of dental plaque incubations from one individual. Control measurements were done in the absence of Na$^{15}NO_3$ (open symbols).

Nitrate was the source for NO and N$_2$O in dental biofilms. This was shown by NO and N$_2$O formation being restricted to the presence of NO$_3^-$, which was actively taken up by the biofilm (Figure 1 a, c and d). Nitric oxide formation in dental biofilms was mediated by both biological NO$_2^-$ reduction and acidic decomposition of NO$_2^-$. Biological NO$_2^-$ reduction was the sole process that produced NO when the medium was buffered at $\sim$ pH 7. In non-buffered medium, bacterial activity decreased biofilm pH below 5 (Figure 1 e) and NO concentrations increased (Figure 1 a). The low pH level causes chemical formation of NO by acidic decomposition of NO$_2^-$ (SI Figure S1), while biological NO formation may still occur in parallel. Thus, the mechanistic model for formation of denitrification intermediates in dental plaque involves a pH-controlled chemical conversion step from NO$_2^-$ to NO in addition to the biological conversion step (Figure 2).
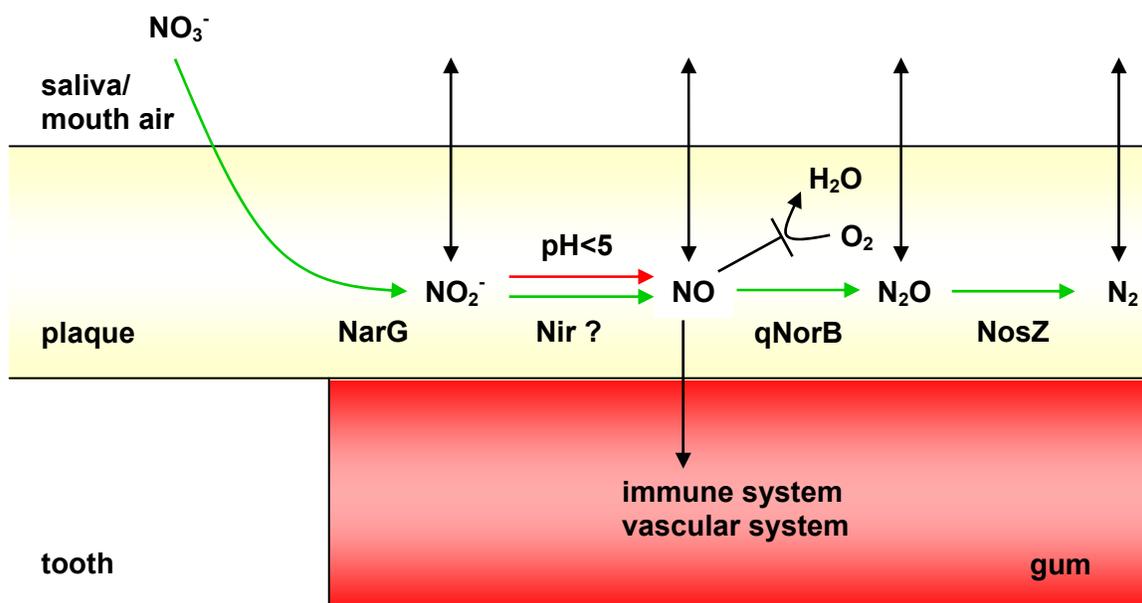
Figure 2. Scheme for conversion of salivary NO$_3^-$ to NO$_2^-$, NO, N$_2$O and N$_2$ by denitrification in dental biofilms. The products of NO$_3^-$ reduction dissolve in saliva, but gases also equilibrate to mouth air and will be subsequently emitted to the atmosphere. The reduction of NO$_2^-$ to NO is chemically driven below pH 5 in addition to biological reduction. Genes encoding for enzymes that mediate steps of denitrification are depicted if detected in dental biofilms with PCR. Genes of the cytochrome c-dependent NO reductase (cNorB) were not detected. Detection of Nir is underway. Nitric oxide generation by denitrification may influence components of the immune and the vascular system of the gum and decreases O$_2$-uptake of the biofilm.

Human cells can produce NO from arginine with NO synthase and respond to NO as a signal molecule produced by other cells (6). In gingival tissue, NO is known to be involved in blood pressure regulation and in inflammatory processes, such as those in periodontal diseases (16, 36). Under acidic conditions, the depth-averaged NO concentration in dental plaque increased from 0.08 to 0.15 µM (Figure 1 a), which is in a physiological effective range (5, 10) for local blood pressure regulation, neurosignaling events and immune system modulation in tissues close to plaque. Hence, we hypothesize that pH fluctuations and plaque denitrification locally affect blood flow, signaling between nerves, and immune response in the gum by modulating the concentration of NO. Nitric oxide-mediated interactions will be different in cariogenic as compared to periodontal plaque, because both are characterized by distinct pH regimes (21). While low pH levels in cariogenic plaque may induce chemical NO formation leading to high NO concentrations, NO formation in periodontal plaque will be restricted to microbial processes, because it is characterized by pH levels > 7.

Until now, it was assumed that denitrification in human-associated microbial communities is not relevant (19). Instead, NO_3^- reduction in humans is thought to be restricted to the dissimilatory nitrate reduction to ammonium, because most bacterial isolates from humans are able to perform this reaction. Nitrate is also present in other body fluids than saliva (e.g. blood 20-40 µM) (20). This suggests that NO production by denitrification and its potentials for interaction with host tissue may occur in microbial biofilms that are associated to other diseased or healthy sites, such as cystic fibrosis lungs, otitis media ears, implants and gut or vaginal mucosa (14).

Like eukaryotic cells, bacteria respond to NO as a signaling molecule. Specifically, NO is involved in the dispersal of bacteria from biofilms (3). This makes NO a possible bacterially-derived factor that balances the development of a natural dental plaque community. Thus, NO might be an important factor from the perspective of the 'ecological plaque hypothesis', which states that environmental factors in the mouth

determine if the dental plaque microbial community is dominated by either health-sustaining or disease-causing microorganisms (21).

Nitric oxide-mediated interactions between plaque bacteria were indeed notable, because high turnover of NO decreased O$_2$-uptake in dental biofilms. Oxygen-uptake in the presence of NO$_3^-$ was lower under acidic conditions than at neutral pH (Figure 1 b and e). Acidic pH alone did not lead to reduced O$_2$-uptake when NO$_3^-$ was absent. Decreased bacterial O$_2$ consumption might result from direct toxic effects of the highest NO concentration (0.15 – 0.2 µM), such as binding of NO to terminal, respiratory O$_2$ reductases (11). However, the absolute increase from 0.08 to 0.2 µM may not affect respiration as concentrations above 0.8 µM were previously shown to be necessary to inhibit O$_2$ reduction in *E. coli* (32). Alternatively, instead of promoting O$_2$ reduction, electrons might be used preferentially for detoxification of NO by reduction to N$_2$O, reconciling inhibited O$_2$-uptake with increased N$_2$O concentrations (Figure 1 a and d). The *absolute* increase of NO due to acidic conditions was small from the perspective of the metabolic homeostasis of denitrification. This was evident because depth-averaged increases of N$_2$O, the product of NO reduction, were approx. two orders of magnitude higher than that of NO concentrations under acidic conditions. This strongly suggests that biofilm bacteria efficiently convert most NO to N$_2$O and thereby keep the steady-state concentration of cytotoxic NO low.

Despite the microbial diversity of dental biofilms (17), we could only detect genes for respiratory NO reductases of the quinol-dependent type (qNorB), but not of the cytochrome c-dependent type (cNorB) (Table 1). Interestingly, genes that code for qNorB are also found in non-denitrifying, pathogenic bacteria, where it contributes to NO detoxification, instead of respiratory electron transport (38). Apparently, respiratory NO reduction is exclusively mediated by qNorB in the investigated dental biofilms. Additionally, qNorB might be used as a protective enzyme against toxic NO derived from host cells, acidic decomposition of NO$_2^-$ and other biofilm bacteria.

We incubated air in the human mouth ('mouth air') and measured the rate of N_2O accumulation to quantify the *in vivo* significance of denitrification in the oral habitat. We related N_2O accumulation in mouth air to the presence of dental biofilms and the salivary NO_3^-/NO_2^- concentrations (Figure 3). N_2O accumulation in the presence of dental plaque varied strongly between the subjects and ranged from 11 to 443 nmol h^{-1} (average of 80 nmol h^{-1}). Based on these data, oral-associated N_2O emissions by humans contribute insignificantly to the global budget of this greenhouse gas (see Supplementary Discussion). N_2O accumulation between subjects increased with increasing salivary NO_3^-/NO_2^- concentrations (Figure 3 a). Increasing the salivary NO_3^-/NO_2^- concentration of a subject by drinking 200 mL beetroot juice that contained 12 mmol L^{-1} NO_3^- increased the rate of oral N_2O accumulation by a factor of 3.8 - 9.1. This shows that dietary NO_3^--uptake influences plaque denitrification.

Dental biofilms were the main sites of N_2O production in the human mouth. This was evident because the combined application of ordinary teeth brushing with an antiseptic mouthwash decreased oral N_2O accumulation rate by 82%, while teeth brushing alone decreased the rate of oral N_2O accumulation by 62% (Figure 3 b). This result and the microsensor data strongly suggest that dental plaque is also the main site for oral formation of NO_2^- and NO. Thus, NO_2^- measurements in saliva (2, 9) are not an adequate proxy for NO formation by human host cells in the mouth. Moreover, NO and NO_2^- measurements in breath and saliva can not be linked to systemic diseases, as it is currently done for renal failure (22, 29), but has been already recognized for cystic fibrosis (37). Rather, measurements of N_2O accumulation rates in mouth air provide a simple and sensitive biomarker protocol to assess the success of oral hygiene. More generally, the importance of dental plaque for the formation of denitrification intermediates as compared to other oral surfaces indicates that plaque bacteria are more relevant for oral nitrogen conversions than bacteria located on the tongue (13). Consequently, dental biofilms might play a crucial role in the regulation of body NO_2^- concentration and affect NO_2^--related physiological functions in the human body, such as hypoxic vasodilatation and antimicrobial activity in the acidic stomach (20).
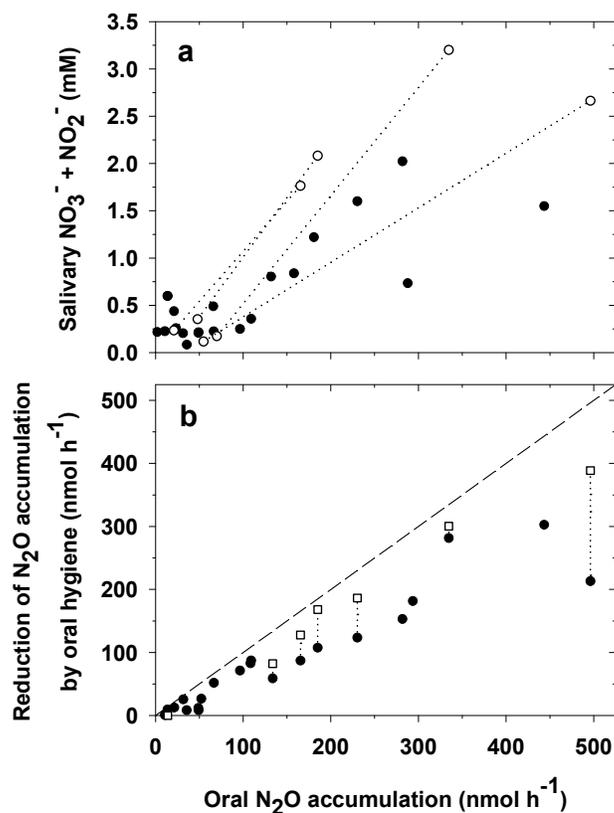
(a) Correlation of oral N_2O production and salivary NO_2^-/NO_3^- concentration in 15 volunteers with unbrushed teeth. Samples of mouth air were collected at two time points to derive the rate of oral N_2O accumulation (black circles). Several volunteers were sampled on more than 1 day. Four volunteers were additionally sampled before and after drinking NO_3^--rich beetroot juice to increase salivary NO_2^-/NO_3^- concentration (white circles connected by dotted line). **(b)** Reduction of oral N_2O accumulation rate by teeth brushing (black circles) and antiseptic mouth rinse (white squares) relative to the oral N_2O accumulation rate before oral hygiene. Each point represents measurements of one subject. Dashed line corresponds to 100% reduction of oral N_2O accumulation. Dotted lines connect hygiene effects within one individual.

Numerous anatomical sites, including the skin, mouth, stomach, colon, and vagina, are inhabited by distinct microbial communities, which are characterized by a large diversity. This suggests a versatile potential of different metabolic pathways mediated by microorganisms that affect human physiology. However, the activity of human-associated microbial communities has rarely been demonstrated *in situ* (12). Thus, we anticipate that investigations of human-associated microbial communities with direct techniques, such as those used in this study, will lead to the discovery of unexpected functions and

interactions between microbes and humans if expanded to elemental cycles of carbon, sulfur, iron and others. Only this approach will allow future interpretation of metagenomic data that is generated in the context of the human microbiome project (35).

Method Summary

Samples of natural, dental plaque were obtained with toothpicks or dental floss from male and female volunteers with an age ranging between 25 to 52 years, who had not taken antibiotics, and not being diagnosed with periodontitis and other severe diseases. Plaque of 2 volunteers was subjected to *in situ* measurements with NO, N_2O, O_2, pH and NO_3^- microsensors outside the mouth in non-buffered medium in the presence and absence of 760 µM NO_3^- and in buffered medium amended with 760 µM NO_3^-. In addition, plaque samples of 3 volunteers were dispersed and incubated in aerobic, buffered media amended with 50 µM $Na^{15}NO_3$ in a time series experiment. Oxygen concentration was measured with O_2 microsensors before inactivating the biological reactions with $ZnCl_2$ at specific time points. Mass spectrometry was used to measure $^{30}N_2$ production. Moreover, DNA was extracted from plaque samples of 5 volunteers and subjected to PCR with degenerate primers for genes encoding for NO_3^- reductase (*narG*), NO_2^- reductases (*nirS and nirK*), NO reductases (*qnorB, cnorB*) and N_2O reductase (*nosZ*). Presence of genes in dental plaque was confirmed by gel-electrophoresis using pure cultures that carry the respective genes as positive control and by cloning and sequencing the PCR products. The accumulation of N_2O in mouth air of up to 15 volunteers was measured by gas chromatography under four different conditions: (i) Before teeth brushing, (ii) after teeth brushing, (iii) after teeth brushing and applying an antiseptic mouth rinse, and (iv) before teeth brushing, but after drinking 200 mL NO_3^--rich beetroot juice. Volunteers incubated 30 mL of air in their mouth ('mouth air') and sub-sampled it after 30 and 90s, which allowed calculating the rate of N_2O accumulation in mouth air. The N_2O accumulation rate was related to the salivary concentrations of NO_3^- and NO_2^- that were measured with an NO_x analyzer.

Methods

Microsensor measurements

Biofilms were carefully recovered with toothpicks or dental floss from the interproximal (IP) spaces of the upper or lower molars by volunteers that did not brush their teeth for at least 24 h. Whole biofilm pieces were placed on solid agar (1.5 %), fixed with a drop of molten agar (0.5 %) and covered with non-buffered sucrose/salt medium (68 mM NaCl, 8 mM MgCl$_2$, 3.6 mM CaCl$_2$, 26.8 mM KCl, 2% sucrose; pH 6.6 - 7.2). Biofilms equilibrated for at least 20 min before the measurements, which were performed within 6-8 h after biofilm retrieval. Manufacturing of NO, N$_2$O, O$_2$, pH and LIX-NO$_3^-$ microsensors (1, 27, 30) and microsensor measurements (30) were conducted as previously described. Steady state micro-profiles were measured before and after 760 µM NaNO$_3$ was added, while an air jet directed on the medium surface created a constant flow regime above the biofilm. To investigate nitrogen cycling at pH 6-7 in the biofilm the medium was supplemented with phosphate buffer (10 mM Na$_2$HPO$_4$, 1.8 mM KH$_2$PO$_4$, pH 7.2; resembling the concentration in 1×PBS), thereby excluding chemical NO$_2^-$ reduction. To increase sensor performance, NO$_3^-$ micro-profiles were measured in medium with lower salt content, and in the presence and absence of 50 µM NaNO$_3$, instead of 760 µM. All presented measurements were performed in the same biofilm spot. Thus, the measurements are suitable to draw mechanistic conclusions. However, the data do not account for biofilm heterogeneity and are not suitable for calculation of average fluxes over a given biofilm surface. We repeated the same experiment with a biofilm from a second volunteer, which essentially showed the same treatment effects (SI Figure S2).

N$_2$ production from isotopically labeled NO$_3^-$

Dental biofilms were collected with a toothpick from dental surfaces and IP spaces of 3 volunteers and were washed twice in phosphate buffered saline (pH 7.2). The protein

content of the sample was determined after Lowry. Biofilms were homogenized by vortexing, the material of each individual was equally distributed to 3 exetainers (3.8 mL) and filled with air saturated incubation medium (phosphate buffered saline and 2% sucrose). The incubation was immediately started by adding 50 µM $Na^{15}NO_3$ and was performed under continuous mixing at 37°C. Dissolved O_2 concentration was measured with an O_2 microsensor, directly before biological reactions were stopped by adding ~0.5 % $ZnCl_2$ at 3 time points ($t_0 = 0h$; $t_1 = 3.5$ h; $t_2 = 5$ h). A quadrupole mass spectrometer (GAM 200, IP Instruments, Germany) was used to measure $^{30}N_2$ after introducing a 2 mL helium-headspace into the closed exetainer and equilibration between the liquid and gas phase.

Molecular analysis of denitrification genes from dental biofilms

Dental plaque was collected from dental surfaces and IP spaces with sterile toothpicks by 5 volunteers that had not brushed their teeth or eaten for 12 h. DNA was extracted according to a protocol optimized for dental plaque (24). PCR amplification of partial sequences of the denitrification genes *narG*, *nirS*, *nirK*, c*norB*, *qnorB*, and *nosZ* was performed in a total volume of 20 µL containing 2 µL of 10x PCR buffer, 250 µM of each deoxyribonucleoside triphosphate, 1 U of *Taq*-polymerase (#), 0.3 mg/ml BSA, 0.5 µM of each primer and 10 to 100 ng DNA. Published primers that target a wide spectrum of organisms were used: narG1960F/narG2650R (25), cd3aF/R3cd (23, 34), F1aCu/R3Cu (15), qnorB2F/qnorB7R (7), cnorB2F/cnorB7R (7) and nosZ1181F_a*/nosZ1880R (33). Thermal cycling conditions were as described in the corresponding protocols with some modifications (see SI Table S1). Amplicons were analyzed by electrophoresis on 1% agarose gels and subsequent ethidium bromide staining. Amplicons of expected size were purified with the QIAQuick PCR purification kit (Qiagen, Hilden, Germany) and cloned using the TOPO TA cloning system (Invitrogen Corp., Carlsbad, CA) following the manufacturer's instructions. The obtained sequences were analyzed with BLAST (www.ncbi.nlm.nih.gov) to confirm that the PCR-products corresponded to the targeted genes.

N_2O accumulation in mouth air

Fifteen volunteers were asked not to brush their teeth the night and morning before the measurement. They were allowed to eat and drink, but not during the last hour before the measurements. To exclusively measure N_2O that is produced in the mouth, but not in the lung or the stomach, we injected ambient air (30 mL) into the empty mouth. Subsequently, volunteers were asked to breathe through the nose with the mouth closed off from the nasopharynx and keep the injected air in their mouth. We defined this air as mouth air in which orally-produced N_2O accumulated. Two gas samples (1 mL) were withdrawn through the blunt canula of a syringe after 30 and 90 s and filled into gas-tight exetainers (3 mL). This sampling scheme was repeated 5 times with teeth unbrushed and 5 times with teeth brushed by the volunteers. The N_2O accumulation rate of 7 volunteers was additionally measured after both teeth brushing and a one-minute antiseptic mouthwash, following the package insert (Chlorhexamed® Fluid 0.1%). Before brushing the teeth, the volunteers collected 1 mL of saliva that was immediately frozen for later analysis of the NO_3^-/NO_2^- concentration. Sub-samples of mouth air were analyzed for N_2O concentration using a gas chromatograph with a ^{63}Ni electron capture detector (Agilent GC7890). From the concentration difference between 30 and 90 s and the incubated volume of air, the rate of N_2O accumulation was calculated in nanomoles per individual and hour. The increase of N_2O concentration in mouth air was shown to be linear for at least 240 s in additional test runs.

In a separate experiment, the N_2O accumulation rate of 4 volunteers with teeth unbrushed was determined before and 2 h after drinking 200 mL of beetroot juice that contained 12 mmol L^{-1} NO_3^-. The volunteers collected 0.5 mL of saliva before and then hourly after drinking the beetroot juice for later analysis of the NO_3^-/NO_2^- concentration. Maximum salivary NO_3^-/NO_2^- and NO_2^- concentrations were generally measured 2 h after drinking beetroot juice. Saliva samples were cleared by centrifugation and then analyzed for NO_3^-/NO_2^- with the VCl_3 reduction method (8) followed by NO measurement on a chemiluminescence detector (CLD 86, EcoPhysics).

1. **Andersen, K., T. Kjaer, and N. P. Revsbech.** 2001. An oxygen insensitive microsensor for nitrous oxide. Sensors and Actuators B-Chemical **81:**42-48.
2. **Aurer, A., J. Aleksic, M. Ivic-Kardum, J. Aurer, and F. Culo.** 2001. Nitric oxide synthesis is decreased in periodontitis. Journal of Clinical Periodontology **28:**565-568.
3. **Barraud, N., D. J. Hassett, S. H. Hwang, S. A. Rice, S. Kjelleberg, and J. S. Webb.** 2006. Involvement of nitric oxide in biofilm dispersal of Pseudomonas aeruginosa. Journal of Bacteriology **188:**7344-7353.
4. **Bayindir, Y. Z., M. F. Polat, and N. Seven.** 2005. Nitric oxide concentrations in saliva and dental plaque in relation to caries experience and oral hygiene. Caries Research **39:**130-133.
5. **Bedioui, F., and N. Villeneuve.** 2003. Electrochemical nitric oxide sensors for biological samples - Principle, selected examples and applications. Electroanalysis **15:**5-18.
6. **Bogdan, C.** 2001. Nitric oxide and the immune response. Nature Immunology **2:**907-916.
7. **Braker, G., and J. M. Tiedje.** 2003. Nitric oxide reductase (norB) genes from pure cultures and environmental samples. Applied and Environmental Microbiology **69:**3476-3483.

8.   **Braman, R. S., and S. A. Hendrix.** 1989. Nanogram Nitrite and Nitrate Determination in Environmental and Biological-Materials by Vanadium(Iii) Reduction with Chemi-Luminescence Detection. Analytical Chemistry **61:**2715-2718.

9.   **Carossa, S., P. Pera, P. Doglio, S. Lombardo, P. Colagrande, L. Brussino, G. Rolla, and C. Bucca.** 2001. Oral nitric oxide during plaque deposition. European Journal of Clinical Investigation **31:**876-879.

10.   **Chen, K. J., R. N. Pittman, and A. S. Popel.** 2008. Nitric oxide in the vasculature: Where does it come from and where does it go? A quantitative perspective. Antioxidants & Redox Signaling **10:**1185-1198.

11.   **Cooper, C. E.** 2002. Nitric oxide and cytochrome oxidase: substrate, inhibitor or effector? Trends in Biochemical Sciences **27:**33-39.

12.   **Dethlefsen, L., M. McFall-Ngai, and D. A. Relman.** 2007. An ecological and evolutionary perspective on human-microbe mutualism and disease. Nature **449:**811-818.

13.   **Duncan, C., H. Dougall, P. Johnston, S. Green, R. Brogan, C. Leifert, L. Smith, M. Golden, and N. Benjamin.** 1995. Chemical Generation of Nitric-Oxide in the Mouth from the Enterosalivary Circulation of Dietary Nitrate. Nature Medicine **1:**546-551.

14.   **Hall-Stoodley, L., J. W. Costerton, and P. Stoodley.** 2004. Bacterial biofilms: From the natural environment to infectious diseases. Nature Reviews Microbiology **2:**95-108.

15.   **Hallin, S., and P. E. Lindgren.** 1999. PCR detection of genes encoding nitrile reductase in denitrifying bacteria. Applied and Environmental Microbiology **65:**1652-1657.

16.   **Kendall, H. K., R. I. Marshall, and P. M. Bartold.** 2001. Nitric oxide and tissue destruction. Oral Diseases **7:**2-10.

17.   **Kolenbrander, P. E., R. N. Andersen, D. S. Blehert, P. G. Egland, J. S. Foster, and R. J. Palmer.** 2002. Communication among oral bacteria. Microbiology and Molecular Biology Reviews **66:**486-+.

18.   **Lloyd, D.** 1993. Aerobic Denitrification in Soils and Sediments - from Fallacies to Facts. Trends in Ecology & Evolution **8:**352-356.

19.   **Lundberg, J. O., E. Weitzberg, J. A. Cole, and N. Benjamin.** 2004. Opinion - Nitrate, bacteria and human health. Nature Reviews Microbiology **2:**593-602.

20.   **Lundberg, J. O., E. Weitzberg, and M. T. Gladwin.** 2008. The nitrate-nitrite-nitric oxide pathway in physiology and therapeutics. Nature Reviews Drug Discovery **7:**156-167.

21.   **Marsh, P. D.** 2003. Are dental diseases examples of ecological catastrophes? Microbiology-Sgm **149:**279-294.

22.   **Matsumoto, A., Y. Hirata, M. Kakoki, D. Nagata, S. Momomura, T. Sugimoto, H. Tagawa, and M. Omata.** 1999. Increased excretion of nitric oxide in exhaled air of patients with chronic renal failure. Clinical Science **96:**67-74.

23.   **Michotey, V., V. Mejean, and P. Bonin.** 2000. Comparison of methods for quantification of cytochrome cd(1)-denitrifying bacteria in environmental marine samples. Applied and Environmental Microbiology **66:**1564-1571.

24. **Parrish, K. D., and E. P. Greenberg.** 1995. A Rapid Method for Extraction and Purification of DNA from Dental Plaque. Applied and Environmental Microbiology **61:**4120-4123.

25. **Philippot, L., S. Piutti, F. Martin-Laurent, S. Hallet, and J. C. Germon.** 2002. Molecular analysis of the nitrate-reducing community from unplanted and maize-planted soils. Applied and Environmental Microbiology **68:**6121-6128.

26. **Pihlstrom, B. L., B. S. Michalowicz, and N. W. Johnson.** 2005. Periodontal diseases. Lancet **366:**1809-1820.

27. **Revsbech, N. P.** 1989. An Oxygen Microsensor with a Guard Cathode. Limnology and Oceanography **34:**474-478.

28. **Robertson, L. A., and J. G. Kuenen.** 1984. Aerobic Denitrification - a Controversy Revived. Archives of Microbiology **139:**351-354.

29. **Rolla, G., M. Bruno, L. Bommarito, E. Heffler, N. Ferrero, M. Petrarulo, C. Bagnis, M. Bugiani, and G. Guida.** 2008. Breath analysis in patients with end-stage renal disease: effect of haemodialysis. European Journal of Clinical Investigation **38:**728-733.

30. **Schreiber, F., L. Polerecky, and D. de Beer.** 2008. Nitric oxide microsensor for high spatial resolution measurements in biofilms and sediments. Analytical Chemistry **80:**1152-1158.

31. **Selwitz, R. H., A. I. Ismail, and N. B. Pitts.** 2007. Dental caries. Lancet **369:**51-59.

32. **Stevanin, T. M., N. Ioannidis, C. E. Mills, S. O. Kim, M. N. Hughes, and R. K. Poole.** 2000. Flavohemoglobin hmp affords inducible protection for Escherichia coli respiration, catalyzed by cytochromes bo ' or bd, from nitric oxide. Journal of Biological Chemistry **275:**35868-35875.

33. **Stief, P., M. Poulsen, L. P. Nielsen, H. Brix, and A. Schramm.** 2009. Nitrous oxide emission by aquatic macrofauna. Proceedings of the National Academy of Sciences of the United States of America **106:**4296-4300.

34. **Throback, I. N., K. Enwall, A. Jarvis, and S. Hallin.** 2004. Reassessing PCR primers targeting nirS, nirK and nosZ genes for community surveys of denitrifying bacteria with DGGE. Fems Microbiology Ecology **49:**401-417.

35. **Turnbaugh, P. J., R. E. Ley, M. Hamady, C. M. Fraser-Liggett, R. Knight, and J. I. Gordon.** 2007. The Human Microbiome Project. Nature **449:**804-810.

36. **Ugar-Cankal, D., and N. Ozmeric.** 2006. A multifaceted molecule, nitric oxide in oral and periodontal diseases. Clinica Chimica Acta **366:**90-100.

37. **Zetterquist, W., H. Marteus, P. Kalm-Stephens, E. Nas, L. Nordvall, M. Johannesson, and K. Alving.** 2009. Oral bacteria - The missing link to ambiguous findings of exhaled nitrogen oxides in cystic fibrosis. Respiratory Medicine **103:**187-193.

38. **Zumft, W. G.** 2005. Nitric oxide reductases of prokaryotes with emphasis on the respiratory, heme-copper oxidase type. Journal of Inorganic Biochemistry **99:**194-215.

Supplementary Information
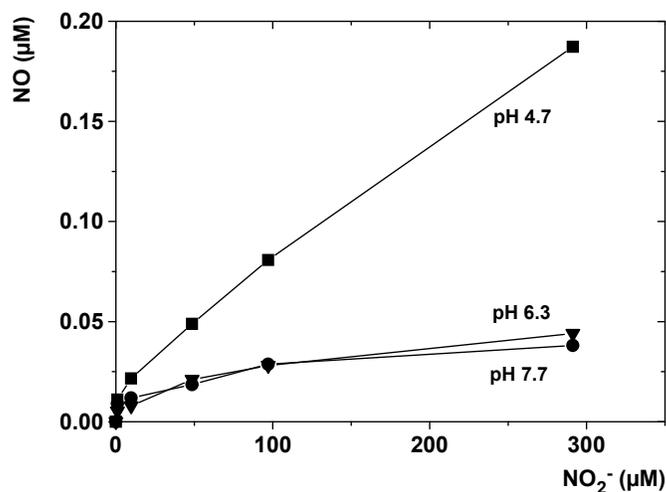
Figure S1. Chemical formation of NO by acidic decomposition of NO_2^- at increasing NO_2^- concentrations and varying pH in phosphate buffered saline.

Table S1. PCR detection of denitrification genes in dental plaque

Target	Primer	Primer sequence 5'-3'	Positive Control	Reference
narG	narG1960f	TAYGTSGGSCARGARAA	*Castellaniella defragrans*	(6) [a]
	narG2650r	TTYTCRTACCABGTBGC		
qnorB	qnorB2F	GGNCAYCARGGNTAYGA	*Castellaniella defragrans*	(2)
	qnorB7R	GGNGGRTTDATCADGAANCC		
cnorB	cnorB2F	GACAAGNNNTACTGGTGGT	*Pseudomonas stutzeri* DSM 5190	(2)
	cnorb7R	TGNCCRTGNGCNGCNGT		
nosZ	nosZ1181F_a	CGCTGTTCMTCGACA GYCAR	*Pseudomonas stutzeri* DSM 5190	(8)
	nosZ1880R	ATGTGCAKIGCRTGGCAGAA		

[a] modified: 10 min at 95°C, touch-down: 38 cycles of 1 min at 94°C, 1 min annealing, 1 min at 72°C, annealing temperature decreased with 0.5°C/cycle from 59°C to 52°C, final elongation for 6 min at 72°C
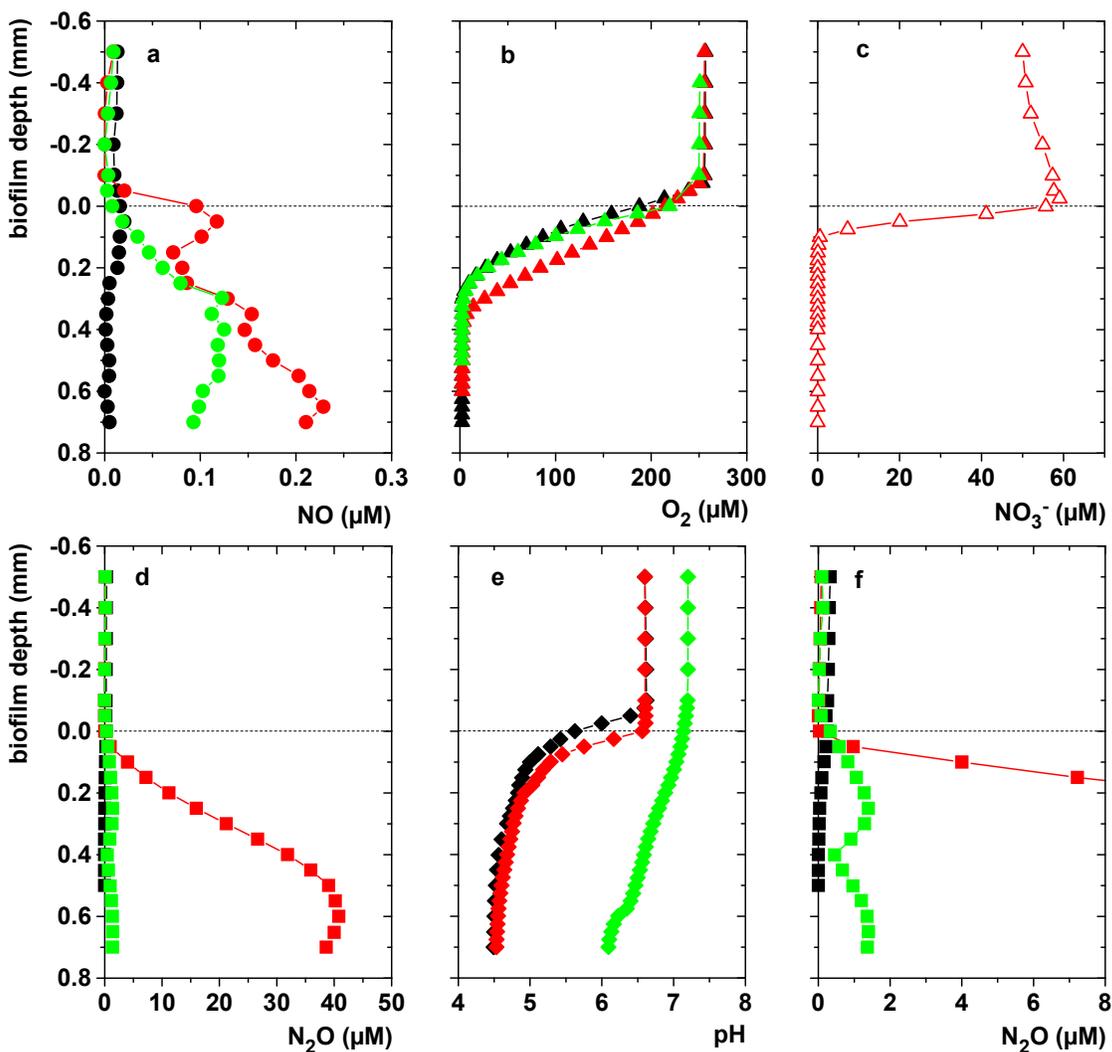
Figure S2. *In situ* concentration micro-profiles measured in a dental biofilm from a different volunteer as presented in the paper **(a-e)**. The medium contained a mineral mix and 2% sucrose in all experiments; (black symbols) non-buffered without $NaNO_3$; (red symbols) non-buffered and supplemented with 760 μM $NaNO_3$; and (green symbols) PBS-buffered (pH 7.2) and supplemented with 760 μM $NaNO_3$. NO_3^- microprofiles were measured in the presence (open red) and the absence (open black) of 50 μM $NaNO_3$ in non-buffered mineral medium with 2% sucrose **(c)**. The horizontal line represents the biofilm surface. **(f)** N_2O micro-profiles as presented in (a), but with a wider x scaling.

Supplementary Discussion

Contribution of oral emissions to N$_2$O budget

The average rate of oral N$_2$O emission from 15 volunteers with unbrushed teeth and non-manipulated salivary NO$_3^-$/NO$_2^-$ concentrations was 80 nmol h-1. While earlier investigations of the breath air of human beings revealed N$_2$O concentrations above the ambient atmospheric level (1, 5, 7), our study presents the first oral-associated emission rates of this greenhouse gas (3) by humans. Extrapolating our data to the world population of currently 6.7 billion people, oral-associated N$_2$O emission by humans is 0.00013 Tg N a^{-1}, representing an insignificant amount of 0.0008% of the global N$_2$O emission of 16.4 Tg N a^{-1} to the atmosphere (4). This picture will probably not be altered when assuming that the worldwide 3.2 billion cows and pigs kept in mass stocks exhibit N$_2$O emission rates similar to those of human beings (USDA 2009).

Suplementary References

1.   **Bleakley, B. H., and J. M. Tiedje.** 1982. Nitrous-Oxide Production by Organisms Other Than Nitrifiers or Denitrifiers. Applied and Environmental Microbiology **44:**1342-1348.

2.   **Braker, G., and J. M. Tiedje.** 2003. Nitric oxide reductase (norB) genes from pure cultures and environmental samples. Applied and Environmental Microbiology **69:**3476-3483.

3.   **Crutzen, P. J.** 1979. Role of No and No2 in the Chemistry of the Troposphere and Stratosphere. Annual Review of Earth and Planetary Sciences **7:**443-472.

4.   **IPCC.** 2001. Climate Change 2001: The Scientific Basis.

5.   **Mitsui, T., and T. Kondo.** 1998. Effects of mouth cleansing on the levels of exhaled nitrous oxide in young and older adults. Science of the Total Environment **224:**177-180.

6.   **Philippot, L., S. Piutti, F. Martin-Laurent, S. Hallet, and J. C. Germon.** 2002. Molecular analysis of the nitrate-reducing community from unplanted and maize-planted soils. Applied and Environmental Microbiology **68:**6121-6128.

7.   **Russow, R., H. U. Neue, I. Wolf, and C. Plath.** 2002. Presented at the 3rd International Symposium on Non-CO2 Greenhouse Gases, Maastricht, Netherlands, Jan 21-23.

8.   **Stief, P., M. Poulsen, L. P. Nielsen, H. Brix, and A. Schramm.** 2009. Nitrous oxide emission by aquatic macrofauna. Proceedings of the National Academy of Sciences of the United States of America **106:**4296-4300.

Chapter 5

Contributed Works

Oxygenic metabolism of an anaerobic bacterium

Aerobic denitrification in permeable sediments of an intertidal sandflat

Nitric oxide generation by tumor-targeting *Salmonella typhimurium* enhances tumor eradication

Oxygenic metabolism of an anaerobic bacterium

Katharina F. Ettwig[1*], Margaret K. Butler[1*], Denis Le Paslier[2,3,4], Eric Pelletier[2,3,4],
Sophie Mangenot[2], Marcel M. M. Kuypers[5], Frank Schreiber[5], Johannes Zedelius[5], Dirk
de Beer[5], Bas E. Dutilh[6], Jolein Gloerich[7], Theo van Alen[1], Francisca Luesken[1],
Mingliang Wu[1], Katinka T. van de Pas-Schoonen[1], Eva M. Janssen-Megens[8], Kees-Jan
Francoijs[8], Henk Stunnenberg[8], Jean Weissenbach[2,3,4], Mike S. M. Jetten[1] & Marc
Strous[1,9]

[1]Department of Microbiology, Radboud University Nijmegen, Heyendaalsweg 135, 6525 AJ, Nijmegen, The
Netherlands. [2]CEA Genoscope, 2 rue Gaston Crémieux CP 5706, 91057 Evry, France.[3]CNRS-UMR 8030,
2 rue Gaston Crémieux CP 5706, 91057 Evry, France. [4]Université d'Evry Val d'Essonne, Boulevard
François Mitterrand CP 5706, 91057 Evry, France. [5]MPI for Marine Microbiology, Celsiusstr. 1 D-
28359, Bremen, Germany. [6]Center for Molecular and Biomolecular Informatics, Nijmegen Center for
Molecular Life Sciences, Radboud University Nijmegen Medical Center, Geert Grooteplein 28, 6525 GA,
Nijmegen, The Netherlands. [7]Nijmegen Proteomics Facility, Radboud University Nijmegen Medical
Center, Geert Grooteplein-Zuid 10, 6525 GA, Nijmegen, The Netherlands. [8]Department of Molecular
Biology, Nijmegen Centre of Molecular Life Sciences, Radboud University Nijmegen Medical Center,
Geert Grooteplein-Zuid 26, 6525 GA, Nijmegen, The Netherlands. [9]Current address: Centre for
Biotechnology, University of Bielefeld and MPI for Marine Microbiology, Celsiusstr. 1 D-28359, Bremen,
Germany; * contributed equally.

*FS contributed, together with KFE, MMMK, JZ, and DdB in designing, performing and
analyzing the experiments for nitrogenous intermediates.*

Abstract

Photosynthesis, microbial chlorite respiration and hydrogen peroxide detoxification are
the only three biological pathways known to evolve molecular oxygen (O_2). Here we
present evidence for a fourth pathway that leads to O_2 formation during anaerobic
methane oxidation coupled to nitrite (NO_2^-) reduction and dinitrogen (N_2) formation.

Metagenomic sequencing of an enrichment culture that performed this reaction showed that the microbial community was dominated by a bacterium, *Methylomirabilis oxyfera*, that is evolutionary distant from all cultivated microorganisms. Surprisingly, *in silico* analyses, metaproteomics and metatranscriptomics suggested that this organism appeared to be aerobic and incapable of complete denitrification. Subsequent ^{18}O and ^{15}N isotopic-labeling indicated that *M. oxyfera* by-passed the denitrification intermediate nitrous oxide (N_2O) by direct decomposition of nitric oxide (NO) into N_2 and O_2. The O_2 produced was used to drive a well established aerobic methanotrophic pathway. These results extend the known possibilities for the degradation of hydrocarbons under anaerobic conditions, and explain the biochemical mechanism of the poorly understood methane sink in freshwater ecosystems, which are presently a major source of atmospheric methane. Since nitrogen oxides were present on early earth before photosynthesis began to oxygenate the atmosphere, the discovery of this pathway may place the evolution of aerobic pathways in a new perspective.
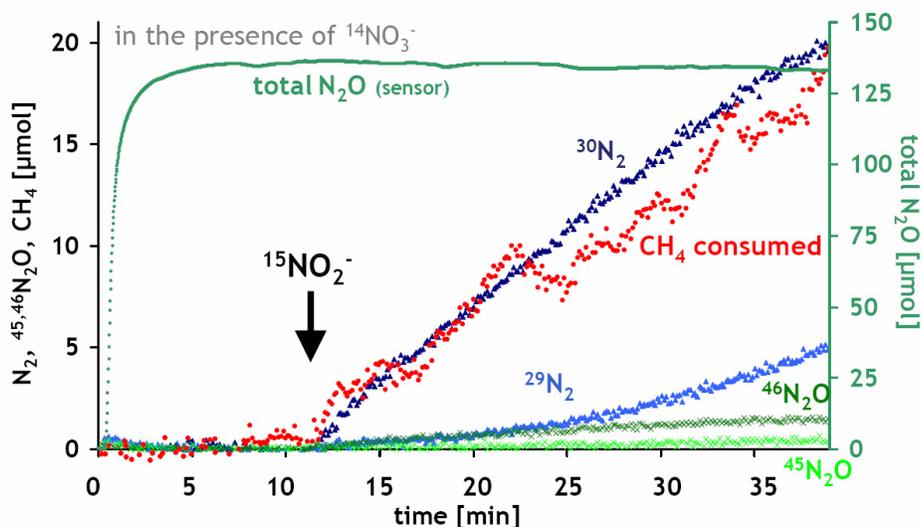
Figure 1. Production of $^{30}N_2$ from $^{15}NO_2^-$ in the presence of a large pool $^{14}N_2O$ with concomitant CH_4 consumption by a sediment-free enrichment culture dominated by *M. oxyfera*. Methane consumption started only after the addition of NO_2^- indicating that $^{14}NO_3^-$ and $^{14}N_2O$ were not used as electron acceptor. Nitrous oxide was not an intermediate since only minor amounts (~ 6%) were trapped in the N_2O pool as $^{45}N_2O$ and $^{46}N_2O$. Concentrations are presented as normalized values. Methane concentrations were additionally multiplied with (-1) to obtain CH_4 consumed

Aerobic denitrification in permeable sediments of an intertidal sandflat

Hang Gao, [a,b,c], Frank Schreiber, [a], Gavin Collins, [a,d], Marlene M. Jensen, [a,e], Joel E. Kostka, [a,f], Gaute Lavik, [a], Dirk de Beer, [a], Huai Yang Zhou, [b,g],

and Marcel M M Kuypers [a]

[a] *Max Planck Institute for Marine Microbiology, Celsiusstr. 1, D-28359 Bremen, Germany;* [b] *Guangzhou Institute of Geochemistry, Chinese Academy Sciences, Kehua Street 511, 401640, Guangzhou, China;* [c] *Graduate School of Chinese Academy Sciences, Yuquan Road 18, Beijing, China;* [d] *Current Address: Department of Microbiology & Environmental Change Institute, National University of Ireland, University Road, Galway, Ireland;* [e] *Current Address: Institute of Biology and Nordic Center of Earth Evolution (NordCEE), University of Sothern Denmark, Campusvej 55, DK-5230 Odense M, Denmark;* [f] *Current Address: Department of Oceanography, Florida State University, Leroy Collins Research Lab 255 Atomic Way, Bldg. 42, 32306-4470, Tallahassee, Florida;* [g] *Current Address: School of Ocean and Earth Science, Tongji University, Siping Road 1239, 200092, Shanghai, China*

Abstract

Sandy sediments dominate the intertidal region of the Wadden Sea but so far little is known about their role in coastal N-cycling. We investigated the potential N-loss rates at a sandflat (Janssand) in the central German Wadden Sea by using a modified version of the whole core incubation technique used for fine-grained sediments. Denitrification assays with permeable sediments incubated with $^{15}NO_3^-$ indicate immediate $^{29}N_2$ and $^{30}N_2$ production. The results show that permeable Janssand sediments are characterized by some of the highest denitrification rates in the marine environment. Surprisingly, several lines of evidence showed that denitrification occurs under aerobic conditions. Gas-tight bag incubations showed that denitrification occurs with maximum rates of 2.30 ± 0.09 mmol m^{-3} h^{-1} at starting O_2 concentrations of up to 90 μM. Additional evidence for

denitrification in the presence of O_2 was obtained by simultaneous O_2 and NO_x measurements with microsensors in percolated cores and Membrane Inlet Mass Spectrometer measurements in well mixed sediment slurries. We hypothesize that the observed high denitrification rates in the presence of O_2 might be an adaptation of denitrifying bacteria to recurrent tidally-induced oscillations in pore water oxygen concentrations in the permeable sediments of Janssand.
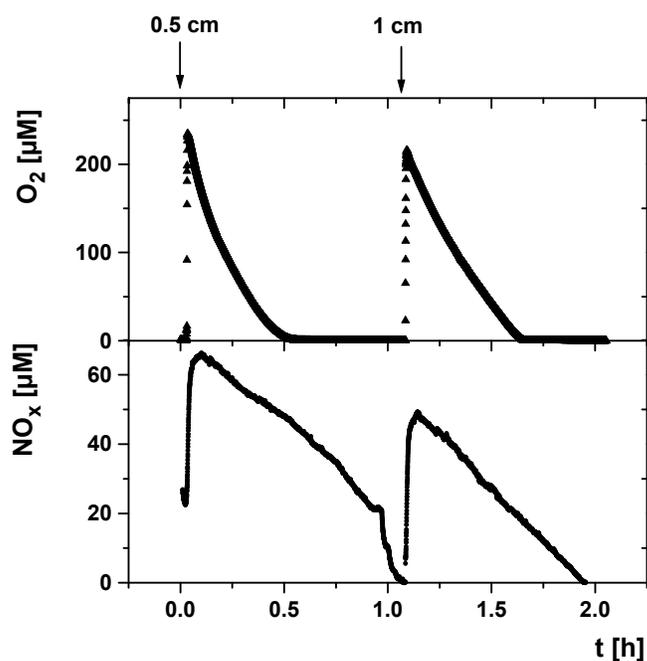
Figure 2. Timeseries measured with O_2 and NO_x microsensors in sediment cores after percolation (indicated by arrows) of overlying water that was air-saturated and contained ~60 μM NO_3^-. Microsensors were adjusted to the same level and measurements were done simultaneously at one depth (0.5 cm and 1 cm). NO_3^- disappears in the presence of O_2 indicating its loss by aerobic denitrification or NO_3^- assimilation. The microsensor measurements corroborated labeling experiments with sediment slurries that showed $^{29}N_2$ and $^{30}N_2$ formation form $^{15}NO_3^-$ in the presence of O_2. Together these results demonstrate the potential for aerobic denitrification in permeable, intertidal sediments.

Nitric oxide generation by tumor-targeting *Salmonella typhimurium* enhances tumor eradication

Yoram Barak[1+], Frank Schreiber[2], Steve H. Thorne[3‡], Christopher H. Contag[3],
Dirk de Beer[2], and A. Matin[1]

[1]*Department of Microbiology and Immunology, Sherman Fairchild Science Building, Stanford University School of Medicine, 299 Campus Drive, Stanford, CA 94305, USA.* [2] *Microsensor Research Group, Max Planck Institute for Marine Microbiology, Celsiusstr. 1 D-28359 Bremen, Germany.* [3]*Department of Pediatrics and Bio-X Program, James H. Clark Center, Stanford University School of Medicine, 318 Campus Drive, Stanford, CA 94305. ‡ Current Address; Department of Surgical Oncology, Hillman Cancer Center, Centre Avenue, University of Pittsburgh, Pittsburgh, PA 15232. + Current address; Codexis Inc. 200 Penobscot, Redwood City, CA 94063.*

FS performed and analyzed microsensor measurements within implanted tumors in mice.

Abstract

Targeting tumors with bacteria is an important strategy for cancer treatment, because they can be used as effective gene delivery agents for activation of non-toxic pro-drugs directly in the tumor environment. Previously, we have shown that the *Salmonella typhimurium* strain SL7838 can target and kill cancer cells without addition of effective pro-drugs. Here we investigate the mechanism of cancer eradication of SL7838 and provide evidence for the involvement of NO. The experiments showed that SL7838 produced NO within different cancer cell types *in vitro*, when NO_3^- or NO_2^- was supplied. In addition, *in vivo* microsensor measurements showed NO production within implanted T1 mouse tumors when infected with SL7838. We constructed mutants with deletions in *hmp* and *norV* genes, which gene products mediate NO detoxification. In the presence of NO_3^-, NO formation and efficiency in cancer cell killing *in vitro* was enhanced in the *hmp and norV* deficient strain SL7842 as compared to the non-deficient strain SL7838. The

killing efficiency of cancer cells by either strain was reduced in the absence of NO_3^-, suggesting that cell death was mediated through NO toxicity. Cancer cell death was accompanied by Caspases 3/7 induction, indicative of apoptosis, and collapse of mitochondrial membrane potential. Together, this suggests that NO produced by these *Salmonella* strains mediated cells death through the mitochondrial pathway. Treatment of implanted mouse tumors by SL7842 was markedly more effective than by SL7838. In conclusion, this study shows that the efficiency of bacterial targeted cancer therapy can be increased when bacteria with high NO generation capability are used as gene delivery agents.
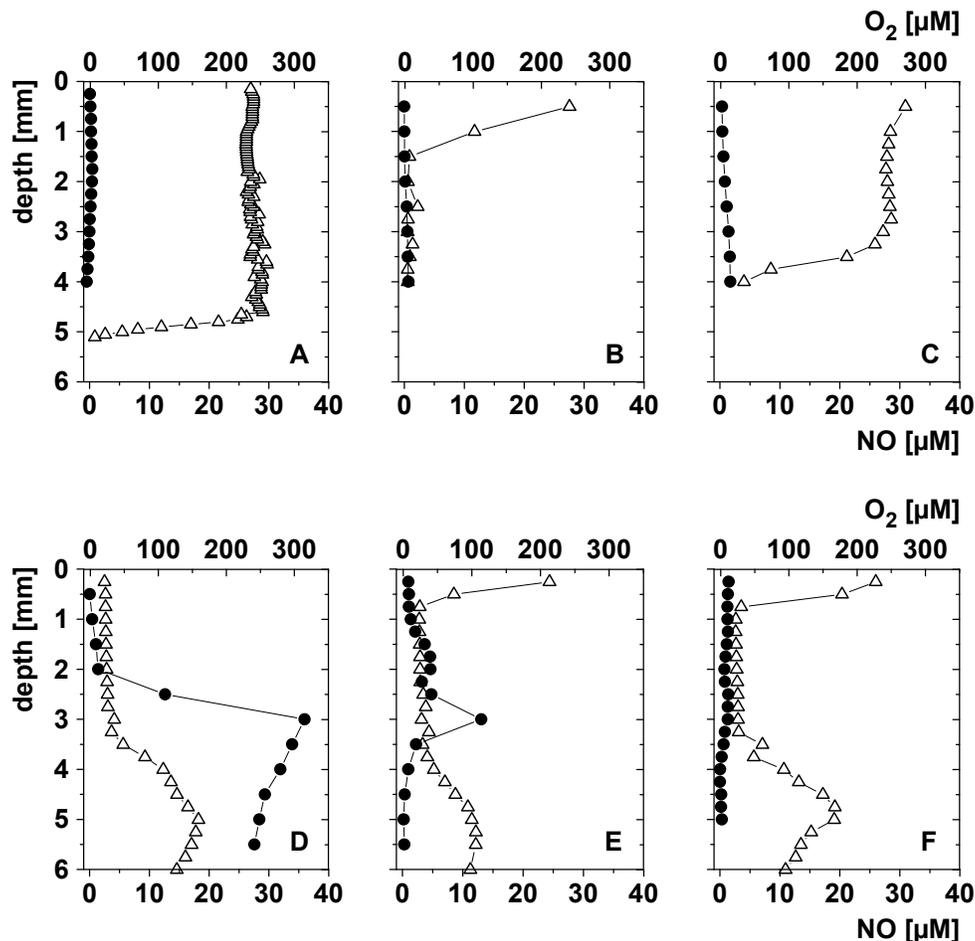
Figure 3. *In vivo* microsensor measurement of NO (filled diamonds) and O_2 (open triangles) in dorsal 14-day old 4T1 subcutaneous tumors in BALB/c mice. **(A-C)** vertical NO and O_2 concentration profiles in 3 different spots of an uninfected tumor. **(D-F)** NO and O_2 microprofiles in a tumor that was infected intra-tumorally with *Salmonella typhimurium* SL7838 24 h prior to the measurement.

Chapter 6

Concluding Discussion and Summary (Zusammenfassung)

Concluding Discussion

Even though NO is a very simple molecule, it mediates manifold biochemical reactions. It is a common misconception that NO is highly reactive. At low concentrations NO is stabile for hours in oxic solution. However, certain proteins are specifically modified and other molecules (e.g. O_2^-) are specifically produced by cells that drastically enhance NO reactivity. This is a common way for cells to use the specific properties of NO. Nitric oxide can also be stored in forms with longer lifetimes, if bound to proteins that release it in a controlled manner (5, 7). Nitric oxide has many different functions in living organism, resulting in a complex picture of interactions and effects (as reviewed in chapter 1). Functions of NO include a wide array of signaling mechanisms in multicellular organisms as well as in microorganisms. In addition, NO is produced as a cytotoxic compound to kill pathogens. Furthermore, NO is produced as an intermediate and as by-product during several reactions of the N-cycle. An important cue to NO function is its concentration range and the chemical conditions of the surrounding media. Thus, the first step in this project was to develop a technique that allows quantification of NO on a scale relevant for microbial communities.

The construction of a NO microsensor for application in biofilms and sediments was successful (chapter 2) and the sensor proved to be a useful extension to the set of microsensors that are already available for biogeochemical studies. The first, specific aim for the application of the novel NO microsensor was to determine micro-environmental NO concentrations in N-cycling communities. The measurements presented in chapter 2, 3 and 4 showed that microbial communities generate steady state NO concentrations in the nanomolar range. However, the measurements of NO formation also showed apparent differences depending on micro-environmental conditions, temporal aspects (steady state vs. transient), and the activity of N-cycling pathways. Thus, I will first compare NO concentrations that were measured in different microbial communities and discuss how those different NO levels could be explained.

In marine sediments maximum NO concentrations were reached in the oxic zone (chapter 2). Concentrations measured in the field were lower (0.5 μM) than those in stored cores,

where NO reached peak concentrations of ~1 µM. The stagnant conditions in the core during sediment storage have led to accumulation of products from organic matter degradation in deeper layers. This caused higher NH_4^+ levels in the oxic zone supporting NO formation by AOB. Indeed, steady state NO concentrations during aerobic NH_4^+ oxidation in a biofilm reached up to 2 µM when it was exposed to 10 mM NH_4^+ (chapter 2), whereas NO concentrations remained in the low nanomolar range when exposed to 400 µM NH_4^+ (chapter 3). In the latter case, addition of NO_2^- (3 mM) induced the formation of 0.3 µM NO at steady state. Much higher NO concentrations were found during perturbations, e.g. after NO_2^- additions or directly after decreasing O_2 in the presence of 3 mM NO_2^-. Nitric oxide steady state concentrations produced by denitrification were lower than those produced by AOB. Nitric oxide concentrations during denitrification were 150-250 nM in the nitrifying/denitrifying biofilm investigated in chapter 3 and 50-200 nM in dental biofilms (chapter 4). In the nitrifying/denitrifying biofilm, steady state NO concentrations during denitrification were almost independent of NO_2^- concentrations. NO concentrations in sediments declined to concentrations below the detection limit in the anoxic zones where denitrifiers may thrive (chapter 2).

Taken together, NO concentrations during nitrification increase up to micromolar concentrations as a result of perturbations or extremely high nutrient input. In contrast, steady state NO concentrations under conditions that allow denitrification are only slightly affected by the environmental conditions and are lower than those produced under conditions where AOB thrive. This can be reconciled with pure culture studies, which suggest that AOB produce NO as a by-product of their metabolism, while in denitrification NO is an intermediate (1, 10). Release of by-products is the result of inefficiency of the metabolic enzymes. This inefficiency is increased by unfavorable environmental conditions, perturbations, or substrate overflow, leading to increased accumulation of by-products. The resulting loss of substrates may not represent a significant energy loss for the cells. In contrast, efficient turnover of intermediates (especially in respiratory processes) is essential for the metabolism, resulting in low concentrations of free intermediates. In fact, NO-consuming enzymes of denitrifiers (Nor) have an extremely high affinity for intermediary NO, which leads to NO consumption long before it reaches cytotoxic levels (9). In contrast, AOB have to control

accumulation of NO produced as a cytotoxic by-product by expressing consuming activities. This will lead to accumulation of almost cytotoxic levels before the consuming activities are expressed and NO is eventually consumed. Accordingly, metabolic modeling suggested that the affinity of NO-consuming processes was the most sensitive parameter to reproduce NO measurements during denitrification, whereas transient NO formation in AOB was partly controlled by the producing process until it accumulated to substantial amounts (chapter 3). Much higher NO concentrations (up to 30 µM) were detected in the very specific environment of tumors infected with *Salmonella typhimurium* (chapter 5; Barak et al.). The high NO concentrations corroborated the benefit of applying *S. typhimurium* in cancer treatment, but how and why these bacteria generate such high concentrations is not completely understood.

AOB and denitrifiers have regulatory mechanisms that control the accumulation of NO, which has been studied previously in pure cultures (2, 6). The experiments presented in this thesis indicate that these mechanisms are also effective in complex microbial communities and limit the accumulation of NO to maximally 2 µM. In contrast, simultaneous measurements of N_2O and NO in nitrifying/denitrifying and dental biofilms (chapter 3 and 4) showed that N_2O accumulates to concentrations, which are one or two orders of magnitude higher than NO concentrations. Comparably to NO, N_2O is a by-product and intermediate of AOB and denitrifiers, respectively. However, the fact that N_2O is not cytotoxic, allows its accumulation to a higher concentration. In fact, NO detoxification often proceeds *via* the reduction to N_2O (reviewed in chapter 1). This is reflected in the data presented in chapter 3 and 4, which shows that whenever the environmental conditions lead to increases in NO, even more drastic increases in N_2O were observed.

How exactly NO is handled in microbial communities is a fascinating subject. The low free NO concentrations in highly active microbial communities may also be caused by reversible binding of NO to proteins and other molecules analogous to albumin and hemoglobin that act as NO and O_2 carriers in blood, respectively. Such molecules may mediate controlled release of NO to concentrations that are cytotoxic to other cells, storage of intermediates, and transport of NO into different strata, where the conditions

favor their release. Medical physiologists have developed several methods to detect proteins with bound NO (3). More research toward the role of molecules that bind NO in complex microbial communities is warranted.

The second, specific aim for applying the NO microsensor was to elucidate the responsible pathways for NO formation in stratified microbial communities. The sensor enabled us to combine the measurement of NO concentrations with micro-environmental characterization and simultaneous measurements of microbial activity. This approach showed that in the nitrifying/denitrifying biofilm, NO formation by AOB was restricted to oxic conditions and by denitrification to anoxic conditions (chapter 3). These results allowed modeling of NO formation under different conditions by applying threshold functions to metabolic pathways. In dental biofilms, nitrification did not play a role, but interestingly, NO was formed by aerobic denitrification. Indeed, aerobic NO_3^- uptake was measured with microsensors and aerobic N_2 formation from NO_3^- was shown by isotopic labeling (chapter 4). Aerobic denitrification has not been observed in many environments and it did not occur in the nitrifying/denitrifying biofilm. However, in a contributed work presented in chapter 5 (Gao et al.) we found evidence for aerobic denitrification in permeable sediments of an intertidal sandflat. The potential for aerobic denitrification is an adaptation of microbial communities to frequent fluctuations of O_2 concentrations during a relatively constant supply of NO_3^-. These conditions apply for both dental biofilms and permeable sediments. Similarly, aerobic denitrification is thought to occur in soil microbial communities, where it is occasionally associated to NO and N_2O formation that is not well understood (4). In conclusion, different pathways can mediate NO formation in complex N-cycling microbial communities. The pathways depend on the incubation conditions and the origin of the sample, and display distinct features and controls for NO formation.

The third, specific aim for applying the NO microsensor was to obtain insights into the regulatory mechanisms behind transient accumulation of NO. This was studied by measuring time series of NO and N_2O concentrations and modeling the transients with dynamic parameters in the nitrifying/denitrifying biofilm. The transient maxima of NO and N_2O after the perturbation with NO_2^- addition and O_2 decrease were followed by an

immediate decrease of NO within minutes (chapter 3). This indicated that NO affected the producing or consuming enzymes directly. The simultaneous increases in N_2O suggested that regulation of NO concentrations is mediated by its reduction to N_2O. Further experiments are needed to show that the underlying mechanisms are active in other complex microbial communities. The sudden accumulation of NO concentrations, and subsequent control of steady state concentrations, will depend on the community type, its cell density and the intensity of the perturbation. Understanding the regulation of dynamic NO formation is important, because it is involved in interactions of microbial communities with multicellular hosts, such as in dental biofilms (chapter 4), and in the emission of the greenhouse gas N_2O from various environments (chapter 3).

The measurements of NO in sediments showed that it is produced in the oxic part and consumed in the anoxic part of stratified microbial communities, suggesting its active involvement in biogeochemical cycling (chapter 2). In the introduction I reviewed all known catabolic reactions of the N-cycle and their ability to produce or consume NO. Moreover, NO affects enzymes in eukaryotes and bacteria based on similar biochemical mechanisms, rendering NO a signaling molecule in multicellular organisms and for microorganisms (chapter 1). Hence, I hypothesize that NO produced during a certain N-cycling pathway may affect microorganisms that perform a different N-cycling pathway. For example, NO may link activity of AOB to the activity of denitrifiers at the oxic/anoxic interface in stratified microbial communities. Here, NO is formed by AOB, because of fluctuating O_2 concentrations (as observed in chapter 3). In turn, NO is a signal for the expression of NO_2^- reductase and NO reductase in denitrifiers (11). Thus, NO produced by AOB can induce denitrification activity. As another example, NO may link the activity of AOB and NOB that commonly live in close association. As reviewed in the introduction, NO produced by NOB is believed to direct cellular electron flux either toward O_2 respiration at high O_2 concentrations or toward NADH synthesis at low O_2 concentrations by reversibly inhibiting cytochrome oxidase (8). Hence, NO produced by AOB at low O_2 concentrations could partially inhibit O_2 respiration and foster the NADH-dependent CO_2 fixation or production of storage compounds (e.g. polyhydroxybutyrate) in NOB. This can be directly tested in microbial communities with carbon-labeling techniques combined with FISH.

The hypothesis that NO links activities of different functional groups within N-cycling microbial communities deserves further investigation. For further research I suggest to study the effect of NO on N-cycling by experimentally supplying non-toxic NO concentrations with NO donor compounds or by decreasing NO concentrations with NO scavenger compounds. The effect can be measured as subtle or drastic changes in the activity of various N-cycle pathways. These effects on the N-cycle will differ depending on the environment, because NO formation by N-cycle pathways depends on the chemical conditions as shown in chapter 3, where NO formation of aerobic NH_4^+ oxidation and denitrification were both affected by O_2 and NO_2^-. Furthermore, NO can be chemically produced at low pH or consumed by reactive metals (e.g. Fe^{2+}). The results shown in chapter 4 provide evidence that environmental pH - induced by fermentation - increased NO steady state concentrations and subsequently its conversion to N_2O.

This thesis showed controlled turnover of NO in different microbial communities indicating that the underlying reactions are a common feature in different N-cycling environments. The contributed work presented in chapter 5 (Ettwig et al.) showed evidence for dismutation of NO to N_2 and O_2 during the anaerobic oxidation of CH_4 coupled to NO_2^- reduction. This surprising finding highlights the biochemical versatility of NO showing that it may undergo unexpected reactions as an intermediate. In addition, targets and functions of NO are divers as has been shown for bacterial pure cultures, but mainly investigated in multicellular organism. It is likely that investigations toward the function of NO in microbial communities will find different functions mediated by biochemical mechanisms similar to those in multicellular organisms. However, bacteria evolved longer than eukaryotes, thus, further investigations will also lead to unique functions and mechanisms that constitute NO bioactivity in microbial communities.

Acknowledgements

I thank Peter Stief and Dirk de Beer for valuable comments on the Introduction and the Concluding Discussion.

References

1. **Arp, D. J., and L. Y. Stein.** 2003. Metabolism of inorganic N compounds by ammonia-oxidizing bacteria. Critical Reviews in Biochemistry and Molecular Biology **38:**471-495.
2. **Beaumont, H. J. E., S. I. Lens, W. N. M. Reijnders, H. V. Westerhoff, and R. J. M. van Spanning.** 2004. Expression of nitrite reductase in Nitrosomonas europaea involves NsrR, a novel nitrite-sensitive transcription repressor. Molecular Microbiology **54:**148-158.
3. **Hausladen, A., R. Rafikov, M. Angelo, D. J. Singel, E. Nudler, and J. S. Stamler.** 2007. Assessment of nitric oxide signals by triiodide chemiluminescence. Proceedings of the National Academy of Sciences of the United States of America **104:**2157-2162.
4. **Morley, N., E. M. Baggs, P. Dorsch, and L. Bakken.** 2008. Production of NO, N2O and N-2 by extracted soil bacteria, regulation by NO2- and O-2 concentrations. Fems Microbiology Ecology **65:**102-112.
5. **Singel, D. J., and J. S. Stamler.** 2005. Chemical physiology of blood flow regulation by red blood cells: The role of nitric oxide and S-nitrosohemoglobin. Annual Review of Physiology **67:**99-145.
6. **Spiro, S.** 2007. Regulators of bacterial responses to nitric oxide. Fems Microbiology Reviews **31:**193-211.
7. **Stamler, J. S., S. Lamas, and F. C. Fang.** 2001. Nitrosylation: The prototypic redox-based signaling mechanism. Cell **106:**675-683.
8. **Starkenburg, S. R., D. J. Arp, and P. J. Bottomley.** 2008. Expression of a putative nitrite reductase and the reversible inhibition of nitrite-dependent respiration by nitric oxide in Nitrobacter winogradskyi Nb-255. Environmental Microbiology **10:**3036-3042.
9. **Zafiriou, O. C., Q. S. Hanley, and G. Snyder.** 1989. Nitric-Oxide and Nitrous-Oxide Production and Cycling During Dissimilatory Nitrite Reduction by Pseudomonas-Perfectomarina. Journal of Biological Chemistry **264:**5694-5699.
10. **Zumft, W. G.** 1997. Cell biology and molecular basis of denitrification. Microbiology and Molecular Biology Reviews **61:**533-+.
11. **Zumft, W. G.** 2005. Nitric oxide reductases of prokaryotes with emphasis on the respiratory, heme-copper oxidase type. Journal of Inorganic Biochemistry **99:**194-215.

Summary

Nitric oxide (NO) is a biologically versatile molecule that serves as cytotoxic agent and signaling compound in microorganisms and multicellular organisms including humans. Microorganisms that catalyze catabolic pathways of the N-cycle produce NO during their activity and consume NO, mainly by reduction to N_2O, leading to emission of both gases form various environments to the atmosphere. This thesis aimed to measure NO concentrations in complex N-cycling microbial biofilms, determine the responsible pathways and obtain insights into the regulatory mechanisms underlying NO turnover. Initially, a NO microsensor that is suitable to detect NO concentrations that are produced within biofilms was developed and applied to a nitrifying biofilm and marine sediments. The microprofiles showed production of NO in the oxic and consumption in the anoxic zone indicating its active involvement in biogeochemical processes. In a following study, NO and N_2O formation was investigated in a biofilm with nitrifying and denitrifying activity. Analyzing the pathways that are active under different conditions, combined with description of micro-environmental conditions allowed the assignment of NO formation to AOB under oxic and denitrifiers under anoxic conditions. Transient measurements, combined with metabolic modeling gave insights into the regulatory mechanisms that were underlying immediate NO production and consumption after perturbation with NO_2^- additions and O_2 decrease. Immediate production resulted from perturbation of active N-cycling pathways, whereas immediate NO consumption was mediated by direct effects of NO on the enzymes that governed its turnover. In a third study, NO and N_2O formation in a dental biofilm was shown to be mediated by aerobic denitrification and highly dependent on environmental pH. NO formation in dental biofilms might mediate interactions between plaque bacteria and gingival cells, because NO is an important signaling molecule for controlling vascular tone and the immune system in the gum. Generally, NO occurs in concentrations in the nanomolar range, but concentrations may increase depending on the environmental conditions and the process that governed its production. Nitric oxide concentrations were always lower than N_2O concentrations, because of fast reduction of NO to N_2O. Control of NO accumulation is important because it is an intermediate of denitrification, a cytotoxic molecule and because it might be involved in signaling processes within complex microbial communities.

Zusammenfassung

NO ist ein biologisch vielseitiges Molekül, das in Mikroorganismen und mehrzelligen Organismen als Signalmolekül dient und zytotoxische Wirkungen ausübt. Die Mikroorganismen des Stickstoffkreislaufes produzieren NO während ihrer regulären Aktivität und verbrauchen es hauptsächlich durch Reduktion zu N_2O. Dies führt zur Emission beider Gase aus verschiedenen Ökosystemen in die Atmosphäre. Das Ziel dieser Arbeit war es, NO-Konzentrationen in Biofilmen, die aktiv Stickstoff umsetzen, zu bestimmen, die NO-Produktion einzelnen mikrobiellen Prozessen zuzuordnen und Einblicke in regulatorische Mechanismen des NO-Stoffwechsels zu erhalten. Als erstes wurde ein NO-Mikrosensor entwickelt, mit dem NO-Konzentrationen in Biofilmen im nanomolaren Konzentrationsbereich gemessen werden können. Die Anwendung dieses Sensors in nitrifizierenden Biofilmen und marinen Sedimenten zeigte, dass NO in oxischen Schichten produziert und in anoxischen Schichten verbraucht wurde und somit aktiv in biogeochemische Prozesse eingebunden war. In einer weiteren Studie wurde die Bildung von NO und N_2O in einem Biofilm untersucht, der sowohl nitrifizierende als auch denitrifizierende Aktivität besaß. Hier konnte die NO-Bildung unter oxischen Bedingungen ammoniak-oxidierenden und unter anoxischen Bedingungen denitrifizierenden Bakterien zugeordnet werden. Dies war möglich, da die Aktivität dieser mikrobiellen Gruppen innerhalb des Biofilms unter experimentell veränderten Bedingungen gemessen werden konnte. Die regulatorischen Mechanismen, die die Dynamik der NO-Konzentrationsänderungen nach Zugabe von NO_2^- und Wegnahme von O_2 bewirkten, wurden durch zeitlich aufgelöste Mikrosensormessungen und Modellierung der metabolischen Prozesse aufgeklärt. Die Produktion von NO setzte unmittelbar ein, wenn ein aktiver Prozess des Stickstoffkreislaufes gestört wurde. Der sich sofort anschließende Verbrauch von NO wurde dagegen durch einen direkten Effekt von NO auf diejenigen Enzyme bewirkt, die die Umwandlung von NO bewerkstelligen. Eine dritte Studie zeigte die Bildung von NO und N_2O durch aerobe Denitrifikation in Zahnbiofilmen. Die Messungen ergaben zudem, dass der pH des Zahnbiofilms einen wichtigen Einfluss auf die Bildung von NO und N_2O hat. Die Bildung von NO in Zahnbiofilmen könnte Interaktionen zwischen Zahnbelagsbakterien und Zahnfleischzellen ermöglichen, da NO ein wichtiges Signalmolekül bei der Regulation des Blutdrucks und des Immunsystems im Zahnfleisch ist. Im Allgemeinen zeigte sich,

dass NO in Biofilmen im nanomolaren Konzentrationsbereich vorkommt, jedoch können die Konzentrationen in Abhängigkeit von Umweltbedingungen und NO-produzierenden Prozessen variieren. Die NO-Konzentrationen waren stets niedriger als die N_2O-Konzentrationen, da NO schnell zu N_2O reduziert wurde. Die Kontrolle der NO Konzentrationen innerhalb mikrobieller Gemeinschaften könnte nicht nur deshalb wichtig sein, weil NO ein Zwischenprodukt der Denitrifikation ist, sondern auch weil hohe NO-Konzentrationen zytotoxische Wirkungen haben und weil NO in verschiedenste Signalprozesse involviert ist.

Anlage zur Dissertation

Frank Schreiber   8. May 2009
An der Kämenade 23d
28327 Bremen

Erklärung
gem.§6(5) Nr.1-3 PromO

1. Ich erkläre, dass ich die Arbeit ohne unerlaubte fremde Hilfe angefertigt habe.
2. ‚keine anderen, als die von mir angegebenen Quellen und Hilfsmittel benutzt habe und
3. die den benutzten Werken wörtlich oder inhaltlich entnommenen Stellen als solche
kenntlich gemacht habe.